UNIVERSITY OF NAIROBI

APPLICATION OF GEOPHYSICAL EXPLORATION METHODS IN MAPPING GOLD MINERALISATION ZONES.

CASE STUDY: MAKINA PROSPECT IN THE BUSIA-KAKAMEGA GREENSTONE BELT, S.E. UGANDA.

BY

OCHOLA KEVIN

REGISTRATION NUMBER: I56/88400/2016

A Dissertation submitted for examination in partial fulfillment of the requirements for award of Degree of Master of Science in Geology, (Mineral Exploration) of the University of Nairobi

2021

DECLARATION

I declare that this Dissertation is the result of my own investigation and research, and has not been submitted elsewhere for examination, award of a degree or publication. Where other people's work or my own work has been used, this has properly been acknowledged and referenced in accordance with the University of Nairobi's requirements.

Signature......................................Date. 15ᵗʰ November 2021

OCHOLA KEVIN

I56/88400/2016

Department of Earth and Climate Science

Faculty of Science and Technology

University of Nairobi

This dissertation is submitted for examination with our approval as supervisors:

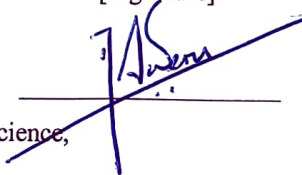|	[Signature]	[Date]
Dr. Aaron K. Waswa		17 November 2021

Department of Earth and Climate Science,

University of Nairobi

PO Box 30197-00100

Nairobi, KENYA.

	[Signature]	[Date]
Dr. Daniel Weru Ichang'i		16ᵗʰ November 2021

Department of Earth and Climate Science,

University of Nairobi

PO Box 30197-00100

Nairobi, KENYA.

UNIVERSITY OF NAIROBI
FACULTY OF SCIENCE AND TECHNOLOGY

DECLARATION OF ORIGINALITY FORM

This form must be completed and signed for all works submitted to the University for examination.

Name of Student: OCHOLA KEVIN

Registration Number: I56/88400/2016

Faculty: FACULTY OF SCIENCE AND TECHNOLOGY

Department: EARTH AND CLIMATE SCIENCES
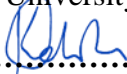
Course Name: MASTER OF SCIENCE IN GEOLOGY

Title of the work

Application of Geophysical Exploration methods in mapping Gold Mineralisation Zones. Case Study: Makina Prospectt in The Busia-Kakamega Greenstone Belt, S.E. Uganda.

DECLARATION

1. I understand what Plagiarism is and I am aware of the University's policy in this regard
2. I declare that this Dissertation (Thesis, project, essay, assignment paper, report. etc) is my original work and has not been submitted elsewhere for examination, award of a degree or publication. Where other people's work, or my own work has been used, this has properly been acknowledged and referenced in accordance with the University of Nairobi's requirements.
3. I have not sought or used the services of any professional agencies to produce this work
4. I have not allowed, and shall not allow anyone to copy my work with the intention of passing it off as his/her own work
5. I understand that any false claim in respect of this work shall result in disciplinary action, in accordance with University Plagiarism Policy.

Signature: …………………………………..……………………………………..

Date: 15 NOVEMBER 2021

ABSTRACT

The geophysical survey exploration programme in Makina was done as a follow up on gold in soil geochemical anomalies delineated by Mayfox Mining Company. The survey grid covered an area of approximately 10 square kilometers. This contained 60-line kilometers of ground magnetic survey and 42-line kilometers of gradient Induced polarization- Resistivity survey that was conducted in the project area. The aim of the geophysical surveys was to determine the extent of gold mineralization and its associated geological and structural controls. The Induced polarization, Resistivity and Magnetic surveys conducted in the project area have produced anomalies consistent with structural and lithological trends relevant to gold mineralization. The chargeability anomalies conform almost perfectly to the trends established from the soil geochemical anomalies. The combined interpretation of the resistivity and magnetic data reveals pertinent rheological variations, suggesting evidence of shear zones or fracture zones, typical of mineralization controls in the Busia-Kakamega greenstone belt. The geophysical maps produced have aided the interpretation of the local geological setting. Distinct lithological boundaries have been inferred and interpreted from analysis of these maps. High chargeability patterns appear to coincide with high magnetic anomalies, supporting the initial association of the area's deposits with sulphide mineralization and more specifically iron sulphides like pyrite and pyrrhotite.

Preliminary analysis of the integrated datasets shows the potential occurrence of mineralization hosted in two geological frameworks. First, there are indications that the Banded Iron formation hosts disseminated mineralization as well as in the accompanying minor shear and contact associated quartz veins and veinlets. The second class is linked to the almost North-South trending fault/fracture zones. The orientation of the latter classification shows resemblance to the Tira deposit.

The two prospective target zones delineated in this project, warrant further exploration and are potentially future drill targets. Pole-Dipole IP/Resistivity surveys have been proposed to target the most prospective chargeability anomalies. The Pole-Dipole data will provide crucial subsurface information on the trend and continuity of the potential ore mineralization besides affirming the veracity of current postulations. The Pole-Dipole data, inversion models and pseudo-sections can then be used to generate drilling targets. For this project area, three initial survey profiles have

been proposed along IP lines; L5200E, L600E and L7200N. The results of this project have emphasized the importance of integrating the IP/Resistivity technique and ground magnetics in gold exploration. Further, the results have shown how suitable the methods can be, especially in the search for potentially deep-lying ores and in the tropical regions, where weathering and leaching processes such as lateritization, may adversely influence soil geochemical surveys. The potential for the regional continuity of the mineralization is evident and intensified exploration works are required to unearth this potential further to the North and West of the survey area and. To the east of Tira and even across the border into Kenya, the grounds are mostly underexplored despite the evident geological potential posed by the rich yet structurally intricate Busia Kakamega-greenstone belt.

ACKNOWLEDGEMENTS

TABLE OF CONTENTS

List of Tables

List of Figures

List of Appendices

List of abbreviations and acronyms

BIF	Banded Iron formation
BRGM	Bureau de recherches géologues et minières
EL	Exploration License
GIS	Geographic Information Systems
GPS	Global Positioning system
GSMD	Geological Survey and Mines Department
GTK	Geological Survey of Finland
HDR	Total Horizontal Derivative
IP	Induced polarization
L.V.G.	Lake Victoria Goldfields
mV/V	Milli volts per volt
Mx/M	Chargeability
PPB	Parts per billion
PPM	Parts per million
REE	Rare Earth Elements
RTP-	Reduction to Magnetic Pole
TDR	Tilt Derivative
TMI-	Total Magnetic Intensity
UNDP	United Nations Development Program
UTM	Universal transverse Mercator
WGS	World Geodetic System

Lithology codes

Avq	Quartz vein
Avqy	Smoky quartz vein
Bed	Bedding
Flc	Foliation cleavage
Frc	Fracture cleavage
Imd	Doleritic intrusion
Ifg	Granitoid
Ifpq	Quartz phyric felsic intrusion
Jt	joint
Mct	Quartzite
Rli	Laterite
Slct	Banded Chert
Slif	Banded Iron Formation
Vm	Mafic Volcanic
Vmlb	Mafic Volcanic breccia

CHAPTER 1   INTRODUCTION

1.1 BACKGROUND INFORMATION

Makina prospect spans approximately 28.4 Km^2, and falls within the Ugandan extent of the Busia-Kakamega greenstone belt, extending further into western Kenya. Makina prospect marks a key anomalous segment of the Busia Gold district in southeast Uganda. The prospect is in Mayfox Mining Company's Exploration License No. EL1646, issued by the Department of Mines and Geological Survey. Gold deposits in the area were initially discovered in the 1930s. Subsequent surveys in the following years led to the opening of Tira mine about 1936. Both alluvial and lode gold mineralization have been mined by local artisanal and small-scale miner ever since. Previous workers have largely been able to distinguish two types of gold deposits in the area. These are, Quartz vein shear-hosted and BIF hosted mineralization. Historical and recent exploration campaigns have continually underscored the significant potential of the gold mineralization in the area, whilst improving the understanding of the mineralization (Davies, 1956; Mroz et al., 1981; Serwanga et al., 1994). The previous exploration data was largely collected from regional exploration programmes involving soil sampling and trenching in addition to regional geophysical surveys in some of the areas. BRGM and GSMD had delineated three gold in soil geochemical anomalies in the region, two of the anomalies around the Tira mines area ranging 50-100 ppb; another in the area around Makina and Osapiri areas. In conjunction with the Finland Geological survey, the GSMD executed a countrywide geology mapping programme as follow up to the Nationwide Aeromagnetic and Radiometric survey. The ground truthing exercise reaffirmed the significant prospectivity of the deposits in Busia. They further recommended the region as a prime prospect for intensified exploration studies.

1.2 STATEMENT OF THE PROBLEM.

Previous gold exploration reports on the region have continually highlighted the rich potential that lies underneath. The magnitude of this potential is yet to be determined either genetically or empirically. The few scientific exploration expeditions executed previously focussed on regional exploration methods, thus leaving more gaps to be filled in the quest to understand the deposit characteristics and quantity. Therefore, more focussed and refined exploration approaches are desirable and necessary in the area. A refined prospect scale approach with tightened sample spacing for both geochemical and geophysical surveys would be ideal. The

area's potential to host significant gold occurrences is not in doubt and this is evidenced by the abundant artisanal and small-scale mining operations. There is also a need to focus on the exploration process towards discovering deeper-lying deposits that may be otherwise been difficult to find using shallow focused methods.

1.3 OBJECTIVES

1.3.1 Main objective

The main aim of the project is to determine the prospectivity and nature of the gold mineralisation in the Makina prospect area by integrating ground geophysical techniques with earlier geological and geochemical data.

1.3.2 Specific objectives

1. To establish suitability of induced polarization and ground magnetics in the delineation of gold mineralisation and the associated geological and structural understanding of the study area.
2. To establish the Economic potential of the gold mineralisation in Makina area by integrating obtained geophysical, geochemical and geology exploration data.
3. To generate target zones for follow up exploration.
4. To establish and design further follow up exploration programmes.

1.4 JUSTIFICATION AND SIGNIFICANCE OF THE RESEARCH

Significant gold resources and reserves have in the recent past been reported in various parts of the craton, including findings in Kenya and Tanzanian. Most known occurrences in the area of focus are underexplored and poorly understood. This is largely a consequent of the nature and limitation of previous studies which were to a greater extent of regional scale. The main type of deposit in the area is known to be Banded iron formation associated. Globally, BIF associated gold deposits are known to host huge amounts of gold, with richer examples occurring in Geita, Tanzania and Lolgorian in Kenya. Detailed geochemical sampling surveys, ground geophysics and drilling programmes are highly recommended if the geological nature and the economic viability of the deposits are to be established. Integration of the latest refined geochemical survey results with ground geophysical data and historical data goes towards improving the understanding of the nature and economic potential of such deposits. Gold mineralisation in the area has been linked mainly to structural and lithological controls, making Magnetic and Resistivity methods the most ideal in identifying these structural patterns. The

sulphide association to gold occurrence in the region is a justification for the suitability of Induced Polarisation (IP) as an exploration tool in this area.

1.5 GEOGRAPHIC SETTING OF THE STUDY AREA

1.5.1 Location

The Makina area is located roughly 10 Km North-West of Busia town see Figure 1.1. Busia town is located at the Kenya-Uganda border. The study area falls in Mayfox Mining Company's License No. EL1646, granted by the Department of Geological Surveys. The licence is 28.4 Km^2 in area. Tororo district borders Busia to the north, Bugiri district is to the west of Busia while to the south the area borders Lake Victoria. To the East is Busia county in Western Kenya.
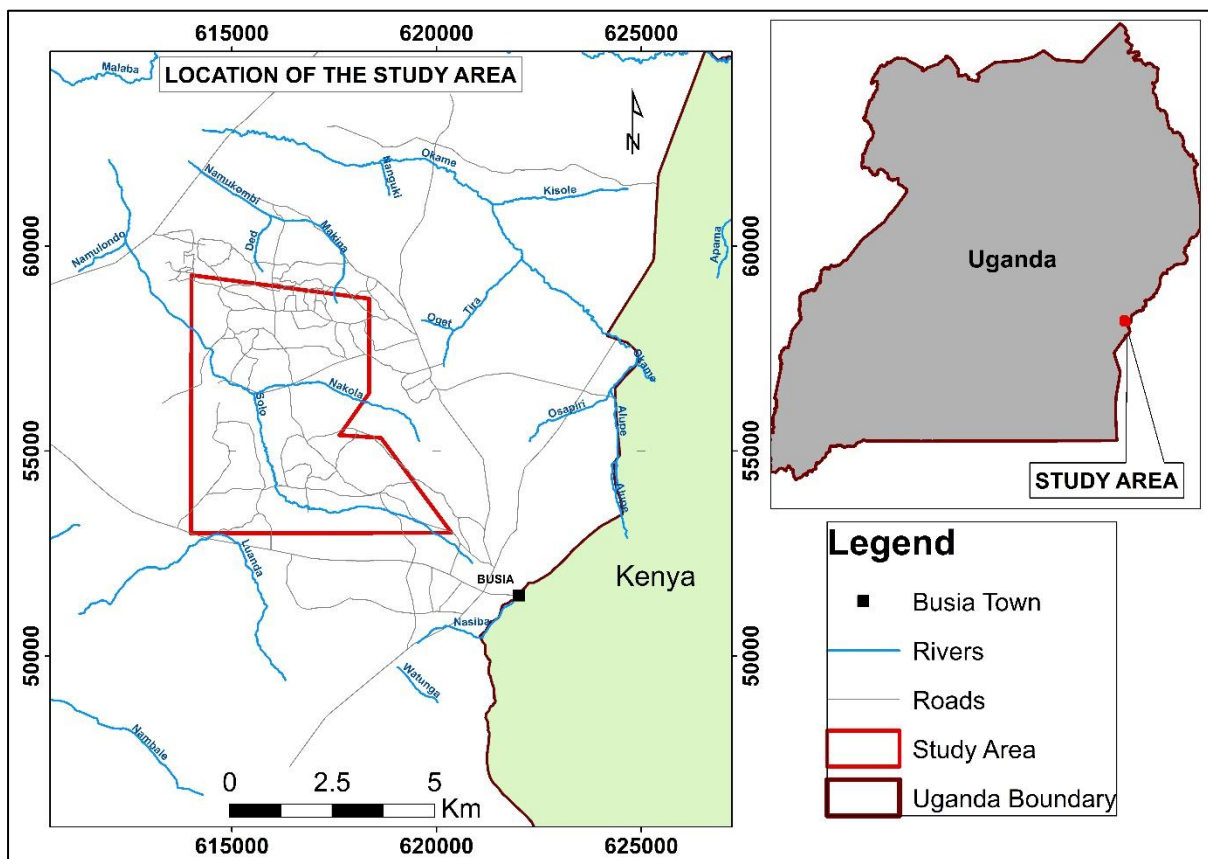
Figure 1.1: Location Map of the Study area. (Inset is the Map of Uganda with the study area highlighted in Red).

1.5.2 Physiography and Drainage

The terrain is generally even with notable hills in Buteba and Bukade areas. The general elevation of the area is between 1070m to 1220m above sea level (Figure 1.2). There are two

known drainage systems, both draining into Lake Victoria. The rivers (Nakola, Tira, Solo and Osapiri) are major tributaries of the River Malaba.
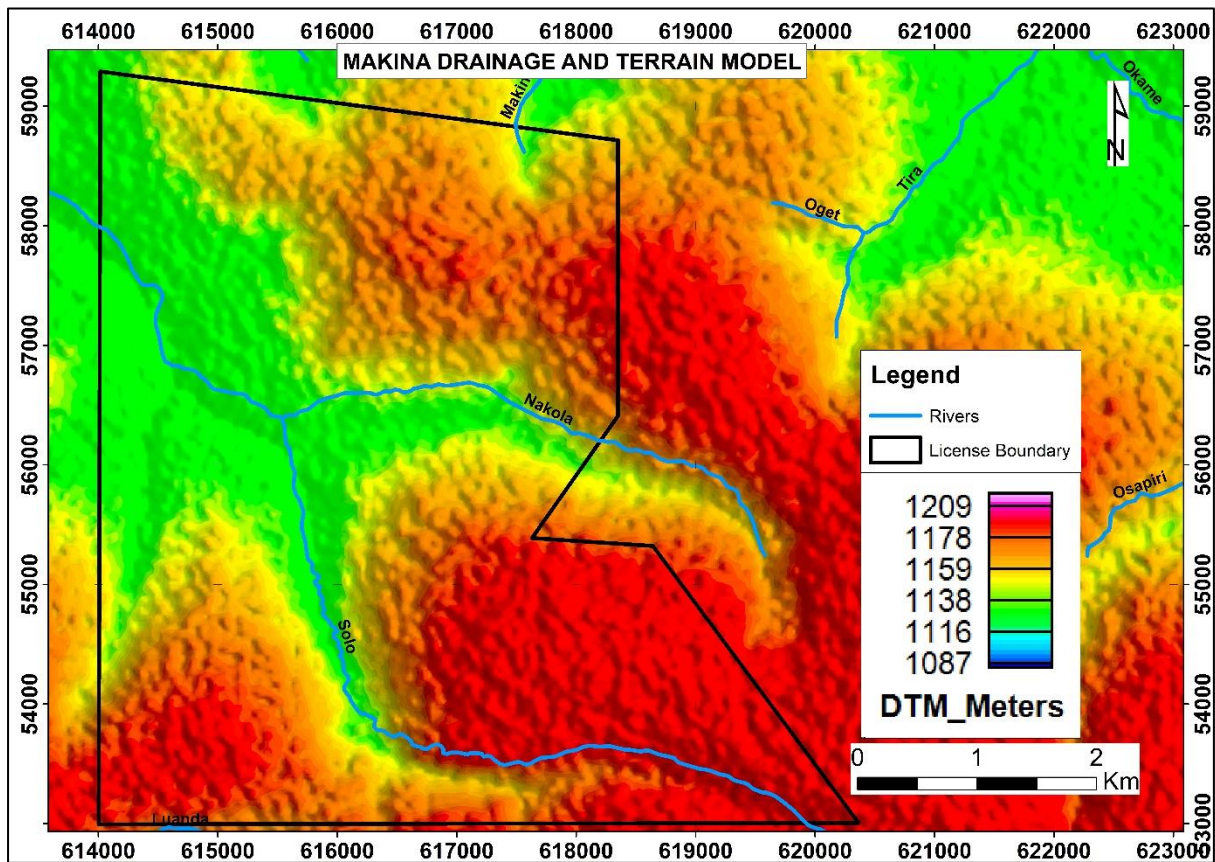
Figure 1.2: Physiography and Drainage map of the Study area.

1.5.3 Climate and Vegetation

Precipitation in Busia is generally of convectional type. The main rain seasons are recorded twice annually, between March and April, with the second period between September and November as depicted in Figure 1.3 below. The mean annual precipitation varies between 1,250 mm and 1,275 mm. The mean annual maximum temperatures are between 25°C to 30°C. Vegetation in the area has been described as dry acacia savannas, with some forested sections, such as Busitema forest and Amonikakinei forest.
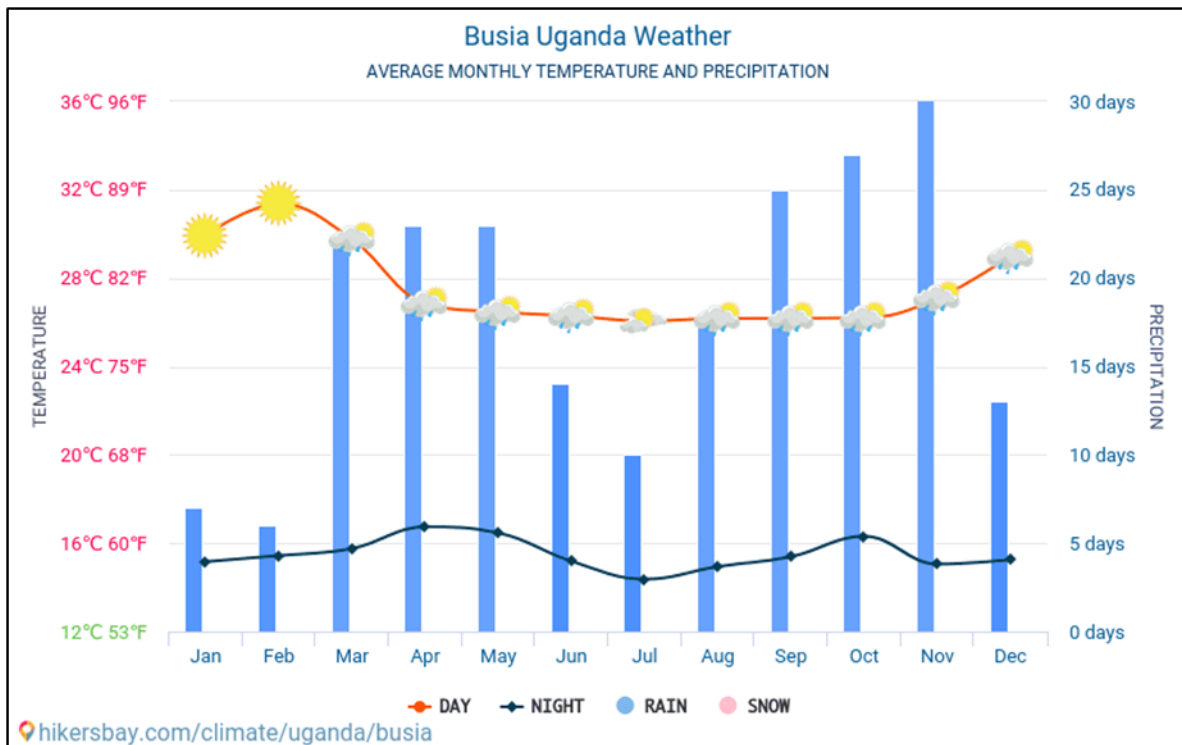
Figure 1.3: Busia Weather analysis (source: hikersbay.com).

1.5.4 Land Use and Settlement

Crop farming and animal rearing are major economic activities in the area. Most of the land system is customary. The small-scale arable farming is majorly for food. Food crops produced include bananas, rice, potatoes, corn, sorghum, cowpeas, cassava and Millet. Cross border trade is also significant economic activity in the area and fishing, especially along the shores of Lake Victoria. The people are also engaged in alluvial and hard rock artisanal gold mining. settlements are scattered with most populated zones distributed near the Kenyan border. This can be attributed the trading activities near the border as well as fertile grounds near the lake.

CHAPTER 2 LITERATURE REVIEW

Davies (1956) categorised the main rock types of Busia can be as follows;

- Bulugwe series- made up of banded quartzites, mudstones, phyllites and shales.
- Samia series- comprising agglomerates, brecciated units that grade into medium and fine tuffs and sediments.

He further genetically associates gold veins in Tira and Busia to the Masaba granitic intrusion, while stressing that the quartzite beds formed barrier to the mineralising fluids. The small-scale mining in Busia is estimated to have produced approximately between 1.0t to 1.5t Au, between 1937 to 1961 (Nyakecho and Hagemann, 2014).

Mroz et al. (1991), suggest that the mineralisation in Busia occurs in the Nyanzian, and that there are two main mineralisation styles in the region. These are:

a) Gold in quartz veins, mostly of tectonic controls and occurs mostly in mafic metavolcanic units.
b) Iron rich banded sediments/ quartzites with either disseminated mineralisation or gold in sulphide rich veins.

Historically, the main anomalies identified by the surveys include two in the Tira mines division, one in Bukade-Makina associated to the quartzites and one at Osapiri.

Nyanzian greenstone belts are said to be the oldest Archean formations in the Tanzania craton (Ogola and Omenda, 1991). They exhibit low-grade metamorphism. Chloritization, carbonatization, silicification and sericitization are alterations that could be evidence of metasomatic activities in the most Nyanzian greenstones. Gold mineralisation is often commonly accompanied by these hydrothermal alterations. The gold deposits in the region are thus associated with the Nyanzian granite greenstone zones. Gold rich quartz veins also occur in banded iron formations, andesites, diorites and basalts.

Some geophysical exploration surveys were carried out in Busia by Serwanga et al. (1994) under the UNDP Uganda Project in collaboration with GSMD and Roraima Mining Company Limited. The survey grid was located 800m northeast of Busia town. The results identified magnetic and IP anomalies with potential for gold mineralisation along the quartzite horizons. The IP survey was able to delineate quartzite horizons near the surface and units favourable for hosting gold mineralisation. The magnetic survey results also identified significant structures.

Mbonimpa et al. (2007) categorised the gold mineralisation as being both quartz vein deposits and BIF hosted deposits, and classified the deposit as being epigenetic. They suggested that the anomaly in Tira area could be associated with the quartz vein styled deposit while the source

of the mineralisation in other areas is probably linked to the BIF, where the gold mineralisation may be disseminated. Their analysis also confirms that there is a positive correlation between gold and other base metals like silver, lead, zinc and copper. They however, recommend more detailed geochemical studies and analyses of the mineralisation, with focus on the sulphide association, to further understand both the quartz vein-hosted deposits and the BIF hosted. Robert (2004) indicates that gold mineralisation in the south east of Uganda is hosted within the Neoarchean Busia - Kakamega granite greenstone belt, which includes the structurally controlled mesozonal Tira gold deposit. He recommends further exploration work and focus on the structural controls on mineralisation. Other recommended geoscientific work include; geochronology of the host rocks and mineral alterations, whole-rock and trace element geochemistry.

Sumner (1976) states that induced polarisation (IP) as a geophysical investigation method is able to detect even small amounts of metalliferous minerals in a rock mass and in order to apply the method effectively in the field one needs to understand physical characteristics of the sought-after deposit including its, shape, size, depth, and electrical properties. With this information, a reasonable IP programme can be designed and one will be able to select the best applicable electrode location spacing, array type, and line spacing. With unknown target characteristics, geological understanding becomes crucial in executing an optimised survey. The IP method picks mostly disseminated concentrations of conductive minerals. Identification of such minerals as sulphides could potentially become a major indicator for gold occurrence. Metal sulphides such as, pyrite, chalcopyrite, pyrrhotite, etc, are usually associated with pathfinders for gold occurrence.

The Gokona gold deposit in North Mara, Tanzania was discovered under younger barren volcanic units through the Induced polarisation technique that was followed up by reverse circulation drilling (Smith and Anderson, 2003). The gold mineralisation in Gokona is associated with potassic alteration with quartz veining accompanied by pyrite and arsenopyrite mineralisation. the resource was initially estimated at 700,000 ounces of gold at 5.4 grams per tonne. That the deposit was discovered between 4m to 60m below a barren phonolite unit is an indication of how effective the Induced polarisation method can be over moderately sulphidic rocks and at various depths.

Magnetic surveys are the most common geophysical exploration techniques in the exploration for gold deposits. Airborne Magnetic surveys are crucial in the early stages of exploration,

since they reliably and affordably provide information on the geology and structure of an area (Kearey et al., 2002).

Interpreted magnetic maps are quite significant in areas where outcrop exposures are limited. Magnetic anomalies would be pronounced in the igneous or metamorphic regions. Intrinsic understanding of the geologic controls of mineralisation is vital in making reasonable interpretations and inferences on the relationships between magnetic rocks and gold mineralisation (Boyd and Wiles, 1984).

Magnetic map interpretations are done to improve geological understanding. Rocks with low magnetic susceptibility like limestone may manifest as sections of low and homogeneous magnetic fields, on the other hand, mafic and ultramafic rocks occur as zones with high and more variable magnetic fields. Comparing magnetic readings in areas of known geology allows extrapolation of the geology into areas where the rocks are under cover (Scott, 2014).

2.1 GEOLOGICAL SETTING AND EXPLORATION HISTORY
2.1.1 Archaean "Busia - Kakamega greenstone belt"

It is among seven major greenstone belts of the Lake Victoria Goldfields (Figure 2.1). The Lake Victoria Goldfields is a segment of the Tanzania craton that is comprised of major gold districts and metal deposits. The goldfields cover regions in Western Kenya, Northwestern Tanzania and Southeast Uganda. The belts are composed mainly of Neoarchean rocks classified as; the Nyanzian volcano-sedimentary sequences that are overlain by younger Kavirondian clastic metasedimentary units. Most parts the greenstone belts have been intruded by later granites.

The Busia-Kakamega greenstone belt occurs to the northeastern most part of the craton and trends North west from Kakamega in Western Kenya to Southeastern Uganda. The belt is bounded to the east by the Neoproterozoic mobile belt (East African Orogen), the Neogene Kavirondo (Winam) rift to the south, and transitions westwards to Late Proterozoic granites and gneisses of the Uganda basement system.
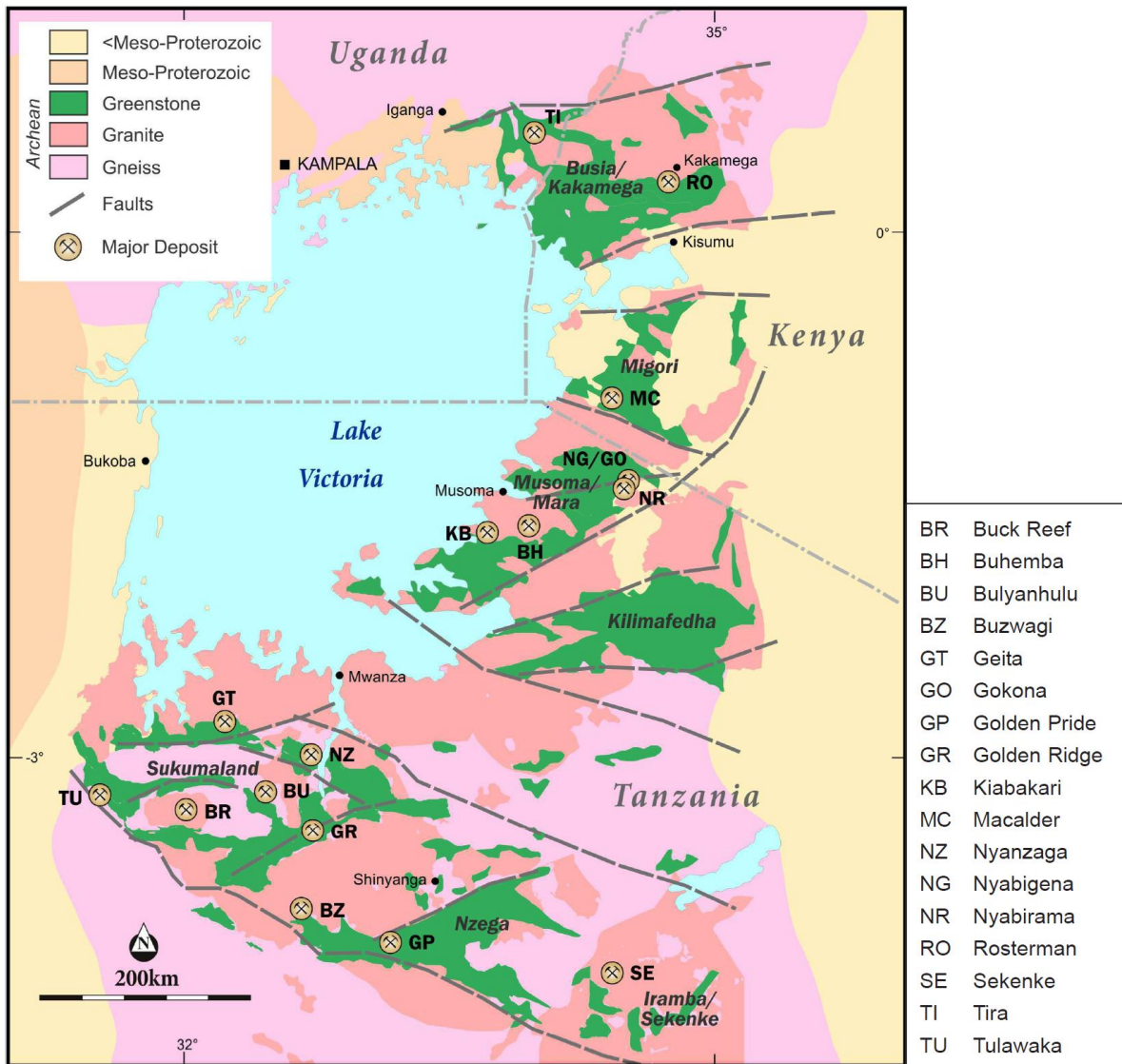
Figure 2.1: Map showing the Nyanzian greenstone belts and the major deposits in the Lake Victoria Terrane. (Adapted from Henckel et al., 2016).
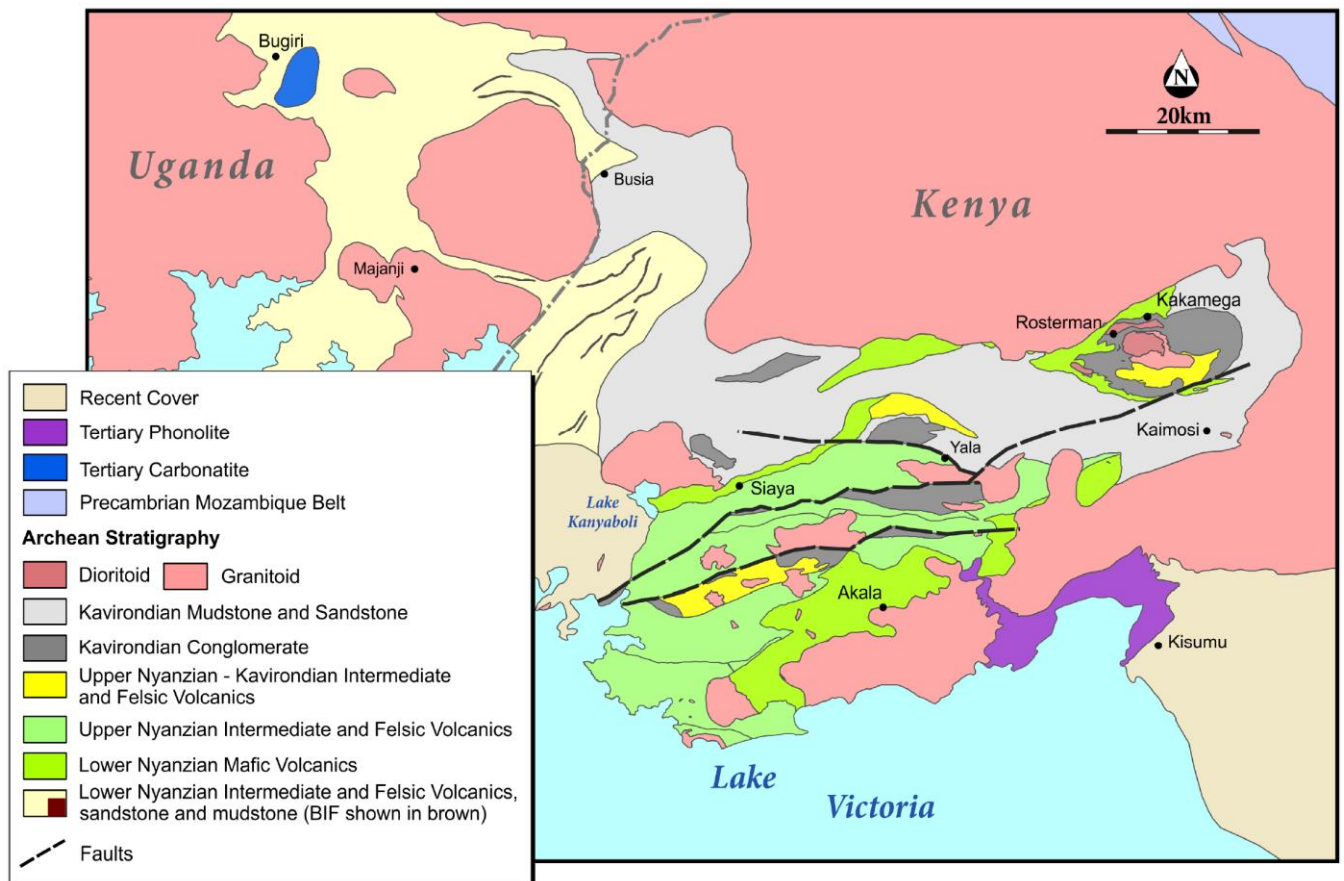
Figure 2.2: Geology of the Busia-Kakamega greenstone belt (Henckel et al., 2016).

Various studies in the belt over the years have distinguished three major stratigraphic units: Gneiss basement system, The Nyanzian (volcano- sedimentary) rocks and the sedimentary Kavirondian as shown in Table 2.1 (Westerhof et al., 2014). Acacia Mining have conducted detailed geological mapping and geological characterization in their exploration properties in the western Kenya segment of the belt (Figure 2.2). A detailed stratigraphy has been established through geochronological work and field relationships in the Kenyan section by Acacia mining.

Previous works in the Archaean terranes of western Kenya have generally concluded that the Nyanzian system, dated as early Precambrian, comprises mafic volcanic units such as metabasalts and pillow basalts, often sheared and chloritized (Ogola, 1987; Opiyo-Akech, 1988, 1991; Ichang'i, 1990, 1993; Ichang'i and Maclean 1991; Ngecu and Gaciri, 1995). These works have also identified the occurrence of felsic and intermediate volcanics such as rhyolites, dacites, andesites as well as their volcaniclastic equivalents (Dindi and Maneno, 2016). The sedimentary rocks of the Nyanzian system include shales, graywackes, conglomerates and banded ironstones.

The Lower Nyanzian clastic volcanic units, Banded Iron Formations (BIF) and various mafic volcanic units underly a sequence of ultramafic-mafic volcanics to felsic volcanics constituting the Upper Nyanzian units (Figure 2.3). Kavirondian conglomerates (polymictic) and sediments unconformably overlie the Nyanzian rocks (Henckel et al., 2016).

Table 2.1: Geological divisions of the Tanzania craton (adapted from Westerhof et al., 2014).

Pinna et al. (1996, 2000, 2004a, 2004b; Schlüter (1997)		BRGM et al. (2004)
Kisii System (2.53 Ga)		
Western Granitic Complex (2.56–2.58 Ga)		Basement Complex, Western Gneissic Terrane
Lake Victoria Terrane	'Younger Granites'(~2.5 Ga)	
(~2.9–2.5 Ga)	Kavirondian System (2.68 Ga)	Kavirondian Supergroup (~2.75–2.50 Ga)
	syn-to post-Nyanzian granitoids	
	Nyanzian System (~2.75 Ga)	Nyanzian Supergroup (~2.9–2.7 Ga)
	pre-Nyanzian basement (e.g. 'Older granitoids', ~3.1 Ga)	
Mtera Terrane (>2.7 Ga)		Isanga-Mtera Terrane (~3.0–2.85 Ga)
Dodoma Terrane (2.9 Ga)		Dodoman Terrane (~2.93–2.50 Ga)
Southern Basement Terrane (>3.2 Ga)		

New stratigraphic and structural framework as summarized by Sharp et al. (2016) indicates that the Busia Kakamega belt comprises a northeastward facing system of volcanics and sedimentary units intruded by granitoids. These units are grouped as follows;

- Samia Hills Group- pre-2.75 Ga.
- Ndori group-2.7 – 2.67 Ga.
- Yala group- 2.67-2.66 Ga.
- Kavirondo group-2.66 Ga.

The volcanics and intrusives are mostly komatiitic, tholeiitic, calcalkaline and high potassium adakitic in composition. The adakites of the Yala group intercalate with sandstone and conglomerates previously included in the Kavirondo group. The komatiitic suite hosted by the Ndori Group hosts the komatiitic units comprising of Mg-rich basalts and ultramafic volcanic rocks (Sharp et al., 2016).

The granitoids are classified into two groups:

- Pre- Kavirondian calcic syn-volcanic granitoids.
- Post-Kavirondian K-rich granitoids (2650 Ma).

Thrusted and folded sections of the stratigraphic units are commonly separated by Faults. Folding on a regional scale is suspected towards the Uganda border (Sharp et al., 2016). Granitic intrusions are extensive throughout greenstone belt.

Throughout the Greenstone Belt most of the rocks show little evidence of strain particularly at the outcrop scale. Except in the minor occurrences of mafic volcanic meta-tectonites, which were to some extent intruded by the Assembo granitoid (2670 Ma), Kavirondo group rocks appear to be locally folded with evident steep cleavage in some outcrops. The evidence of this younger cleavage points towards there being no less than two generation sets of structures in the belt. East-North-East faults have been inferred across the belt from several lines of evidence. These faults are naturally discordant, most likely representative of younger deformation. The major structural orientation of rocks in the central part of the belt is NE (Sharp et al., 2016).

Like most parts of the Lake Victoria terrane, mineralized deposits predominantly comprise of shear zone hosted quartz veins and extensional fractures in the Nyanzian host lithologies. Some deposits are hosted in folded banded iron-formation. Various mineralization styles occur in the LVG, and thus indicate the existence of a broad spectrum of host lithologies and mineralized structures.

The age of mineralization in this belt and LVG is still a matter of large debate. The belt is consistent with other known greenstone-hosted orogenic gold deposit models (Groves et al.,1998; Hagemann and Cassidy, 2000). Emplacement of the abundant late to post orogenic granites may have major faults and shear zones coincidental with the linear trends of deposit distributions (Sharp et al., 2016).
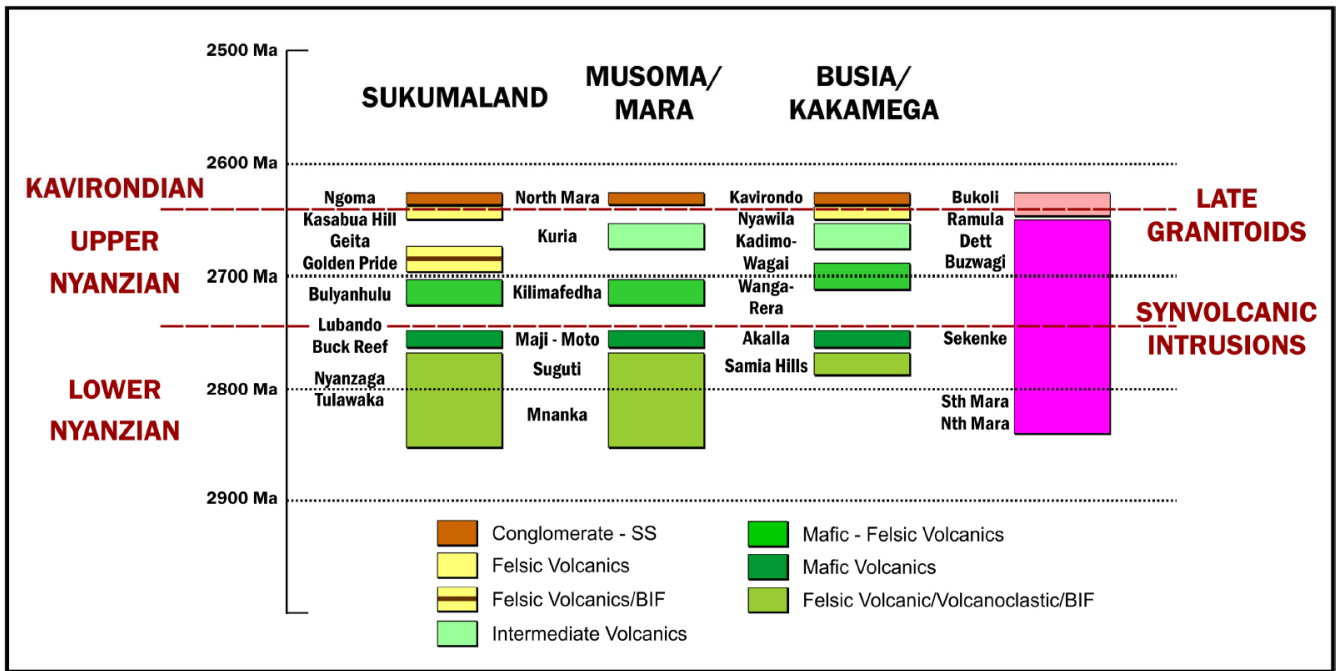
Figure 2.3: Stratigraphic column of the LVG (Henckel et al., 2016).

2.2 REGIONAL GEOLOGY OF BUSIA GOLD DISTRICT
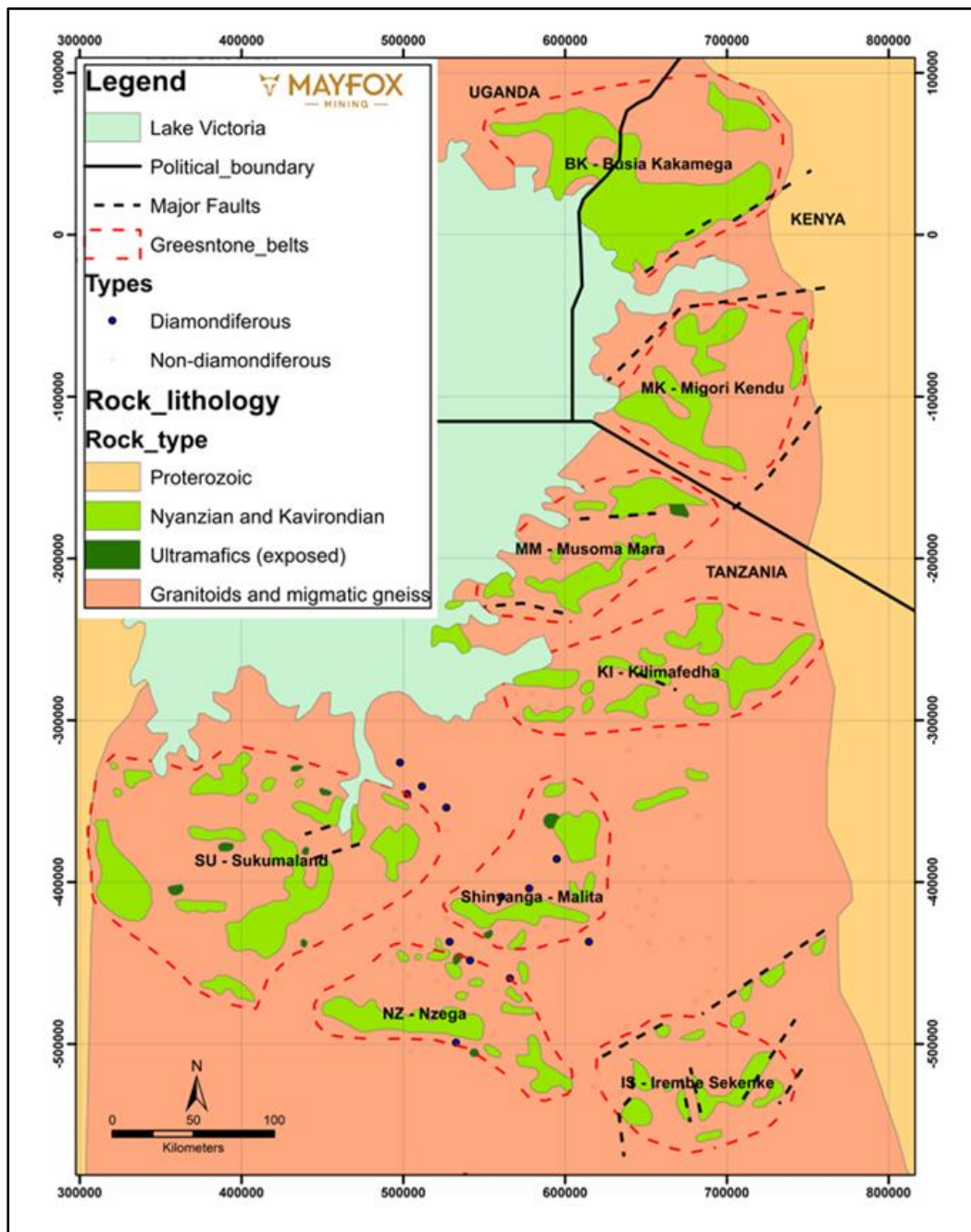
Figure 2.4: The Archaean- greenstone belts in the Tanzanian craton. (Mayfox Mining exploration report, 2018).

The Busia gold district represents a significant part of the extension of the Archaean Tanzania Craton into south-eastern Uganda as shown in Figure 2.4.

The geology of the Busia Gold District of S.E. Uganda is represented mainly by the Kavirondian and the Nyanzian groups or supergroups - 2.7–2.5Ga (Nyakecho and Hagemann, 2014), pre-and post-tectonic granitoids later intruded these units. Metasedimentary sequences

related to the Paleoproterozoic Rwenzori belt and the volcanic rocks of the East African Rift appear to border the Busia terrane to the south west and north east respectively. The GTK consortium have indicated that the terrane in southeastern Uganda is comprised of Nyanzian mafic metavolcanics, underlying felsic volcanics and metasediments of the Kavirondian system in addition to syn - post Nyanzian Granites.

Nyanzian rocks include mainly, mafic metavolcanics and minor intermediate to felsic metavolcanic and metasediments. Westerhof et al. (2014) have subdivided the Nyanzian in SE Uganda into two groups:

1. The lower "Bulamba" group, dominated by mafic metavolcanic rocks, and minor felsic and intermediate metavolcanics units. Felsic to intermediate metavolcanic segments occur as ridges and include rhyolites and metatuffs.
2. The Top/ Upper "Sitambogo" Group- it's made up of sedimentary units e.g. cherty quartzites, shale, black shale and BIF. The cherty quartzites occur as cryptocrystalline to fine-grained rocks visible layering in most outcrops.

The Kavirondian rocks that occur around the border with Kenya have been associated with Samia series rocks (Davies, 1956). The rocks include fragments of the Bulugwe series (Nyanzian). The Kavirondian units of SE Uganda are subdivided into two formations (Westerhof et al., 2014);

1. Malaba river formation

This is a sequence of psammitic metasediments overlying Nyanzian metavolcanics in Western Kenya (Westerhof et al., 2014). This succession is comprised of sandstones, greywackes, polymictic conglomerates, shales and mudstones.

2. Busiro formation

Consists of felsic metavolcanic rocks some of which are exposed to the North of Iganga town. The rocks are accompanied by leucogranite dykes with common fragments of pyroclastics in the granites. The felsic metavolcanics (pyroclastics) vary in grain size from medium to fine grained, and they can be massive and weakly.

Most granitoids of the goldfields of the Lake Victoria greenstone belts have been classified as either post-Nyanzian or post-Kavirondian. This includes Masaba biotite granite, the Iganga

granite suite and the three granite plutons; Lunyo, Namagenge granodiorite and the Kayango granite (Westerhof et al., 2014).

The Busia gold district rocks are said to have undergone relatively late northeast- southwest trending movement on steep faults. Metavolcanics are generally NE–SW trending with steep dips (Nyakecho and Hagemann, 2014). According to Old (1968) and Tanner (1973) the Nyanzian rocks have been metamorphosed to greenschist grades, exhibiting regional development of biotite and chlorite. Most common mineral assemblages are indicative of regional to greenschist facies metamorphism.

The gold mineralization is in quartz veins hosted in mafic metavolcanic units, and in Banded quartzites and iron formations (Mroz et al., 1991). According to Harris (1961) most lode- gold deposits are epigenetic in nature and are hosted by mafic, carbonate altered metavolcanics, while others are structure controlled like in the case of shear-zone hosted mineralization.

Figure 2.5 shows localities in Busia, known for small scale gold mining. About 10 kilometers north of the Tira workings, in Amonikakinei, locals extract mineralized veins from open pits with numerous vein bands, extending up to 1km and approximately 6–7 km in strikes (Nyakecho and Hagemann, 2014). Isolated veins can be about 0.4m wide and occur in weathered dolerites and metasedimentary units. Artisanal workings have been opened up in the areas surrounding Tira Mine and Makina. According to Mbonimpa et al. (2007) the two-principal gold mineralization styles in Busia are: Gold in quartz veins and BIF hosted gold deposits. Quartz vein mineralization is associated with pyrite, galena, magnetite, pyrrhotite, chalcopyrite, ilmenite and covellite. The basaltic country rocks are rich in secondary calcite (Mbonimpa et al., 2007).
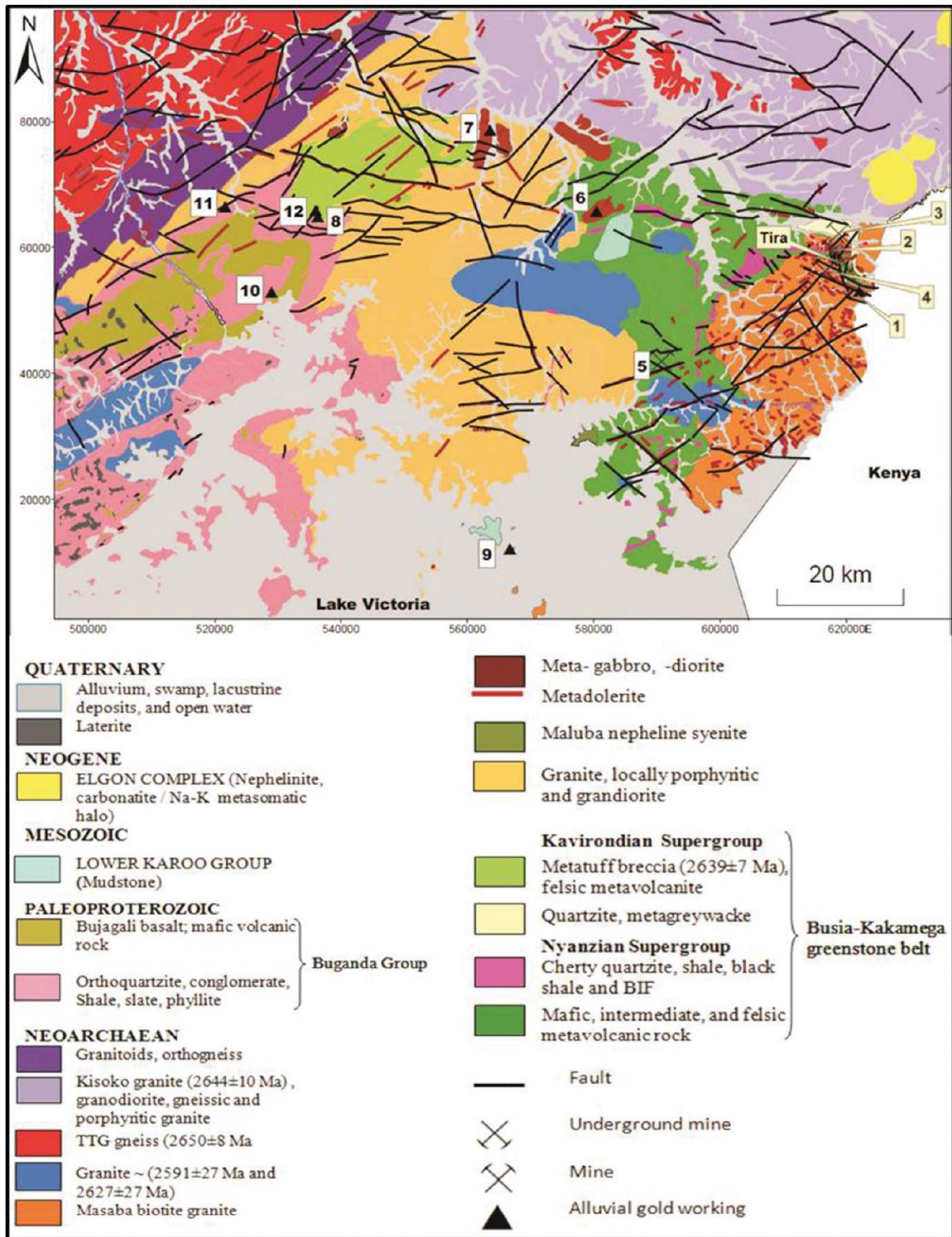
Figure 2.5: Geology and mineralisation of the Busia district (adapted from Nyakecho and Hagemann, 2014). 1. Osapiri; 2. Amonikakinei; 3. Makina; 4. Busia; 5. Bude-Kitoja; 6. Bukiriri; 7. Butamakita; 8. Bulomba valley; 9. Kaza Island; 10. Mwiri-Walube valley; 11. Kagoma ridge; 12. Nakatama valley.

The Tira mine formation is hosted in a suite comprised of metasediments, metabasalts and metadolerites (Figure 2.6). The metasedimentary assemblages are represented by metashales, phyllites, sandstones and quartzite (Nyakecho and Hagemann, 2014). The granite- dolerite contact strikes in the NW–SE direction to NNW–SSE direction. Mineralization control is mainly credited to the NW and NS shear zones. These subvertical ductile shear/ fault zones are associated with massive quartz lodes. The shear zone also contains small mineralized veinlets at various local scales. The main mineralized zone contains fractured, smoky to white, crystalline quartz veins and in some zones, quartz-carbonate veining. The ore minerals include pyrite, hematite, chalcopyrite and gold. The wall rocks in the mineralized zone are fine grained and foliated dolerites, basalts and gabbros exhibiting significant hydrothermal alteration (chloritization and carbonatization).
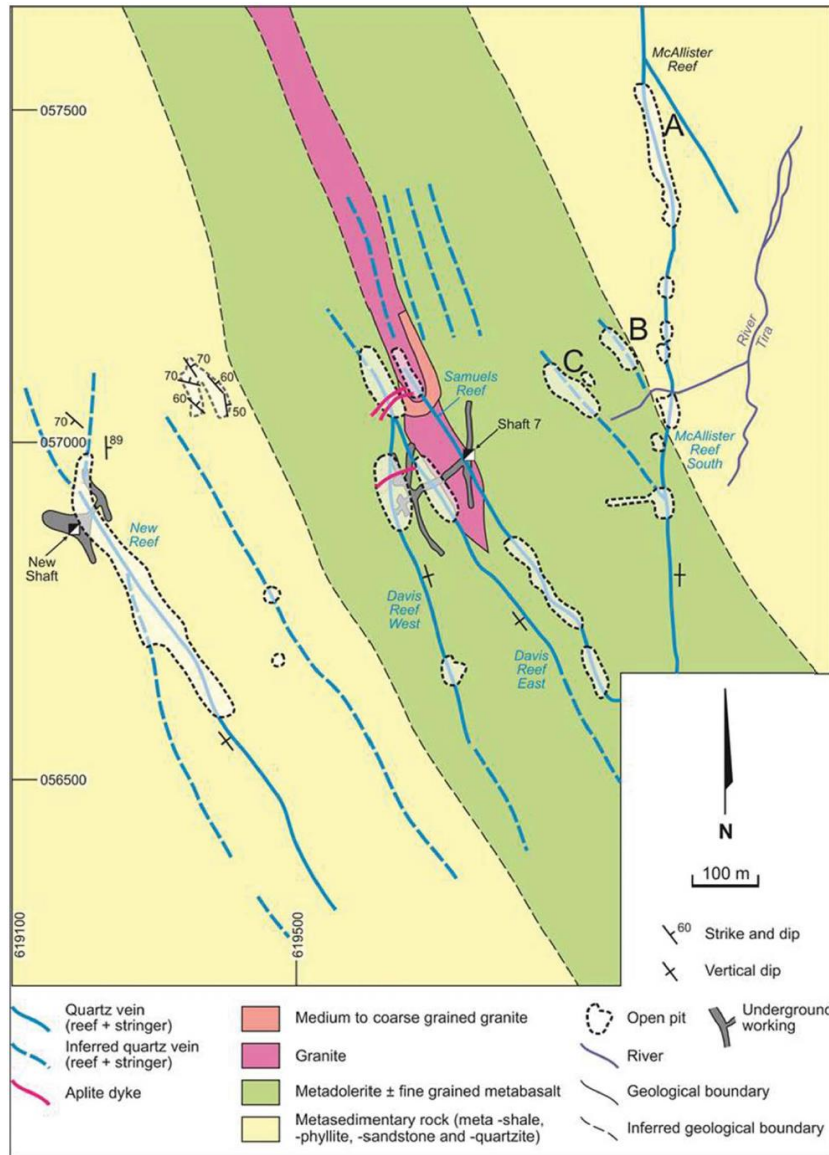
Figure 2.6: Geology of the Tira mine. Nyakecho and Hagemann (2014). A= Main pit; B= Eastern pit; C= Western pit.

2.3 GEOLOGY OF THE MAKINA PROSPECT

Prospect-scale mapping was carried out by Mayfox Mining which resulted in the identification of some important lithologic units that had previously not been reported by earlier workers (Figure 2.7). Generally, the rock types encountered to the north of the prospect include both massive and banded iron formations. Massive and banded chert, quartzite, granodiorite intrusions, mafic volcanics, and clastic mafic volcanics. The BIF unit which plays a major role as a dependable marker horizon has a variable magnetite enrichment. Figure 2.8 shows a BIF outcrop in Makina with clear magnetite bands. Both the BIF and chert generally have an east-

west trend, truncated to the east along strike by north-south trending regional fault structures. At this location, these chemical sediments appear to display dextral en-echelon left step faulting that extends into the lower Nyanzian group. Further, folding and thrusting observed on a banded chert outcrop in this area elucidates the possibility of even more structural complexities. The clastic mafic unit mapped to the south of soil line 3500E forms an intercalation with banded chert and BIF. In the southern area of the license, a dyke swarm of mafic-felsic compositional variation possibly explains the localized spatial existence of sheared quartz-feldsparthic intrusions, magnetic dolerites, and intermediate intrusions. Mafic volcanics are also infrequently encountered. The mapping exercise successfully demonstrated that previous regional geology studies may have heavily relied on airborne geophysics to delineate geological units, hence the discrepancies between observed and inferred geology is common (Figure 2.7). In some segments however, conformity between observed and inferred geology is evident. Rock exposure in the project area is quite limited, especially in the zones presumed to be mafic volcanic zones. Some banded Iron Formation outcrops have been mapped recently (Figure 2.8) and appear to have magnetite bands in narrow cherty bands. This thin Banded Iron Formation layer occurs within a zone of mafic volcanics. The quartzites and their associated banded sediments to the north form distinct ridges and are thus most easily accessible (Figure 2.9).

The main alteration types that have been observed in the area include, pervasive carbonate alteration and propylitic (chloritization) in some of the mafic volcanic rocks. Sericitization is not commonly encountered except in some segments of the Tira deposits. Kaolinization is evident mostly in exposed walls and mining pits giving an indication of the proximal association of the alteration type to gold mineralization. Historically, similar evidences were reported in pits and shafts of the Tira mining area.
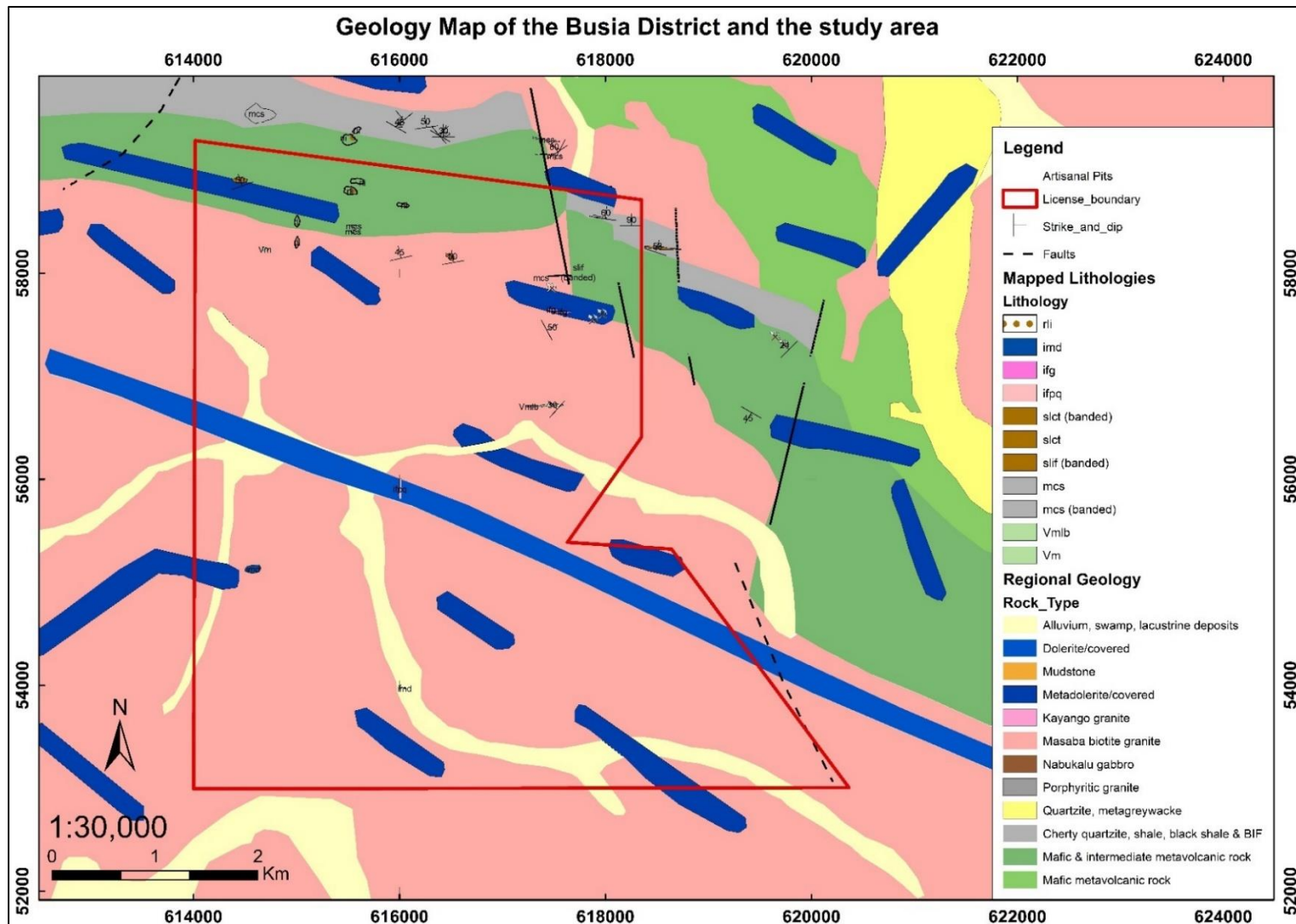
Figure 2.7: Busia geological map with both regional geology and outcrops mapped by Mayfox team (Modified from, Westerhof et al, 2014). Lithology codes are as adopted by Mayfox mining and have been described in the list of abbreviations and acronyms.

Figure 2.8: Outcrop of Banded cherty iron formation striking almost west-south-west.

Figure 2.9: Deformed outcrop of banded quartzite (Facing North). Evidence of folding and faulting indicating the significant deformation episodes.

2.4 EXPLORATION HISTORY

The Uganda Geological Survey discovered Gold in Busia in 1932. Initial mining works targeting alluvial deposits continued between the years 1932-1936. Exploration works after 1936 progressed all the way until 1939 which led to the discovery at Tira. Artisanal and small-scale mining have been ongoing ever since. Operations in the Tira mine have been on and off over the years as it changed ownership between different operators.

BRGM/DGSM (1990-1991); Mroz et al. (1991) carried out systematic exploration over an area of 1500 km^2. This was mainly a stream sediment geochemical survey with a grid soil sampling survey spaced at 1000m line spacing x 250m sample spacing. Mroz et al. (1991), recommend further detailed investigations in most parts of the Busia District.

In 1994, Roraima Mining Company (RMC) employed geochemical soil sampling and geophysical surveys (IP, resistivity, and magnetics) and geological mapping in their Busia license areas. The surveys concluded outlined a geochemical gold anomaly of up to 2.6Km long with a width of 50m.

Mbonimpa (2005) conducted an analysis on the potential of the gold mineralization in Busia using rock, soils and stream sediment geochemical samples of the larger Busia District. He suggests in his analysis that apart from the Tira deposit, surrounding deposits in Osapiri, Bukade and Makina were equally highly prospective. Mbonimpa et al. (2007) indicate that gold in soil anomalies in the Tira area were as high as 4.8ppm and Osapiri at 2.8 ppm, with the best values in the Bukade-Makina segment being 0.6 ppm. Mbonimpa (2005) also posits that the possible source of the Tira anomaly could be auriferous quartz veins whereas the other two anomalies are largely associated with Banded Iron formations, where the gold mineralization is possibly disseminated.

Lead (Pb) correlates positively with gold in all types of geochemical samples, hence a more reliable pathfinder element for gold. Cu, Ag and Zn could also be used as indicators for gold mineralization (Mbonimpa et al., 2007). It is further suggested that future analysis be conducted to establish the association of the common pyrite mineralization with the quartz veins, particularly in the metabasalts zones.

The Department for geological survey in Uganda together with the Finnish Geological survey conducted a nationwide geological mapping as a follow up to the airborne geophysical survey and they recommended Busia as one of the regions requiring advanced investigations to

establish the economic potential of the gold mineralization. The findings of the surveys have been recorded in the Geological Survey of Finland Special Report Number 55, 2014 (Westerhof et al., 2014).

Mayfox mining company has embarked on a detailed exploration program that encompasses geological mapping and geochemical sampling in Makina. Over 1000 soil samples have since been collected in a systematic sampling program. Mineralized rock samples were also obtained from the mapping exercise.

Interpretation of assay data obtained from the geochemical soil sampling program in Makina identified two significantly anomalous gold trends that appear to have a strong correlation with regional and local structures. The major anomaly trends interpreted are oriented East- west and another North- South. The North-South anomaly appears to be constrained within a structural setting, where north-south oriented faults intersect west North West – east south east structures.

Anomalous zones appear to be associated with contacts of major lithological units observed, such as, Nyanzian banded Iron formations (BIF) and Nyanzian metavolcanics contacts, and the interpreted Nyanzian metavolcanics and metasediments contacts.

2.4.1 Summary of recent exploration findings.

- *Preliminary analysis of Airborne geophysics and Regional geological data*

Airborne magnetics and radiometric data were acquired for the exploration in Busia. The set of data acquired from the Department of Geological survey also included updated geological maps of the block as had previously been mapped by the GTK consortium and the DGSM. Preliminary interpretations revealed relationships in the geology of the area and both the radiometric and magnetics signatures. Structural associations and lineaments were extracted and related with the mapped lithological units to establish potential trends and occurrence of gold mineralization.

- *Fact mapping of geology and Artisanal workings (Mineral occurrences)*

Interpretation of Airborne geophysical data and the regional geological maps informed reconnaissance survey and a ground truthing programme to identify main features and rock units considered critical for gold occurrence in the area. During mapping, several grab samples were collected and assayed for gold and other elements. Artisanal Mining sites were also

mapped out for the purpose of understanding their distribution in the area possible identification of trends that enrich the understanding of the mineralization styles in the area. Figure 2.10 is a photograph taken at one of the artisanal mining sites in Makina.

Figure 2.10: Artisanal mining site in Makina. (Note thickness of the weathered overburden encountered in most parts of the prospect).

- *Geochemical soil sampling*

The geochemical sampling was conducted in three phases with the sampling grids cutting across(N/S) the potentially mineralized zones from the inferred granite- volcanics contact in the south, to the edge of the metasediment in the north the sampling grids and plotted result as shown in Figure 2.11. From the geochemical soil sampling program in Makina two significantly anomalous gold trends that appear to have a strong correlation with regional and local structures were inferred. The major gold in soil anomaly trends interpreted are oriented East- west and another North- South. The North-South anomaly appears to be constrained within a structural setting where north-south oriented faults intersect West North West – East South East structures. There is also evidence of thrust faulting in these zones and the mineralization also appears to resemble that of the Tira deposit.

Anomalous zones appear to correspond with contacts of major lithological units observed, such as, Nyanzian banded Iron formations (BIF) and Nyanzian metavolcanics contacts, and the interpreted Nyanzian metavolcanics and metasediments contacts (Figure 2.11).

Recommendations were made based on the conviction that the soil and rock anomalies coupled with the improved geological understanding of the area were strong enough basis to warrant further exploration work. The proposed follow up exploration activities were as listed;

- ➤ Ground magnetic survey
- ➤ Gradient Induced polarization and Resistivity survey
- ➤ Pole- dipole IP/Resistivity survey (dependent upon the results of the gradient IP/Res survey)
- ➤ Anomaly testing/ Test drill holes.

This project focusses on the activities carried out during the ground magnetic survey and the Gradient IP/Resistivity survey and the subsequent results as well as implications on the future of the exploration programme.
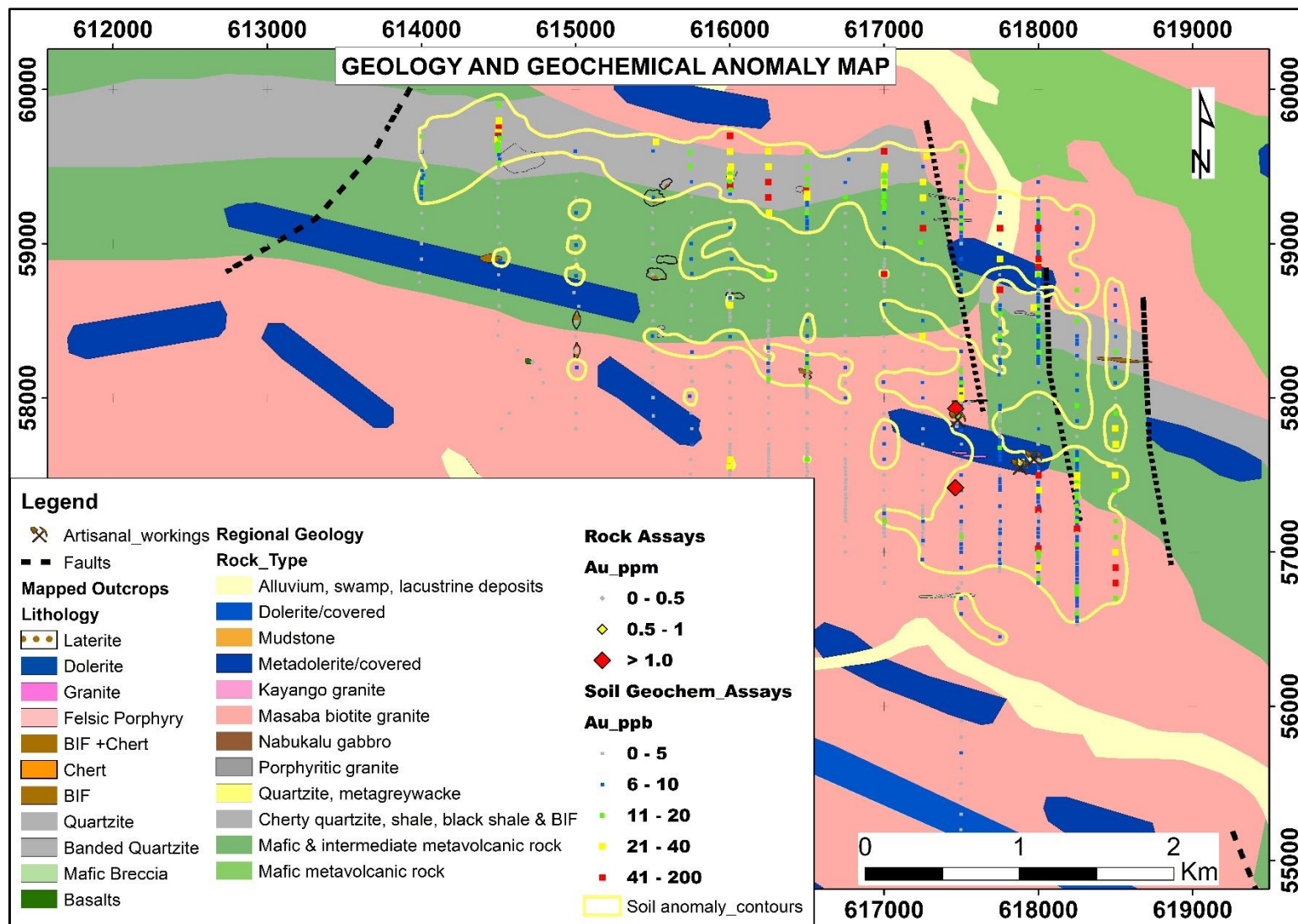
Figure 2.11: Soil geochemical results superimposed on the Makina Geological Map (Adapted from Aseto et al., 2018).

CHAPTER 3 MATERIALS AND METHODS

3.1 MATERIALS

The materials and resources used in the project from project planning to data acquisition and data processing were provided by Mayfox Mining Company. The data acquisition was carried with the help of company geologists and field technicians.

The field equipment used in the project were;

Gradient IP/Resistivity equipment

- Zonge GGT-3-time domain transmitter
- Honda GX240 Power generator
- Zonge VR1B voltage regulator
- Single core, multi-strand steel wires on reels
- Steel rods (used as current electrodes.
- Scintrex IPR-12-time domain receiver
- Non-polarizable porous pots (copper sulfate electrodes) as potential electrodes.
- Copper sulphate crystals.
- Motorola radio calls (walkie talkies)
- Garmin GPSMap62 handheld GPS units.

Ground magnetic survey equipment

- Geometrics G- 857 Proton Precession Magnetometer
- Scintrex Envi- magnetometer (Base station magnetometer).
- Scintrex- Envi-Cs - Cesium sensor magnetometer
- Garmin GPSMap62 handheld units.

Data processing and Map production software.

- Geosoft oasis montaj version 8.5.
- ArcGis ver. 10.6
- RES2DINV

Historical exploration data was acquired from Uganda's Geological survey and Mines Department through Mayfox Mining Company.

3.2 BASIC CONCEPTS OF GEOPHYSICAL METHODS IN GOLD EXPLORATION

Gold generally occurs in low grades in most deposits, therefore, getting direct signatures for gold is often difficult except in cases where individual shallow nuggets have been targeted by electromagnetic detectors (Doyle, 1990). Physical associations of gold and the host rocks or structures however, present geophysical characteristics that can be investigated. Some of these associations include the following:

- Magnetization
- Density
- Electric polarization
- Electrical conductivity
- Electrical resistivity

The common units investigated are BIFs, Magnetite bodies, sulphide bodies, altered and fractured zones, shear zones and faults that ore often associated with gold mineralization.

The most commonly applied geophysical techniques in gold exploration are the Magnetics, Radiometrics, Gravity, Electromagnetics, Induced Polarization and Resistivity methods. The selection appropriate method for an exploration programme is largely dependent on:

- The nature and characteristics of the deposits being probed and mineralization styles.
- Geological understanding of the area of interest and structural setting.
- Interpretation of previous exploration data.

It is important in any gold exploration program to develop an understanding of the deposit's geological model and its environment, and subsequently, identify the geophysical properties of the host rocks.

This research is focused on Magnetics, Induced Polarization and Resistivity methods.

3.2.1 Magnetic Methods

This is the most commonly applied method in the exploration for gold as well as most metal deposits. Magnetic surveys are done either as airborne or ground surveys. Aeromagnetic data is useful in early-stage mineral exploration as the aeromagnetic maps are used in generation of regional geological maps, and potential mineralization targets.

The magnetic technique is used to investigate subsurface geology with regard to signals in the magnetic field of the earth attributed to the magnetic character of different rocks (Kearey et al., 2002).

3.2.1.1 Rock Magnetism

Some minerals, such as magnetite produce easily detectable magnetic anomalies. Magnetization is either induced or remanent (Moon et al., 2006). When magma/lava cools, minerals start forming and subsequently, the magnetic minerals in the material become aligned to the extant magnetic field. After solidification, these minerals retain this magnetic orientation. In the case of sedimentary rocks, during the deposition of iron rich sedimentary minerals from the water column, they also become aligned with the ambient field. The magnetism remains intact unless the rock is heated above its Curie point (temperature where magnetic materials lose magnetization). On cooling below the Curie point, the rocks will record the later time field as the old magnetic field will be lost. It is, therefore, important to find out whether a rock's magnetism is primary or otherwise (Reeves, 2005). Generally, rock-forming minerals have very low magnetic susceptibility. Magnetic character in rocks is mostly due to the proportion of their magnetic minerals. The two groups of minerals that constitute such magnetic minerals are;

- Iron–titanium–oxide group – they contain magnetic minerals in the solid solution series- Magnetite [Fe_3O_4] to ulvöspinel [Fe_2TiO_4] (Kearey et. al., 2002).
- The iron–sulphide group (pyrrhotite) [FeS_{1+x}, $0 < x > 0.2$].

Magnetic anomalies are usually indicators of features such as faults, mafic intrusives, dykes, folded sills and lava flows, metamorphic rocks and magnetite bodies. Mafic igneous rocks are usually highly magnetic. Felsic igneous rocks usually are less magnetic than mafic rocks. In the case of metamorphic rocks, magnetic character depends on partial pressure of oxygen levels and metamorphism grades.

3.2.1.2 Magnetic Susceptibility

Refers to ability of materials to get magnetized on exposure to a magnetic field. Magnetization is influenced by composition and the concentration of the magnetizable elements in a particular material. Some magnetizable minerals include the ferromagnetic minerals - strongly magnetizable, paramagnetic minerals (moderate magnetization) minerals among others (Telford et al., 1990).

Magnetic susceptibility is largely the main physical parameter in magnetic surveying. Rocks with high amounts of ferri or ferro-magnetic minerals exhibit highest susceptibilities. Figures 3.1 and 3.2 illustrate the common susceptibility ranges of rocks.
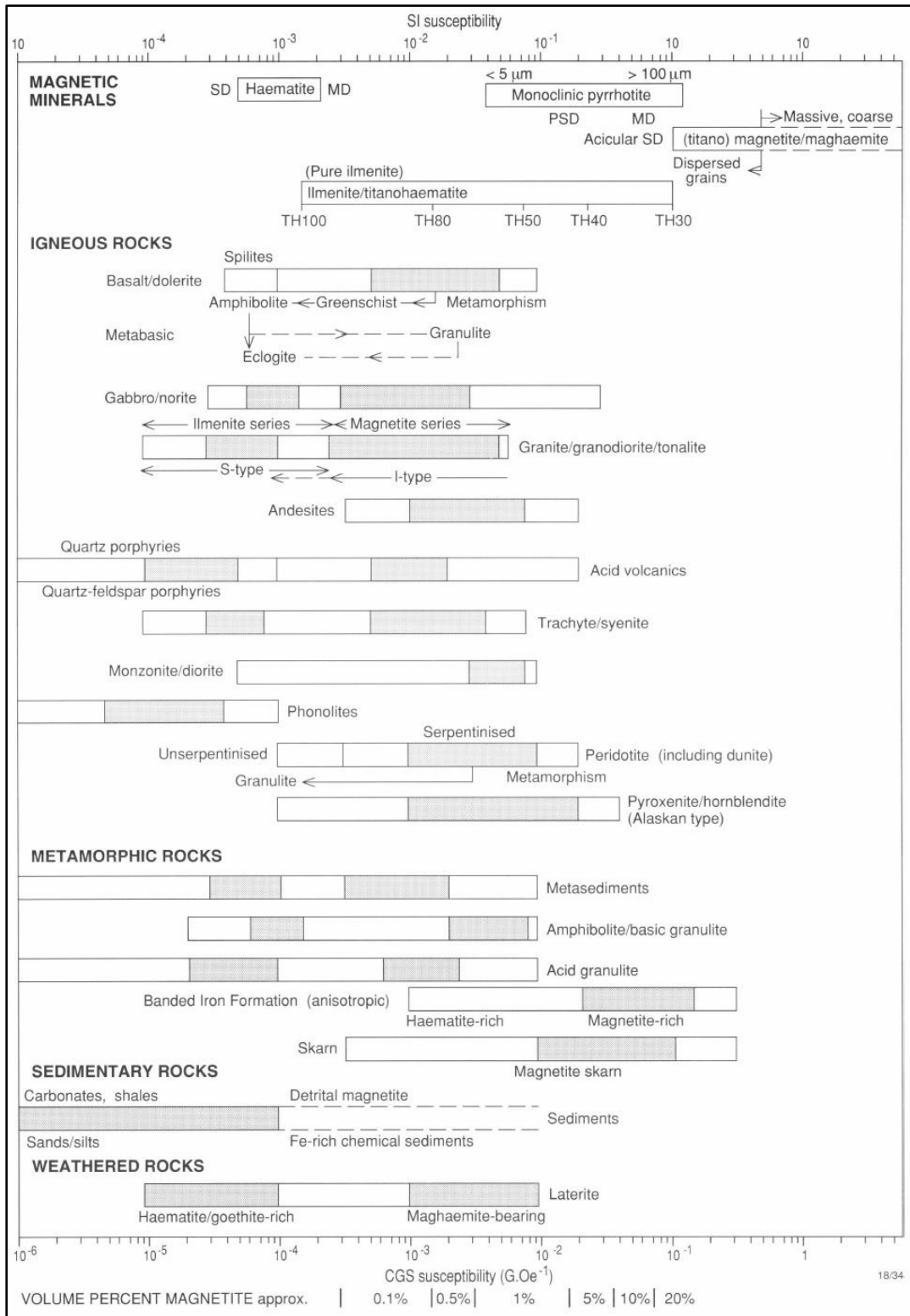
Figure 3.1: Common susceptibility ranges for rocks (Clark, 1997).
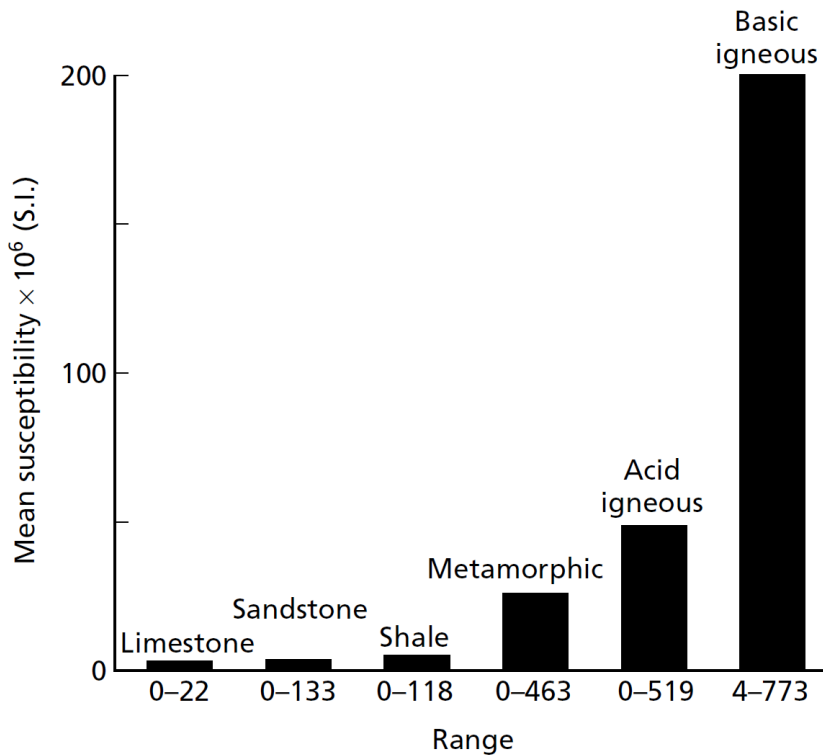
Figure 3.2: Magnetic susceptibility ranges of common rock types (Kearey et al., 2002).

3.2.2 The Earth's magnetic field

This field is said to resemble a magnetic dipole at the Earth's center, inclined at about 11 degrees to its own rotation axis (Moon et al., 2006). The dipole's magnetic moment can then be computed from the observed field. If the dipole field is removed from the observed field, the resultant (residual) field can thus be estimated by the effects of a second dipole. This process can be continued by fitting dipoles of ever decreasing moment until the observed geomagnetic field is simulated to any required degree of accuracy (Kearey et al., 2002).

The International Geomagnetic Reference Field (IGRF) is a formula that describes variations in magnitude and direction in space and time. This is the estimation of the regional field in adequately surveyed regions with great formulation control (Figure 3.3). There are also daily variations in the field strength, usually about 20– 60 nT in amplitude (Moon et al., 2006). They are usually low in the night time but begin to rise by dawn, with peaks at around mid-morning and declines fast to a low of about 1600hrs, and gradually rises to the overnight figure. Diurnal variation during survey is corrected using base station magnetometers readings stationed within the survey area and free from magnetic interference (Waswa, 2015).
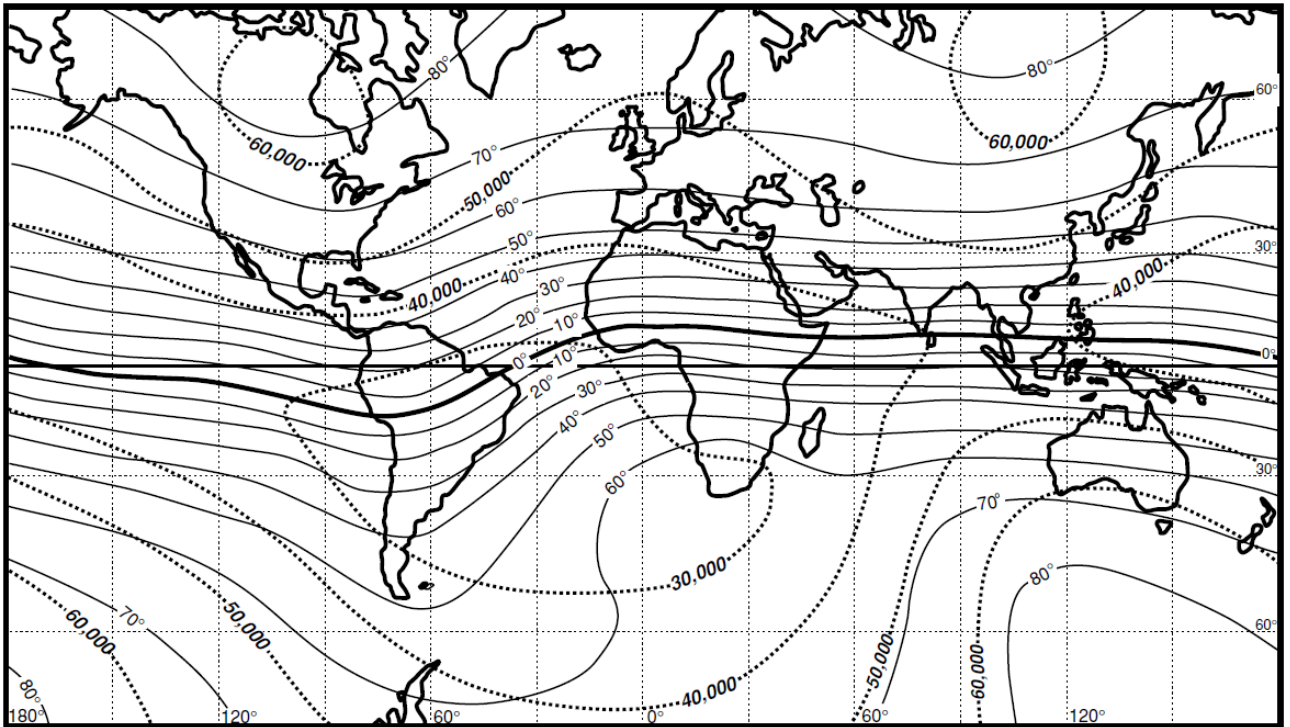
Figure 3.3: Image showing the magnetic field of the earth. Thick lines represent contours/ lines of constant dip. The dotted lines are zones of a constant total field strength (nanoteslas). Adapted from Moon et al. (2006).

3.2.3 Magnetic anomalies

The usual sources of magnetic anomalies are magnetite (Fe_3O_4), pyrrhotite, and maghemite. Hematite (Fe_2O_3) anomalies are rarely large enough to be detected by aeromagnetic surveys. Almost all local features on magnetic maps have a crustal origin. Variations in the magnetic field in sedimentary terranes are usually very small in amplitude, higher changes are common in areas of exposed basement rocks. Anomalies as high as 150,000 nT have been recorded (Moon et al., 2006), which is much higher than that of the Earth's normal field. Magnetic data is always crucial in qualitative interpretation of rock and structures since magnetite is considered a common accessory mineral in various rock types.

At different magnetic latitudes, bodies that have been magnetized produce different magnetic anomalies (Moon et al., 2006), and for interpretation purposes, the regional variations in dip are regarded as the most important compared to the regional variations or changes in the absolute magnitude.

The total magnetic flux is normally zero since all magnetic anomalies possess positive and negative parts. This applies also to sources magnetized at the magnetic poles, negative flux is however, usually broadly dispersed. Thus, magnetic field maps for regions proximal to the

poles can be easier to interpret as opposed to other regions. The reduction to pole (RTP) filter is commonly used to translate the maps of the low and mid-latitude into high latitude variants.

Various image processing techniques have been advanced to enhance features in Magnetic maps. Magnetization intensities are not always linked to occurrence of economically significant features. Other processing methods can be employed to focus on depth determination and causative bodies. Such methods include the Werner and Euler deconvolution. Horizontal gradient in airborne installations is measured using either the nose and tail or wingtip sensors (Moon et al., 2006).

3.2.4 Magnetic survey instruments

The standard instrument in use at the moment are the Optically pumped (Cesium Sensor Magnetometers). The Proton Precession Magnetometer is still in use although the Cesium Sensor ones are considered to be more sensitive. Both can used on an aircraft or in towed birds. Aircraft fields vary slightly, the variations in aircraft fields due to heading.

3.2.5 Induced Polarization

Induced polarization (IP) is an electrical phenomenon caused by transmission of electrical current into the ground. It is an out-of-phase voltage response in subsurface materials. Induced polarization refers to the electrical polarization in subsurface rocks, enhanced by metallic minerals and fluid filled pores. The IP effect is hence observed in units rich in metallic minerals. However, the relation between IP response and the amount of mineralization and/or polarizable material is quite complex. Therefore, the most important attribute of this method is the ability to detect present ores (Sumner, 1976). Geological units may also be differentiated by use of this method depending on content of metallic minerals (Gallas, 2015). Time-domain Induced Polarization measurements monitor the rate of voltage decay after turning off current transmission.

Chargeability (M) is the main property measured by IP surveys; Chargeability (M) is given by the area under the decay curve divided by the interval (t_1–t_2) normalized by the steady-state potential difference, ΔVc. Chargeability is therefore measured within a time interval immediately after switching off the current transmission. The area under the curve can then be determined by the equipment. Minerals have distinguishable chargeability values as shown in Figure 3.4. Pyrite for example has a chargeability of = 13.4ms/s while magnetite has a chargeability of 2.2ms/s (Kearey et al., 2002).

On switching primary current off, the resultant voltage's decay becomes detectable, and thus the measurement of the location and magnitude of a chargeable body can be determined. The Induced Polarization technique is the most reliable method capable for directly detecting concealed disseminated sulphide bodies (Marjoribanks, 2010).

IP measurements are done either in time domain or in frequency domain. In time-domain, IP effect can be determined from the residual voltage decay after current transmission has been put off. The SI units for chargeability are in millivolts per volt (mV/V) or milliseconds. (Loke, 2015).
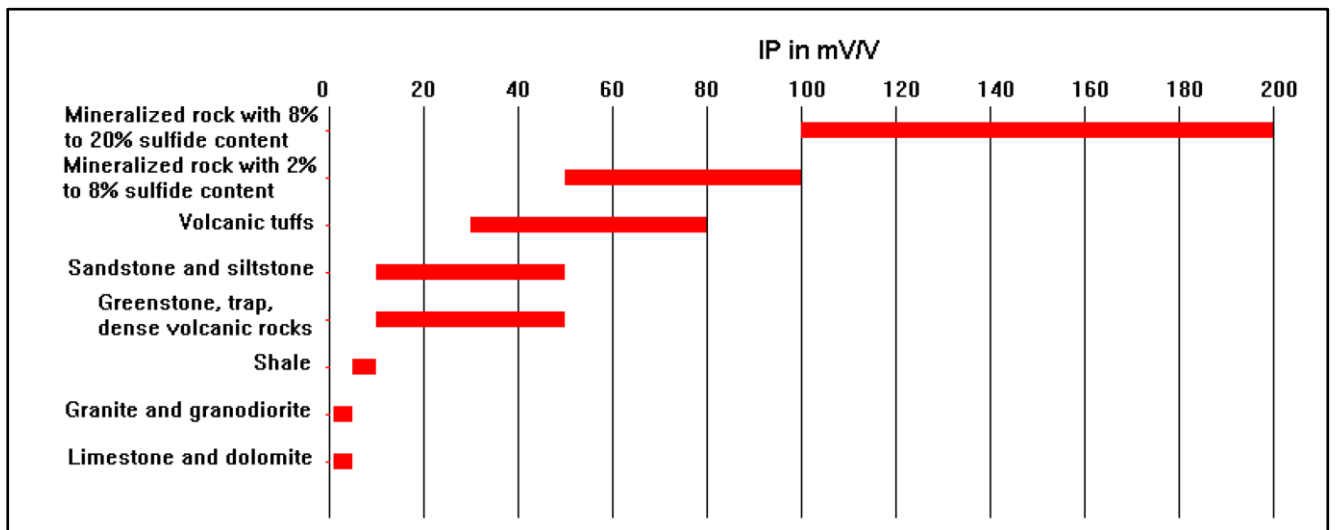
Figure 3.4: IP values for some common rocks and minerals (adapted from Loke, 2015).

The IP method has been utilized consistently in mineral exploration programs especially where metal sulphides are among the ore minerals of interest.

3.2.6 Resistivity

This is among the oldest geophysical surveying techniques (Loke, 2015). These surveys aim to measure how resistivity is distributed in the subsurface materials through measurements done on the surface. True resistivity can then be estimated from the ground measurements. The ground resistivity is influenced by geological factors like the minerals present, fluid content, porosity and water saturation level. Electrical resistivity surveys have been applied in the field of hydrogeology, mining, engineering, environmental studies and hydrocarbon exploration (Loke, 2015).

The resistivity method is governed by Ohm's Law. Ohm's Law in vector form for current flow in a continuous medium is given by equation (3.1):

$$J = \sigma E \qquad\qquad\qquad\qquad\qquad\qquad\qquad\qquad\qquad (3.1)$$

Where J is the current density, σ is conductivity of the sounding medium, E is the Potential gradient (electric field at location).

Resistivities of rocks and minerals

Resistivity is the resistance between the opposite faces of a unit cube of that material. In the case of a conducting cylinder of resistance δR, length δL and cross-sectional area δA (See Figure 3.5), the resistivity therefore is; $\rho = \dfrac{\delta R \delta A}{\delta L}$ $\qquad\qquad\qquad\qquad (3.2)$
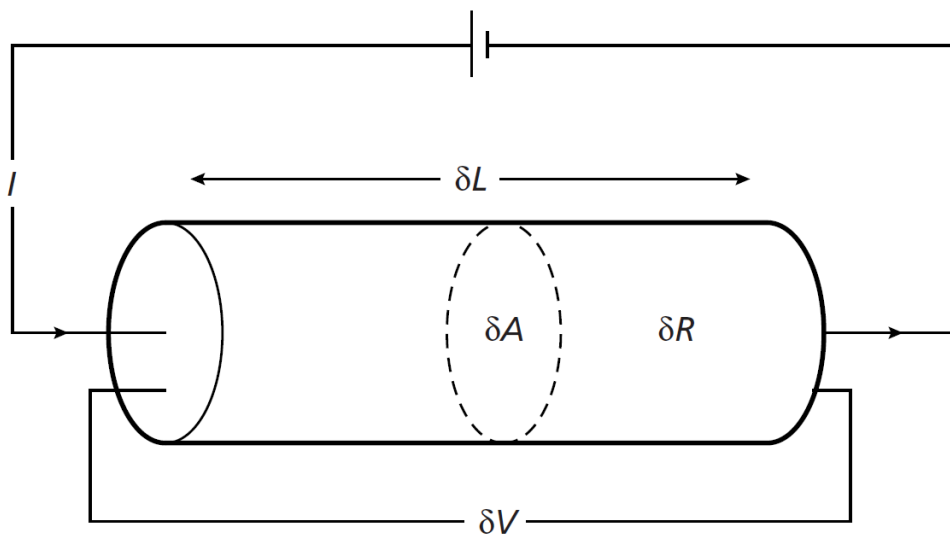
Figure 3.5: Parameters used in defining resistivity (from Kearey et al., 2002).

Resistivity is recorded in ohm-meter [ohm.m] and it is the reciprocal of conductivity, given in Siemens (S) per meter; $1Sm^{-1} = 1ohm^{-1}m^{-1}$. Some minerals like the native metals and graphite are mostly good conductors of electricity, while most minerals are insulators. When current passes through a mass of rock, it is usually through ion movement through pore water. Therefore, rocks are said to conduct electrical current through electrolytic processes and not electronic processes. Porosity therefore, is a major controller of resistivity in rocks. Resistivity tends to increase when porosity decreases. Some crystalline rocks may, however, conduct through cracks and fissures, especially where there is some intergranular porosity (Kearey et al., 2002).
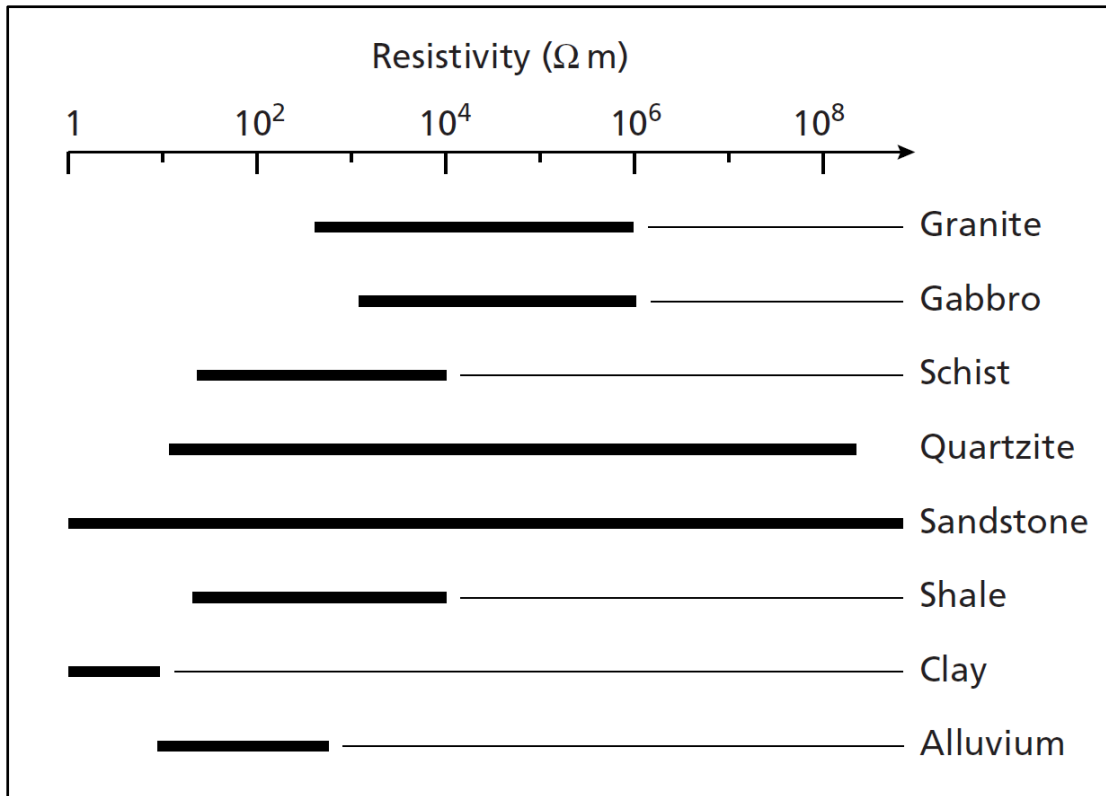
Figure 3.6: Resistivity values for common rock types (after Kearey et al., 2002).

Igneous rocks and metamorphic rocks are typified by high resistivity (Figure 3.6). Their resistivities depend largely on their fracture density, and subsequently, the percentage moisture filled fractures. This means that one rock type could have different resistivity values, depending on its moisture content. This characteristic is utilized in geotechnical surveys as well as groundwater surveys to identify subsurface fracture zones and weathering effects.

Resistivity values in sedimentary rocks are usually very low owing to their porous nature and moisture content. The resistivity values of rocks are also dependent on the salinity levels of the moisture in the rocks.

Unconsolidated sediments tend to have low resistivities compared to sedimentary rocks. Clay content in soil also tends to lower the resistivity of soils. Hence, clay soils are normally lower in resistivity value than sandy soils. The resistivities of several types of ores are also shown in Figure 3.7. Metal sulphides typically have low resistivity values. The resistivity values of certain ore bodies may differ from those of their constituting crystals. Most oxides do not have significantly low resistivity values, except for magnetite (Loke, 2015).
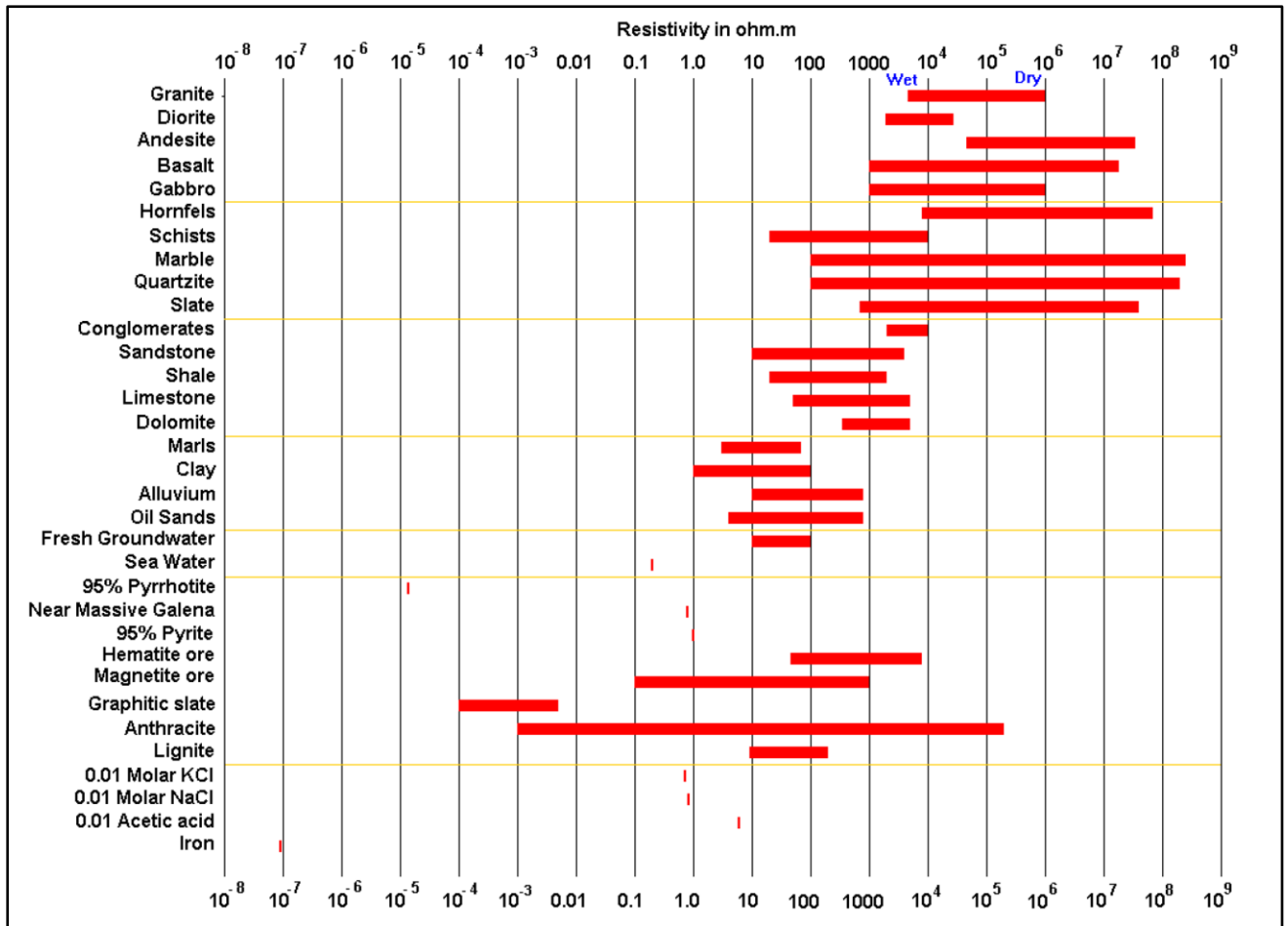
Figure 3.7: Resistivity of rocks, soils and minerals (Loke, 2015).

3.3 GEOPHYSICAL EXPLORATION/ SURVEY PLANNING

3.3.1 Overview

The planning phase of the ground geophysics was done based on interpretation of geological, geochemical and structural data obtained on the area. The structural interpretations and the soil geochemical anomaly trends from Mayfox Mining exploration were mostly applied in designing the survey grids.

Analysis of the soil geochemical anomalies presented two possible trends that the mineralization in Makina is believed to be oriented in. The first geochemical anomaly appears to be aligned with the almost N-S faults towards the east of the study area. This anomaly lies in a zone of significant fracturing and possible strike slip/ thrust faulting. The second anomaly appears to manipulate the Nyanzian lithologies, possibly along the lower contact of the narrow-Banded Iron Formation and the mafic volcanic unit.

The grids were designed in such a manner as to ensure the measurement lines cut across the strike of the anomalous trends and the anomaly being investigated. Thus, two sets of survey grids were established. The first set investigating the N/S anomaly was designed with east-west survey lines (East/west survey direction). The second set of survey lines were designed over the E/W anomaly (over the BIF). These Survey lines are in the N-S heading direction.

3.3.2 Survey specifications for Gradient IP/Resistivity

The survey was conducted at 900m current electrode spacing and a potential electrode spacing of 50m with survey line spacing of 200m. The survey coverage was 42-line kilometers in total. Figure 3.8 is a map showing the IP survey grid, with measurement points overlaid on contoured geochemical trends and regional faults.
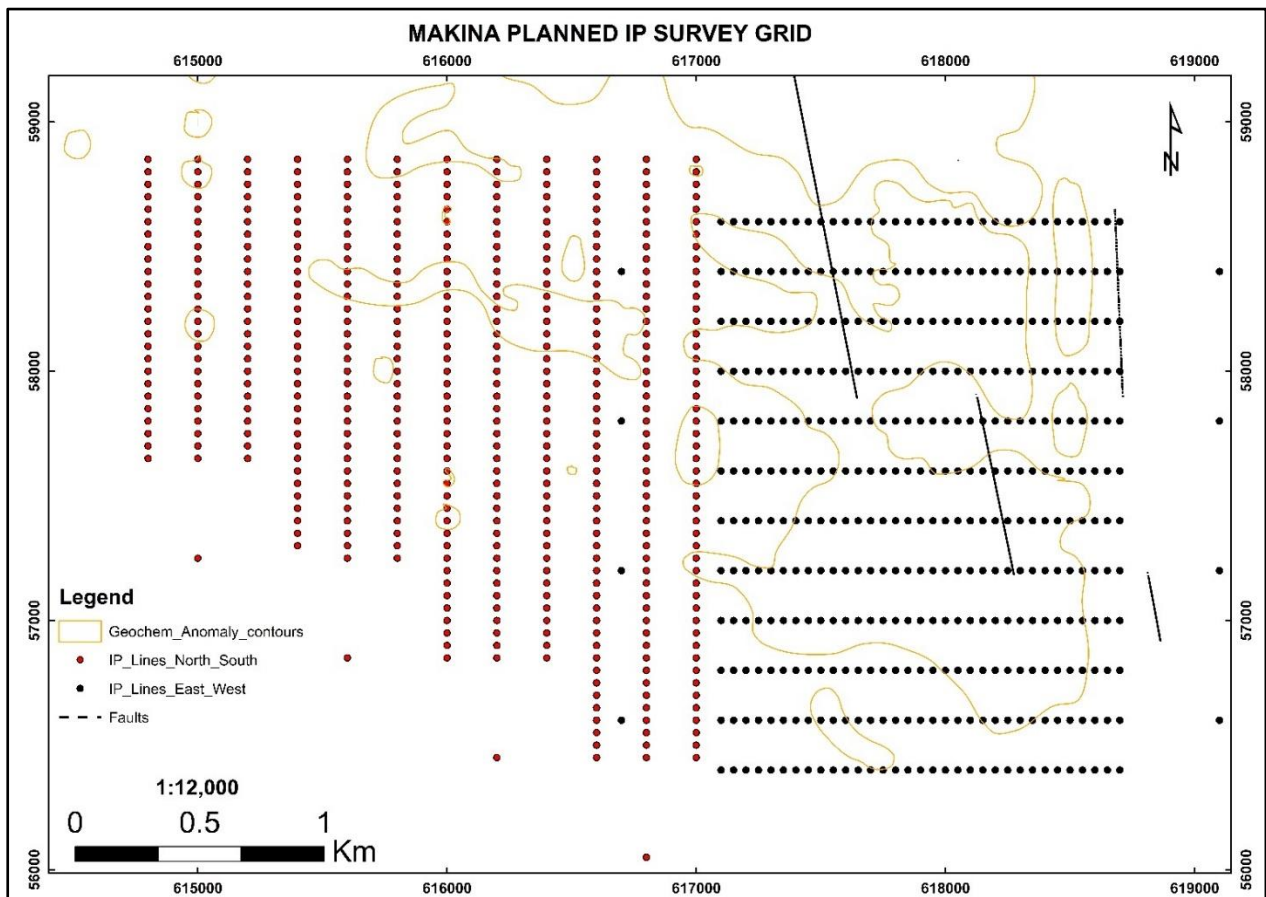
Figure 3.8: Map of Makina proposed IP/Resistivity grid.

3.3.3 Survey specifications for Ground Magnetics

A ground magnetics survey covering the same area at 100m line spacing and 10m spaced sample points. The total coverage of the ground magnetics survey was approximately 60-line Kilometers. Figure 3.9 shows the magnetic survey lines superimposed on soil anomaly contours and regional faults.
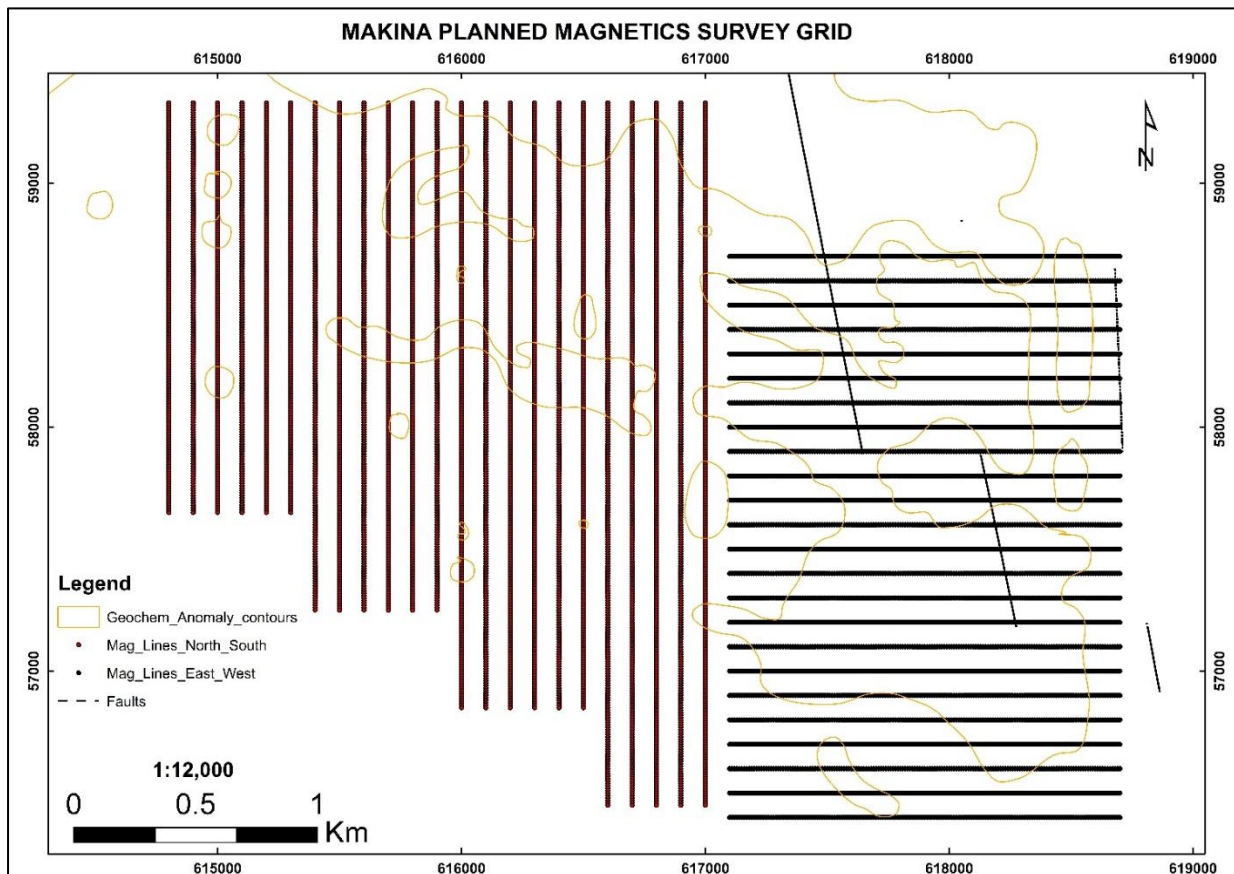
Figure 3.9: Map of Makina planned ground magnetics survey lines.

3.4 GRADIENT IP AND RESISTIVITY

3.4.1 Overview

Current pulses are injected into the ground via two current electrodes. Time pulses were set to a 2 seconds on-off sequence. The current electrodes are usually steel rods hammered into the ground normally after digging out top resistant material. The pits are ideally very shallow and just enough to ensure good conductivity. Salt water would then be poured into the pits just to improve the conductivity of the ground, at the contacts at least. Figure 3.10 shows the laying out of the measurement wire and Figure 3.11 shows the typical current electrode setup.

The Potential difference decay is measured by an IP receiver. A potential dipole constitutes two potential electrodes. The voltage decay measurements are taken during current transmission. The apparent resistivity is computed immediately, as a function of the measured voltage and the array coefficient. During the off time the receiver records the potential decay due to Induced Polarization and subsequently the ground chargeability is calculated. The chargeability is the ratio between the measured IP at a point during the off-time duration and initial on time voltage. The non-polarizable pots electrodes are used for the collection of the potential readings. The pots are normally filled by a saturated copper sulphate solution. The contact of the pots and the ground may require moistening, depending on the contact resistivity signatures sent to the receiver for the electrodes.

3.4.2 Data acquisition

The gradient array is designed to acquire measurements of the ground IP and resistivity at multiple points using one current line. According to Edwards (1977), the estimated depth of investigation (Z_e) is determined by the current electrode separation (L), whereby; $Z_e=0.191L$. In the case of this survey, L=900m, therefore, $Z_e=171.9m$.

The data collection operations were carried out using two field teams. One team stationed on the Current transmission line and the other on the Potential line or the measurement line.

Figure 3.10: Photo showing laying out of the measurement lines during the gradient survey.

Each set up had the current electrodes stationed at 900m apart, and connected to the Transmitter through steel wires. The Generator was used as the power source and the Transmitter had an operator in station to monitor the function as well as regulating the current being transmitted whenever necessary. The potential line was always laid on the middle third of the current line. The potential line had the potential electrodes stationed 50m apart. The potential electrodes were then connected to the IP receiver. The IP and resistivity measurements are recorded automatically.

Figure 3.11: Photograph of the current electrode set up.

The usual field procedures began with first laying out the current and potential lines and confirming coordinates for the measurement points and electrode locations. The current electrodes would be hammered in to the ground for good conductivity. A set of five electrodes wound together with a copper wire would be used. In case of poor current transmission or in resistant surfaces, salt water would be poured in the ground to improve the transmission. Figure 3.12 shows a laid out potential line with measurement electrodes in locations. Figure 3.13 shows the typical non polarizable electrode used collect potential measurements. Figure 3.14 illustrates the gradient array/ configuration set up as applied in this survey. After the setup was completed, the transmission would begin and the transmitter operate then communicates the status of the current transmission and the amount of current as indicated on the display. The communications in the field were always via radio/ walkie talkies. The measurement team would then proceed to take the readings from the IP receiver (Figure 3.15). Each current electrode setup was used to take measurements for three potential lines, that is, one along the current line and two on either side of the current line as shown. This process is then repeated for the entire day or shift. The coordinate system used for the survey was UTM, Zone 36N, Datum: WGS84. Figure 3.16 shows the Scintrex IPR-12 receiver that was used in the survey measurements. The typical current transmission set up used in the survey is illustrated in Figure

3.17, showing the connection from the power generator to a voltage regulator and to the Zonge GGT-3 transmitter.

Figure 3.12: Potential measurement line laid out during gradient measurements.

Figure 3.13: Potential electrode at a measurement point.
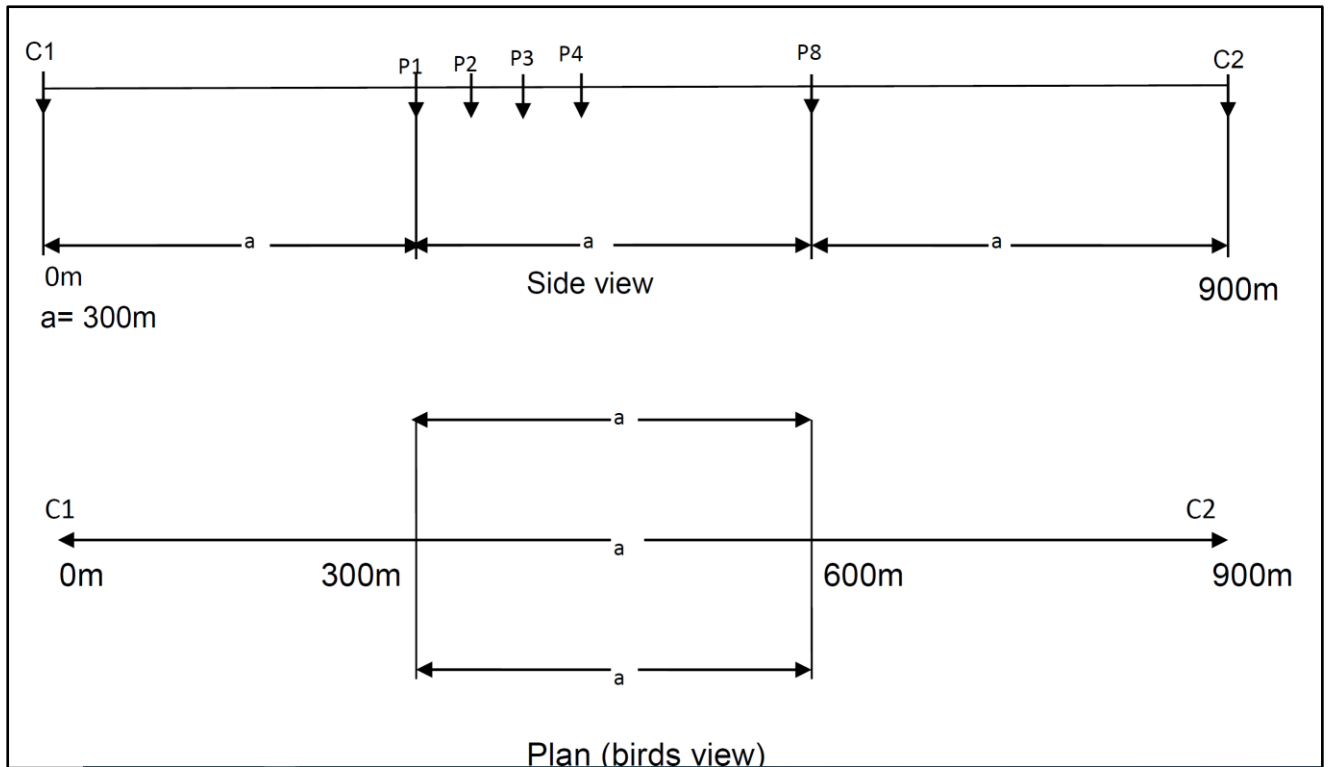
Figure 3.14: Typical measurement set up for gradient array IP/Resistivity survey. The potential dipole spacing used was 50m that is, distance between each of the potential electrodes (P1 - P2).

Figure 3.15: Measurements of gradient IP using the IPR-12 receiver.

3.4.3 Data processing

Quality control and data transfer

The IPR-12 receiver (see Figure 3.16) system contains quality check parameters that can be used to detect noise or bad data while taking measurements in the field. This ensures that the geophysicist discards data that is compromised and can continue taking more readings after ascertaining source of the interference. These quality check parameters are:

a) The Standard Deviation readings, which qualify the chargeability data. The recommended normal admissible readings are always below 1. Values of this parameter that appeared out of the ordinary would indicate an error.

b) The root mean square deviation checks the fit between the master curve and the measured decay curve. Readings with RMS values above 3 were not accepted, and, were remeasured.

Equipment quality assurance is also key to ensuring quality of the data. Maintenance and monitoring of the copper sulphate in the electrodes is important. Maintaining good quality of the connecters and wires, ensuring proper insulation and minimal flux leakage. Regular maintenance of the genset to ensure constant and reliable power supply.

Figure 3.16: Scintrex IPR-12 Receiver

Figure 3.17: Typical set up of the current transmission station; A- Generator, B- Voltage regulator, C- Zonge GGT-3 transmitter.

Data transfer and Advance processing

On conclusion of the day's fieldwork, the acquired data can then be transferred onto a computer from the receiver. The data is the checked in text format (Figure 3.18) for any visual inconsistencies on the input parameters such as station number, as well as editing the header files in text format.

```
------------------------      S C I N T R E X      ------------------------------

                  IPR-12 MULTI-CHANNEL IP-RECEIVER V4.0

Job #:            1                        Date:      18/04/23

Operator:      KO                          Serial #:      1

P-Line:      7200N                         Units:      Metre

Array:      Gradient                       Mx From:   960 ms  To:  1050  ms

-------------------------------------------------------------------------

Station    P1      P2      P3      P4      P5      P6      P7      P8      P9

        C-Line    C1      C2    Curr.   Timing        Time   |

 D:        VP      SP      Mx     S.D.    Res.          Dur. K-Fact.      Rho

           M1      M2      M3      M4      M5      M6      M7|    M"       Tau

           M8      M9     M10     M11     M12     M13     M14|   RMS%       Wi
*
  8700E    8700E   8650E   8600E   8550E   8500+   8450E   8400E   8350E   8300E

           7200N   9000E   8100E   1800      2       09:07:05|

 1:      37.71       8    3.51    0.61    1.1             15  10009.8      210

                                  14.31   12.27   10.51   9.03| 67.5   0.12500

           7.60    6.49    5.41    4.29    3.66    2.98    2.39|   1.663      9

 2:      32.76      22    3.18    1.03    1.4             15  11658.0      212

                                  14.06   12.04   10.28   8.86| 69.5   0.06250

           7.45    6.26    5.18    4.10    3.35    2.70    2.12|   1.002      7

 3:      34.19      -8    2.92    0.50    1.6             15  12566.4      239

                                  12.12   10.44    8.95   7.78| 58.1   0.12500

           6.57    5.61    4.71    3.73    3.07    2.48    1.94|   1.247     10

 4:      23.05     -25    3.49    0.66    1.3             15  12566.4      161

                                  13.82   11.94   10.27   8.94| 64.2   0.25000

           7.59    6.48    5.49    4.36    3.65    3.01    2.41|   1.348      9

 5:      39.54     -12    4.64    0.35    1.2             15  11658.0      256

                                  18.15   15.80   13.69  11.92| 82.5   0.50000

          10.16    8.66    7.26    5.89    4.89    4.01    3.24|   0.903     11

 6:      21.45      60    5.32    0.55    0.8             15  10009.8      119

                                  20.59   17.99   15.64  13.59| 93.3   0.50000
```

Figure 3.18: Snapshot of IP data in text format

The Scintrex IPR-12 dump file (Figure 3.18) is then imported into Geosoft Oasis Montaj version 8.5 for further quality control processing.

The Geosoft IP system extracts standard required information channels such as IP average, apparent resistivity, chargeability, Self-Potential, voltage potential and metal factor from the instrument dump file into a database (Figure 3.19). With the QC tool, one can inspect the data and eliminate data sets that appear incorrect. Masking essential data ensures the data integrity is maintained.

The clean chargeability and Resistivity channels were then subsequently gridded and maps plotted to present the respective data. The gradient array data is best presented in the form of profile maps. Bi- directional interpolation gridding was used for this dataset.

The final grids produced were as follows:

- Average chargeability grid: The grid enhancement methods performed for the grid include:
  - ➢ Average chargeability, coloured by histogram equalization colour stretch
  - ➢ Average chargeability coloured by linear colour stretch
- Resistivity grid
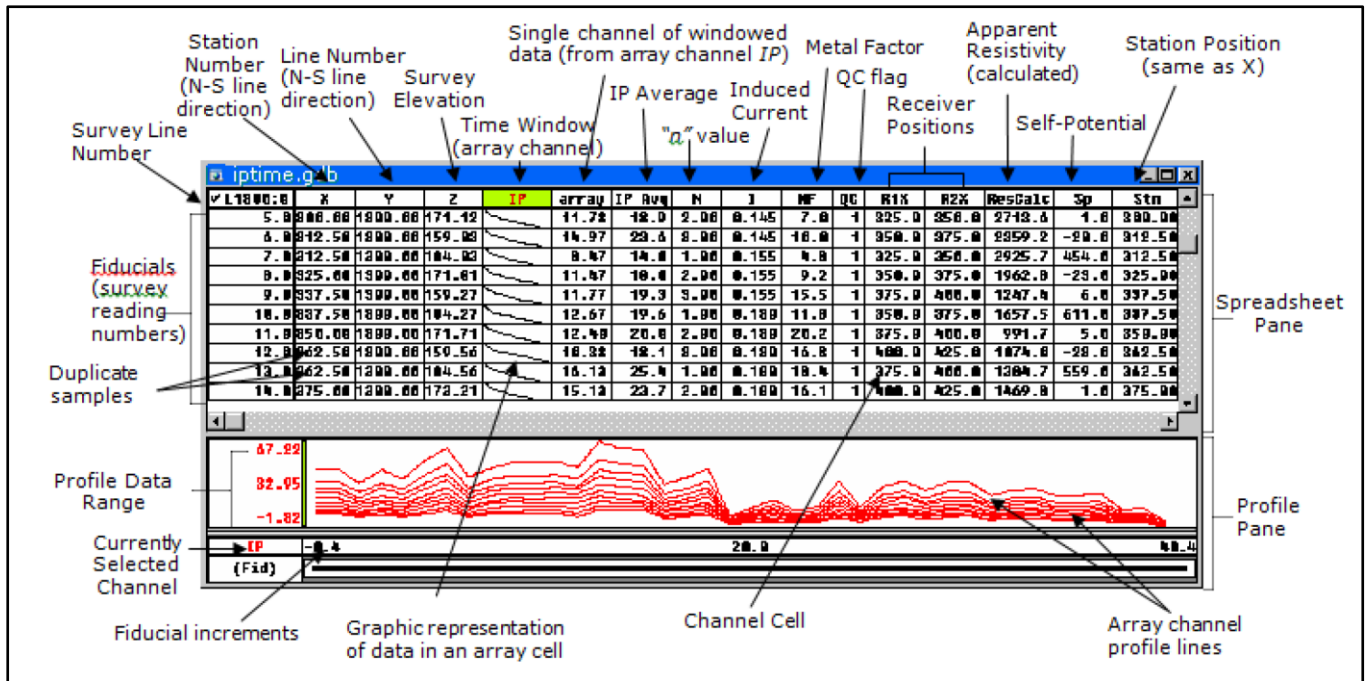
Figure 3.19: Geosoft display of IP database during processing. (Geosoft).

3.5 GROUND MAGNETICS

3.5.1 Data acquisition

Total Magnetic Field data was collected with the use of the Geometrics G-857 proton-precession magnetometer (Figure 3.20) and Scintrex Envi-Cs - Cesium sensor magnetometer (Figure 3.21). The Envi-mag was used as the base station magnetometer (Figures 3.22 and 3.23). The base station was placed in a magnetically quiet location near the survey area. One location was used for the entire duration of the survey.

Figure 3.20:Magnetic surveying using the Geometrics, G857 Proton Precession Magnetometer.

The first activity of a normal field day was setting up the base magnetometer. Throughout the survey, the base station magnetometer was tuned to the nearest magnetic field strength of 34000 nanoteslas (nT). The Envi mag (Base station) was set up to take readings at 2 second intervals. The base magnetometer was then time-synchronized with the rover magnetometers. After the base station set up is completed, the field surveying begins. The two field magnetometers were set to operate on lines spaced over 1km apart. The field magnetometers were both integrated with an external GPS that recorded the position coordinates as magnetic measurements were taken. The magnetometer was configured to collect data at a frequency of 5 seconds and 10 seconds for the Envi-Cs and G857 respectively.

Before commencing the field measurements, the operator is cleared of any metallic materials. The Geometrics G-857 proton precession magnetometer comprises a console for taking measurements and a sensor on a staff. The sensor head was always aligned towards the north for adequate signal acquisition of the magnetic field. The console is strapped over the operator's shoulder while the integrated GPS is also connected and maybe held by the operator or strapped by the side. The operator would then walk along the survey direction guided with the GPS, while holding the sensor staff. The Envi-Cs magnetometer, on the other hand, comprised of a back pack set up of the magnetometer and the GPS component with the cesium sensor hanging over the head together with the GPS antenna. The operator handles the console and keys in necessary information like line number among other metadata as may be required.

At the completion of a field surveying day or shift the operators would proceed and stop the base magnetometer. The data would then be downloaded at the field camp onto a computer. The survey data would then be imported as ASCII files into a Geosoft database for further processing. The coordinate system used was UTM ZONE 36N and Datum, WGS84.

Figure 3.21: Field operation of the Envi-Cs Magnetometer during magnetic survey in Makina

Figure 3.22: Setting up of the Base station Envi-mag (BaseMag).

Figure 3.23:Sensor and console of the Scintrex Envi- mag

3.5.2 Magnetic Data Processing

Processing was done using Geosoft Oasis Montaj ver. 8.5. The lines were then plotted to check the accuracy of the survey measurement and adherence to the line spacing. The general measurement spread was also checked. The magnetic data was check for noise and spikes in the signal. Any noise or irregular spikes were cleaned (despiked) manually. The base station magnetometer data was equally checked for any irregular signal before diurnal corrections were applied.

Diurnal corrections were followed by calculation of Geomagnetic Reference Field (IGRF) to enable the generation of the residual magnetic field. The residual magnetic field is obtained by subtracting the IGRF from the base/diurnal corrected data:

(Observed Magnetic data - diurnal variation) – IGRF = Residual magnetic field

Diurnal Variation = (Base station data - Base mean).

Minimum curvature gridding was applied to the final corrected magnetic array resulting in the Residual Magnetic Intensity map. For this study, data corrected for diurnal variation was found to be good enough for final gridding and processing as the signals were as good as those of IGRF corrected data.

Further enhancement steps involved the utilization of 2D - Fast Fourier Transform filters. Enhancement filter techniques employed; Reduction to magnetic pole, first vertical Derivative, Tilt Derivative, Upward Continuation, Horizontal Tilt derivative and the Analytic Signal. Some of the filters utilized can be described as presented in Table 3.1:

Table 3.1: List and description of magnetic data processing techniques and products.

Base-corrected **TMI**:	Total magnetic intensity, corrected for diurnal variations
Upward continuation	Upward continuation is a frequency domain filter used to calculate the effective potential field at a higher survey height. The technique provides a useful means for smoothening out point related anomalies and has been used in combination with additional derivative products
RTP: Reduction to pole	Reduction to pole is a mathematical function applied to TMI data in the frequency domain, with the resultant product being the equivalent TMI data situated at the magnetic pole thus replacing the dipolar magnetic response with a simple peak positioned above the magnetic source. There are a few limitations to this filter, which need to be understood when interpreting data: • The filter assumes the magnetic response to be due to induced magnetisation and ignores the effect of magnetic remanence. This results in incorrect solutions where the remanent magnetic contribution is large and differs in orientation from the induced magnetic contribution (often manifested as a smearing of anomalies). The filter is unstable at low magnetic latitudes where it results in a smearing and exaggeration of NS trending features. This is mitigated to some degree by using an amplitude correction, although at the expense of under-correcting NS trending features
Analytic signal of the Total Magnetic Intensity (TMI).	Analytic signal refers to the mathematical square-root of the total sum of squared derivatives of the total magnetic field. The analytic signal is used for locating edges of magnetic source bodies while spatially positioning anomalies correctly, especially where remanence or low magnetic latitude may complicate interpretation. This filter accentuates shallow features at the expense of deeper (or longer wavelength) features.
First vertical derivative	This is a standard product, which is calculated either in the space or the frequency domain. The filter accentuates shallow features and structures and enhances magnetic textural changes, which often characterize lithologies. As a result, the vertical derivative images typically provide a good match with mapped geology.
TDR: Tilt derivative	This filter calculates the angle between the horizontal and vertical derivatives providing a useful edge detection and structural mapping tool. As a phase measurement, the filter includes more of the deeper structural information compared with conventional derivative products. The tilt derivative is generally applied to reduced-to-magnetic pole data and is a useful product for direct spatial positioning of magnetic anomalies. In addition to the standard tilt-derivative filter, a residual product was also created which highlights shorter wavelength anomalies.
THDR: Total Horizontal Derivative TMI	Directional derivatives highlight structures and trends in a particular orientation. The Total Horizontal derivative is the square-root of the sum of the squared x- and y-derivatives. This filter is useful for delineating edges and internal magnetic fabrics of near surface structures.

CHAPTER 4   RESULTS AND DISCUSSION

The results of the two geophysical surveys conducted in the study area after final processing were presented in the form of Geosoft grid files and maps representing the measured parameters. IP/ Chargeability maps and Resistivity maps were processed from the Gradient survey data. The various enhancement and filter methods applied on the magnetics data have also been presented in maps for purposes of interpretation and identification of possible mineralization trends. The further discussions and interpretations were based on the following set of maps/grids:

4.1 GRADIENT MAPS

The chargeability and resistivity data were plotted into colour coded maps showing the various zones of chargeability and resistivity distribution in the area. High chargeability zones represent zones of chargeable material, either at shallow depths or deeper (See Figure 4.1). High resistivity means zones of highly resistive bodies or poor electrical conductivity (Figure 4.2).
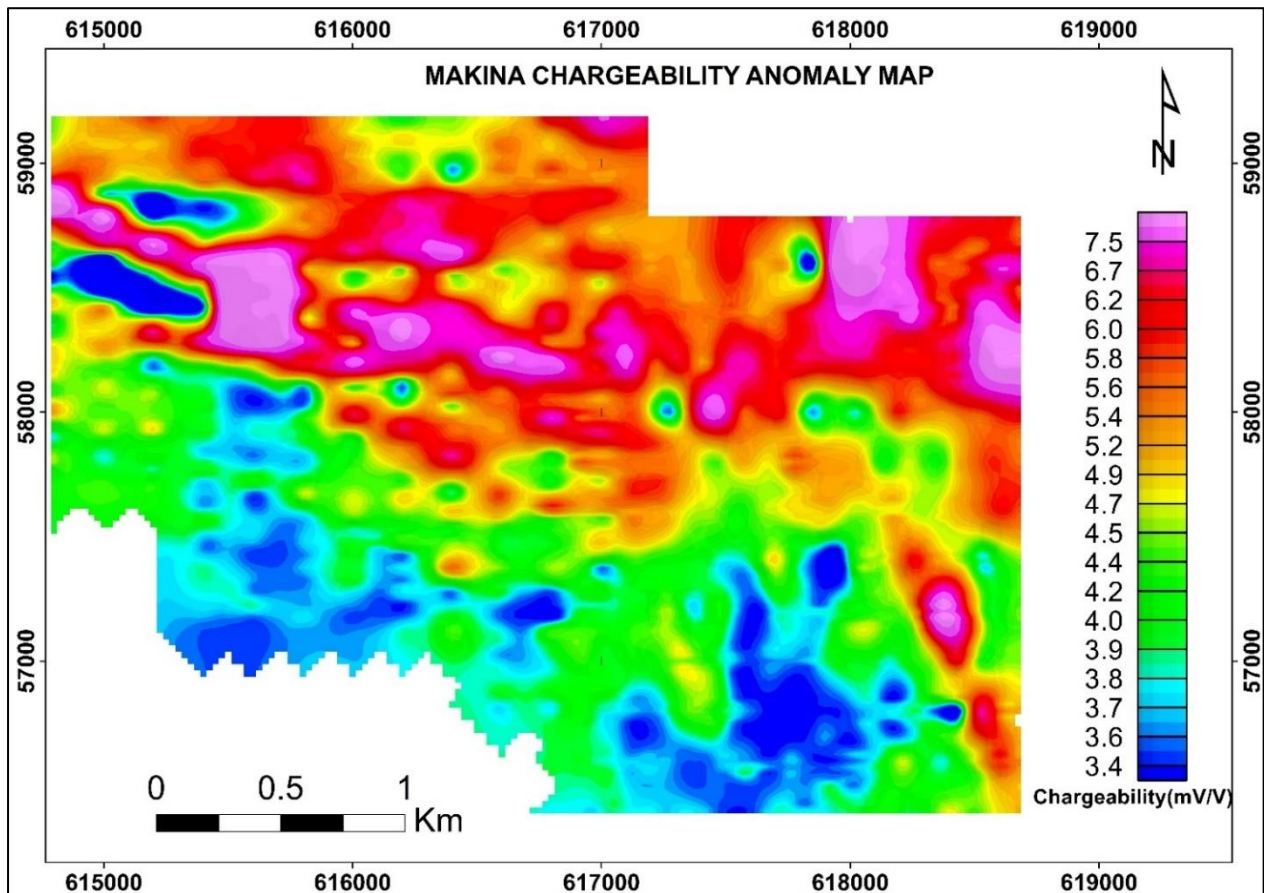

Figure 4.1: Makina Chargeability map of collected IP survey data.
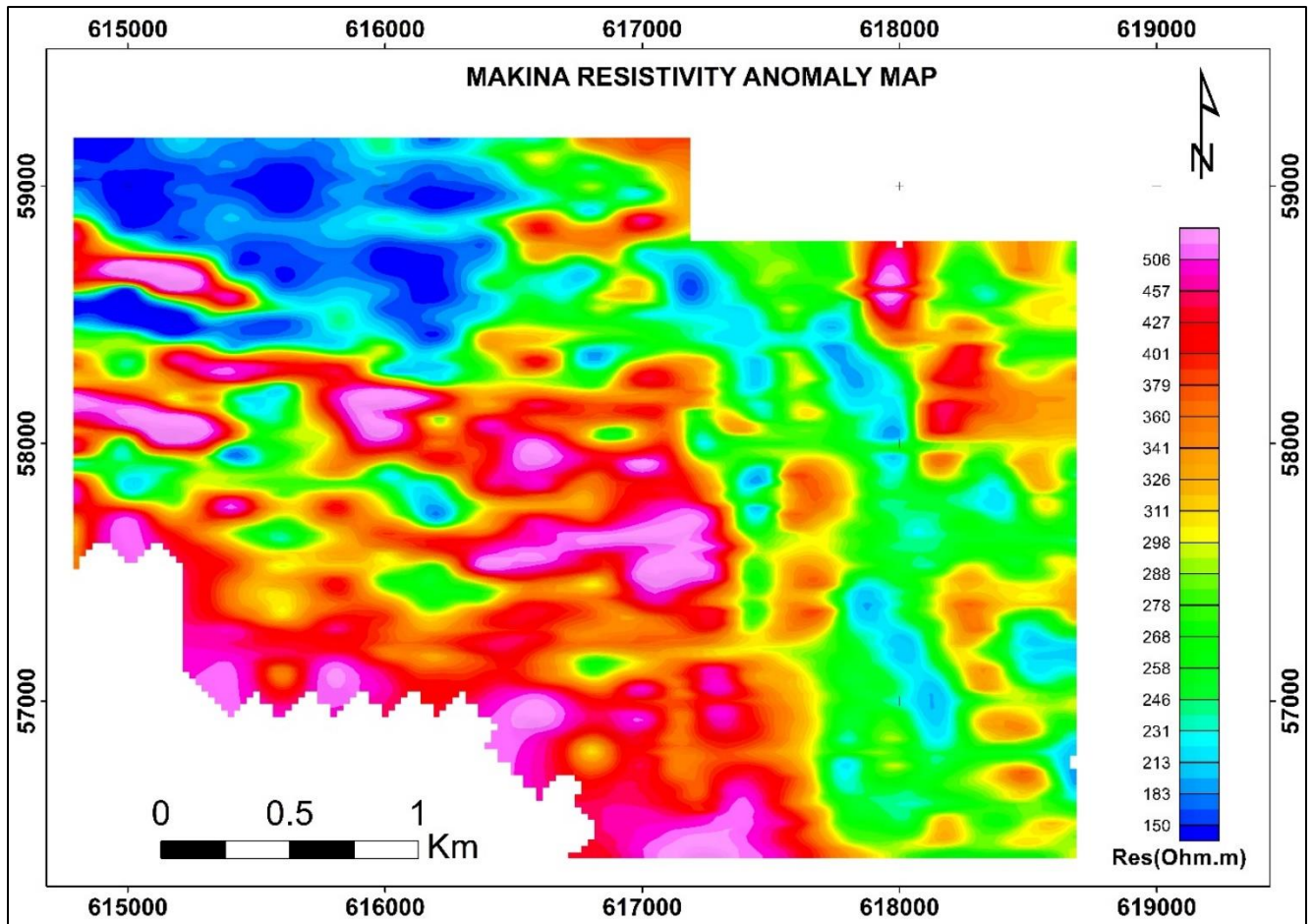
Figure 4.2: Resistivity map of the surveyed area.

4.2 GROUND MAGNETICS MAPS

Magnetic anomaly maps often represent geological and structural features. The mineralization style in the study area is believed to be both structurally controlled and lithology based. The produced magnetic maps provide an improved understanding and interpretation of structures such as faults and intrusions, in addition to indicating various areas of competency contrast that can be correlated to available exploration geochemical data further delineated potential trends.

4.2.1 Total Magnetic Intensity- TMI

The total magnetic Intensity map (Figure 4.3) was generated form the diurnal corrected residual magnetic field data using minimum curvature gridding in Oasis montaj.
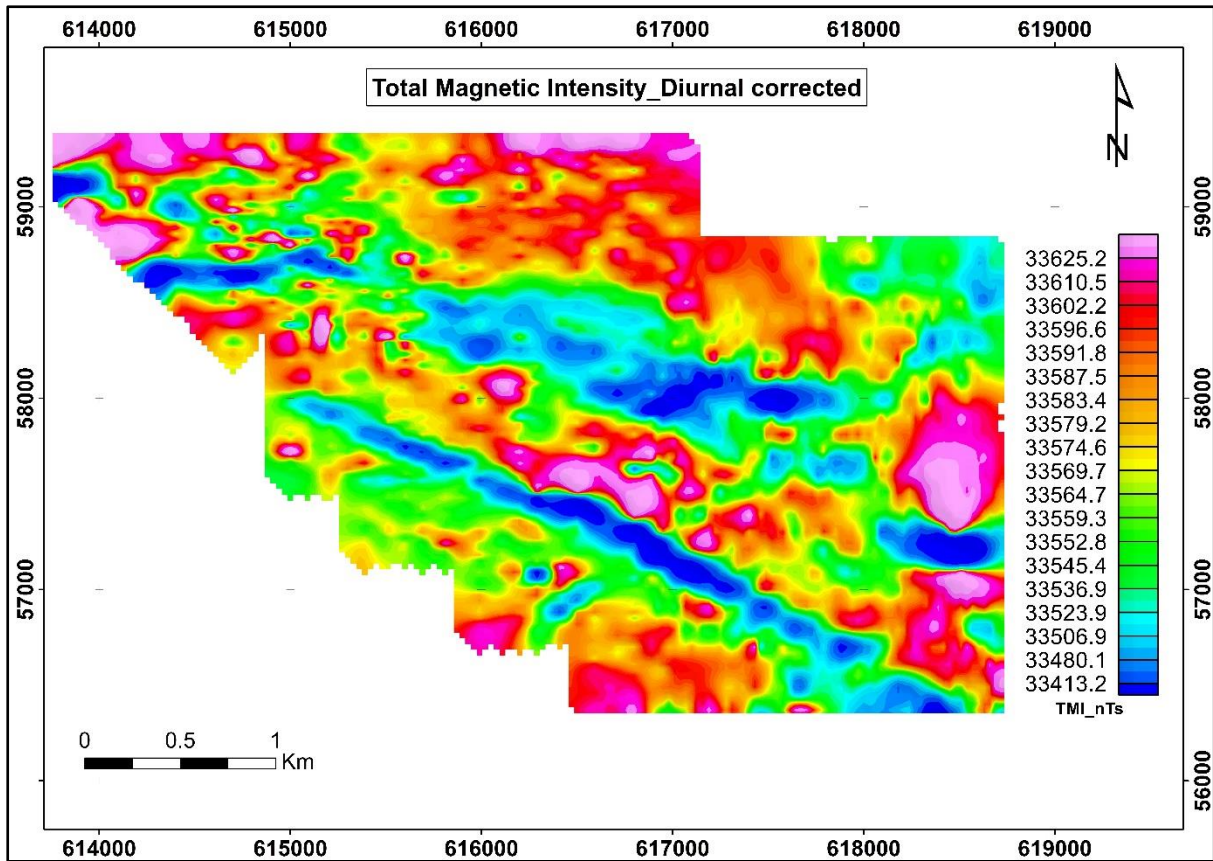
58

Figure 4.3: The Total Magnetic intensity (Diurnal corrected) map of Makina.

4.2.2 Analytic signal

The analytical signal is used to locate the edges of magnetic source bodies and correctly positioning anomalies in space, particularly where remanence or low magnetic latitude complicates interpretation. This filter accentuates shallow features at the expense of deeper (or longer wavelength) features. The Analytic signal of the map for Makina (Figure 4.4) was generated from the Total Magnetic intensity grid file using Oasis montaj 2D filtering softwares.

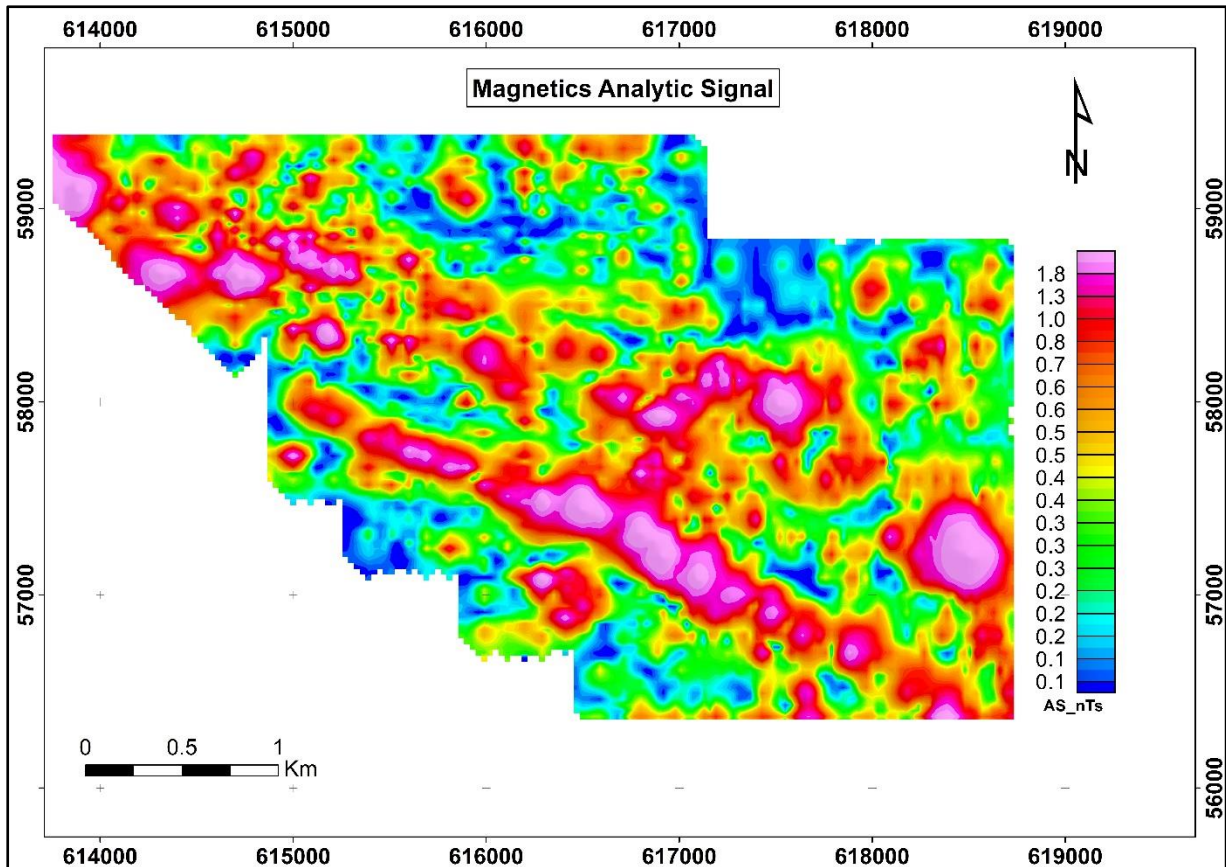The analytic signal map in Figure 4.4 begins to show some of the distinct magnetic anomalies in the surveyed area.

Figure 4.4: Analytic signal of Makina.

4.2.3 Upward continuation

The technique provides a useful means for smoothing out point related anomalies and has been used in combination with additional derivative products. This potential field filtering technique was performed on the, Total magnetic intensity. The TMI was upward continued by 15m. The upward continued map shows the smoothened trends and bodies initially observed in the TMI map (Figure 4.5).
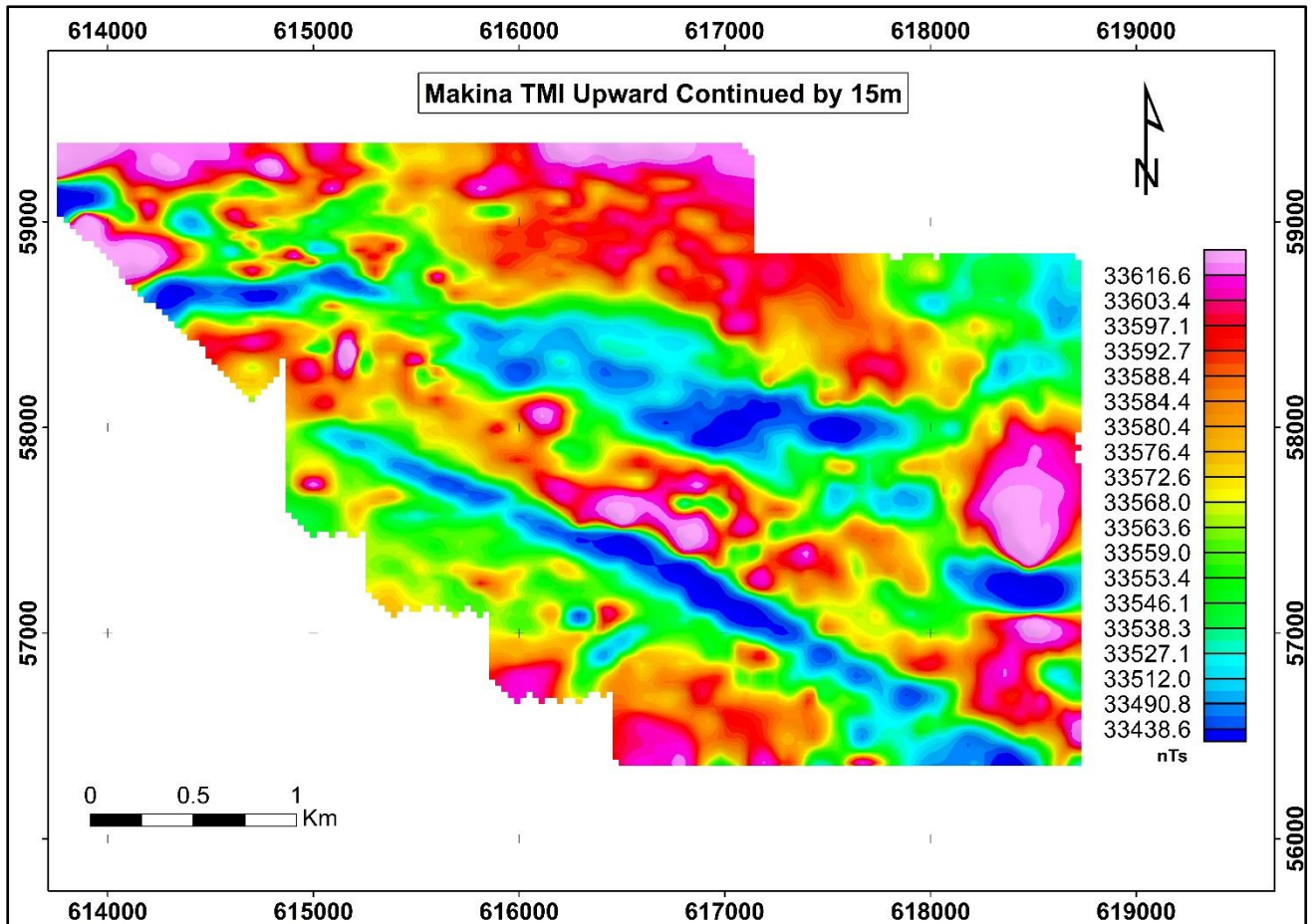
Figure 4.5: Residual Magnetic Intensity Upward continued by 15m.

4.2.4 Reduction to pole

The upward continued residual magnetic intensity output was reduced to the magnetic pole in this case (Figure 4.6). This produces magnetic field equivalent to that at magnetic poles, replacing dipolar magnetic response with peaks positioned above the magnetic source. In the case of the Makina RTP product, the anomalous bodies can be easily identified and various trends are distinguishable.
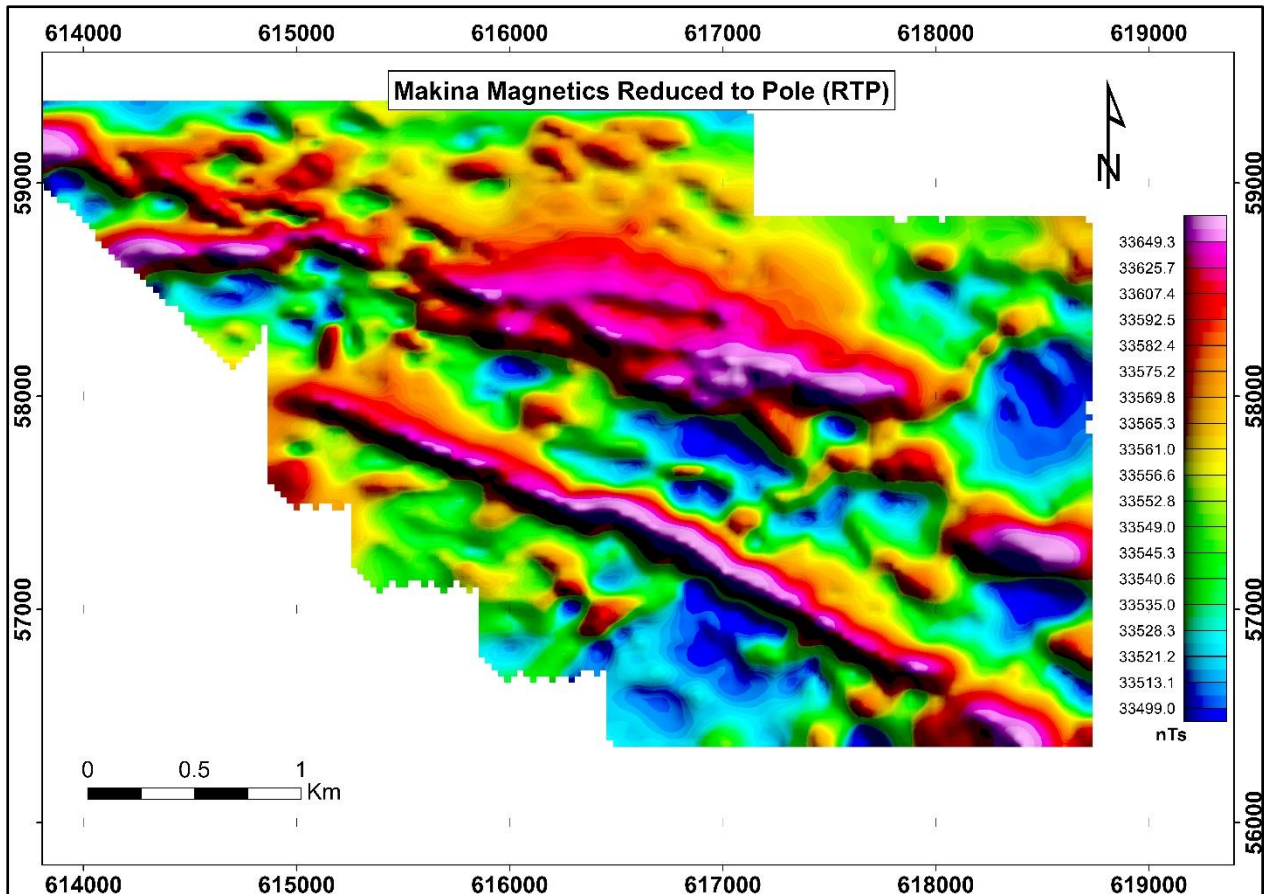
Figure 4.6: Makina Residual Magnetics Reduced to Pole.

4.2.5 Tilt Derivative Map

The Tilt Derivative 2D-filtering method is a useful edge detection structure mapping tool. The Tilt derivative (Figure 4.7) is applied to the reduced to magnetic pole (RTP) data. Distinct structural trends and patterns mostly coincidental with the RTP data can be observed from the Makina Tilt Derivative data.
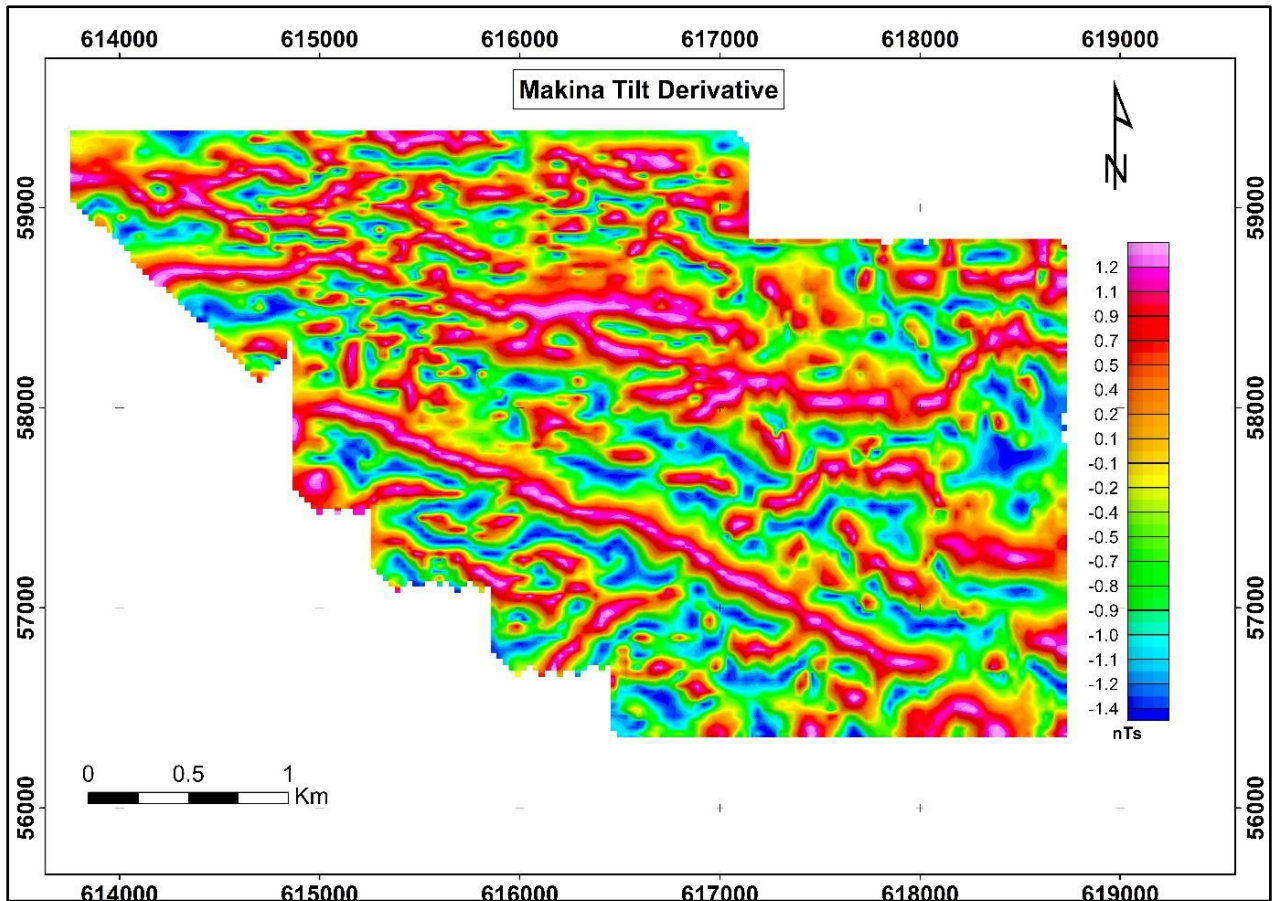
Figure 4.7: Makina Tilt derivative.

4.2.6 Total horizontal derivative map

This filter is useful in delineating edges of near surface structures. The Total Horizontal Derivative map of Makina (Figure 4.8) depicts significant magnetic signatures of interpretable structures.
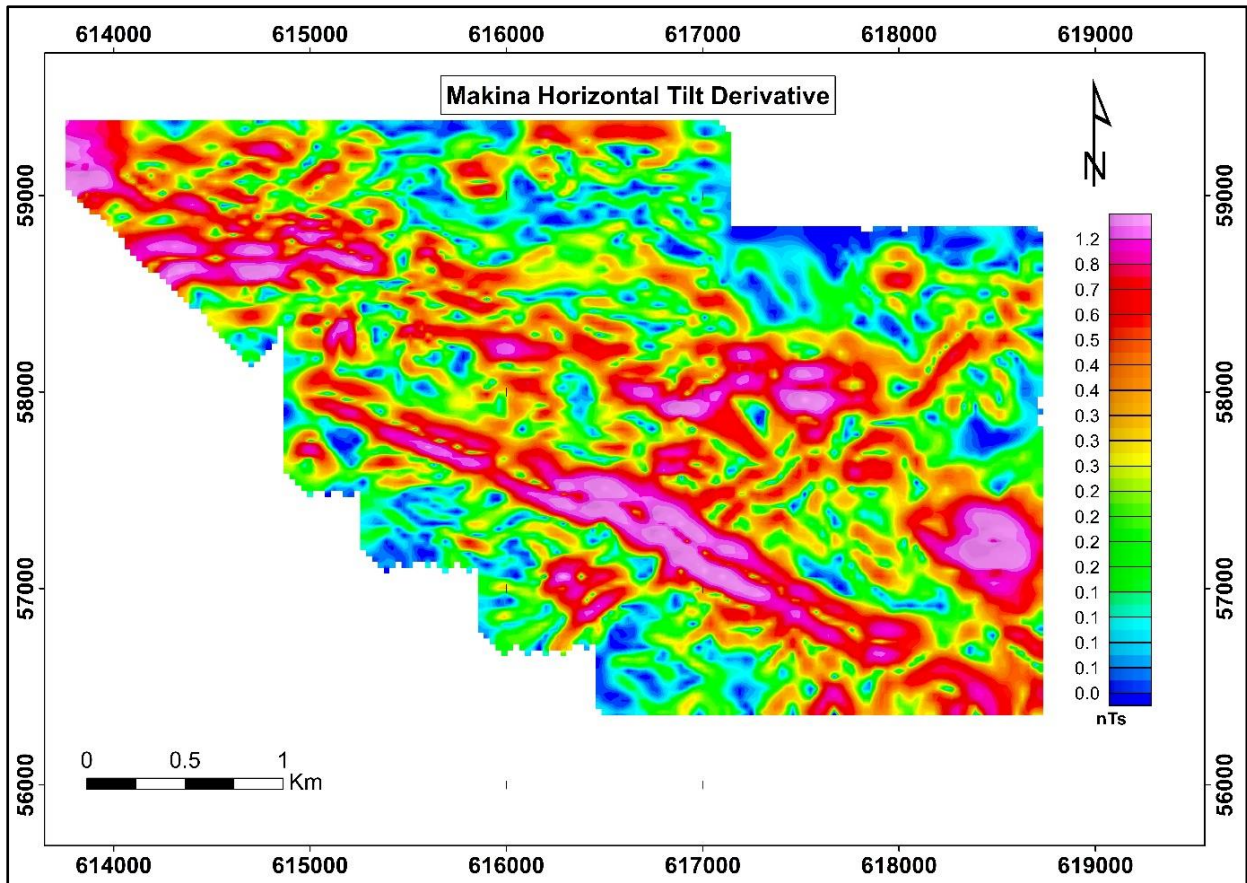
Figure 4.8: Horizontal Tilt Derivative.

4.2.7 Unconstrained magnetic susceptibility inversion volume

An unconstrained magnetic susceptibility 3D Volume Voxi model was completed and various depth slices show significant continuity of the magnetic signatures at the various depths with resolution and delineation improving with depth. Depth slices were plotted through the 3D susceptibility volume at 0m, 10m, 100m, 250m and 500m below surface terrain. Figures 4.9 to 4.14 illustrate the 3D Voxi model and the resultant depth slices generated through Oasis Montaj respectively.

The susceptibility inversion model (Figure 4.9) indicates the existence of magnetic anomalies that may be related to mineralization in the study are. Some of the anomalous trends and structures appear to have persistence consistency even with depth. Figure 4.10 is a depth slice of the surface depiction of the magnetic susceptibility. At the surface however, no distinct patterns can be established possible due to the various magnetic factors influencing the susceptibility signatures at the surface such as effect of soil and surface debri with contained

magnetic material. At about 10m below surface (Figure 4.11), the patterns and structures begin to appear mildly but are mask possibly by surface magnetization effects.

At 100m depth (Figure 4.12) the magnetic field patterns appear more distinguishable and shapes and trends of certain anomalous bodies are identifiable. The magnetic signatures at 250m (Figure 4.13) are clearly defined and show some consistency with the upper slices with regard to the main magnetic high signatures and trends. At 500m, fewer seemingly voluminous magnetic high signatures are observed (Figure 4.13). This could be as a result of reduced resolution, however, a continuity in the downward trend of some of the anomalies is evident.
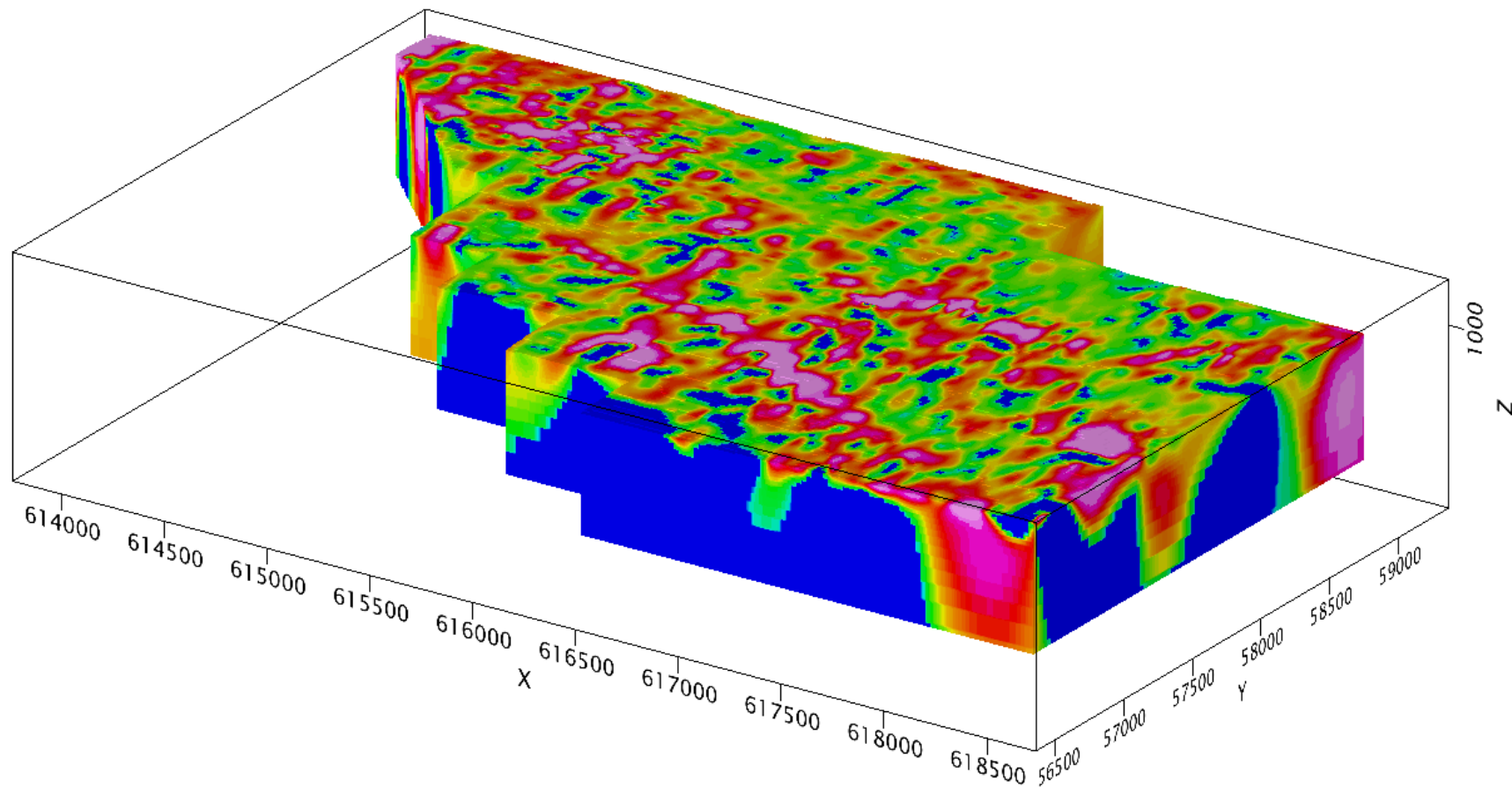
Figure 4.9: Unconstrained magnetic susceptibility inversion volume- 3D- Voxi model. The pink-red zones represent zones of high magnetic susceptibility. The inversion model represents observations upto 600m below the surface.
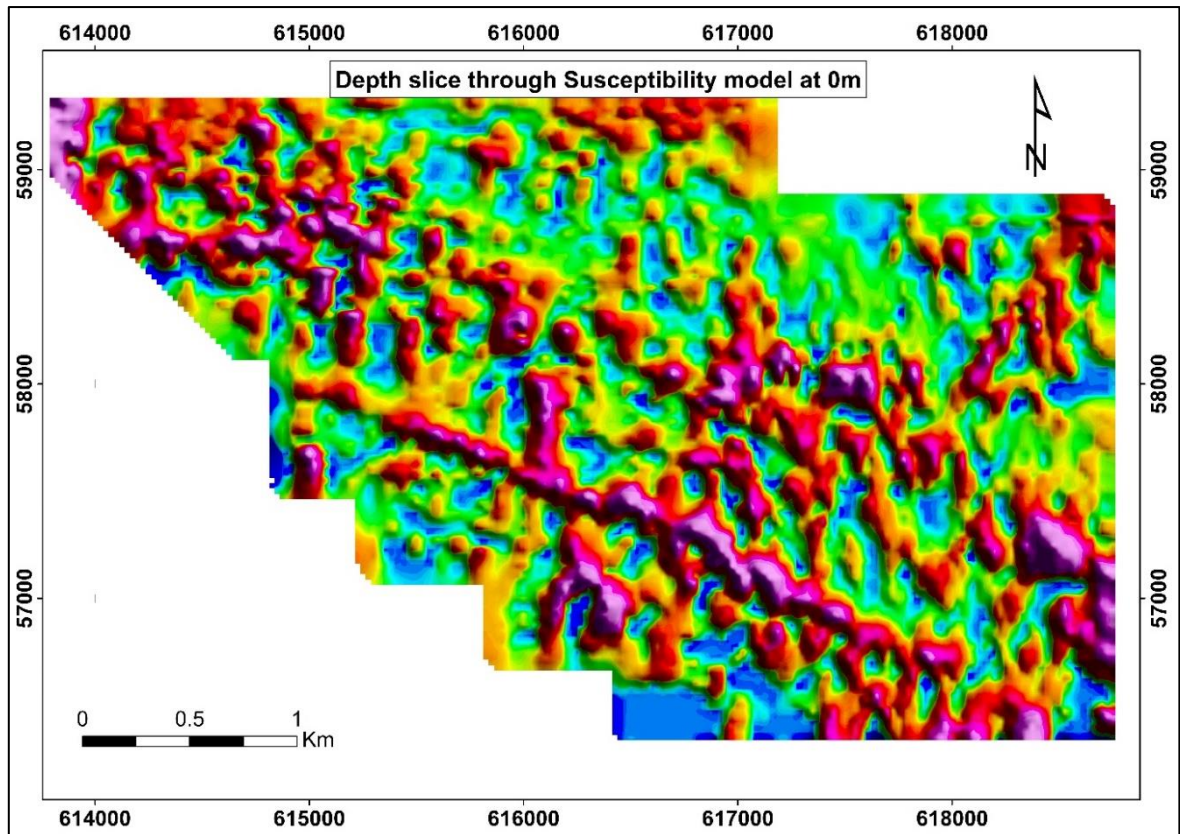
Figure 4.10: Depth slice through 3D susceptibility volume taken at 0m below terrain
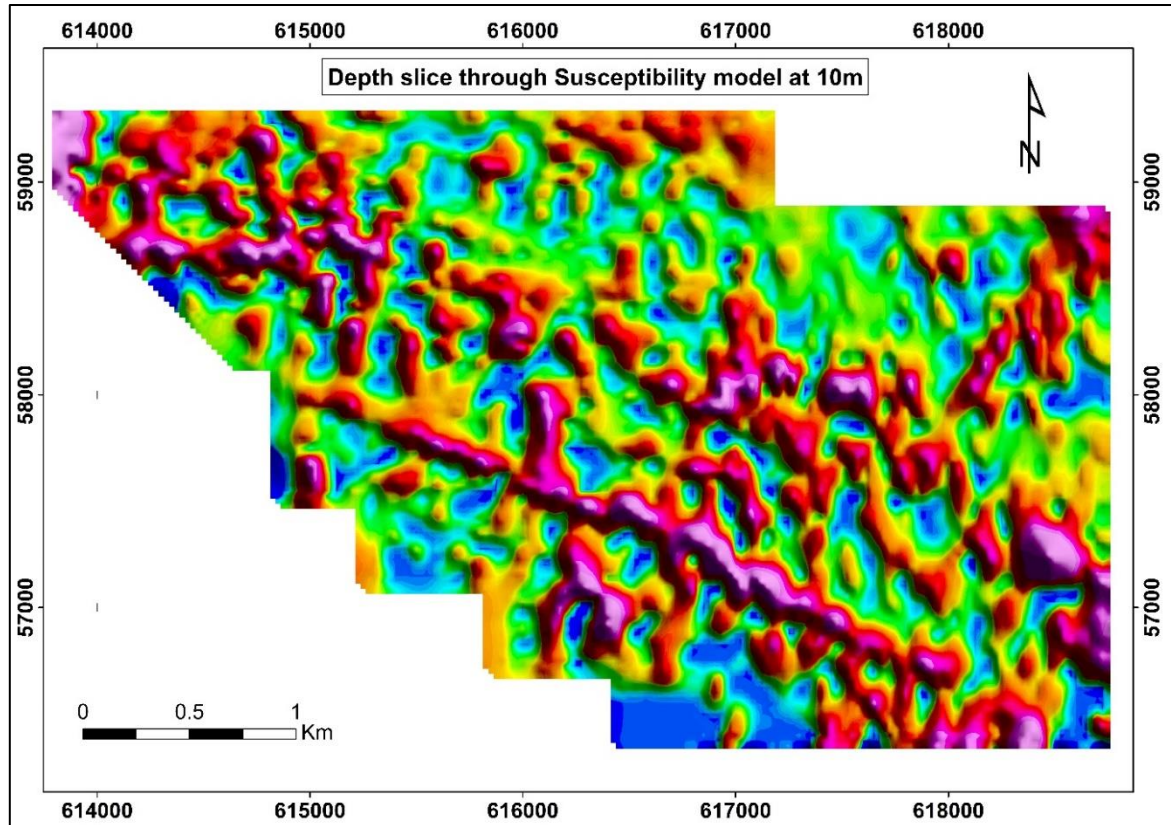

Figure 4.11: Depth slice through 3D susceptibility volume through 10m below terrain
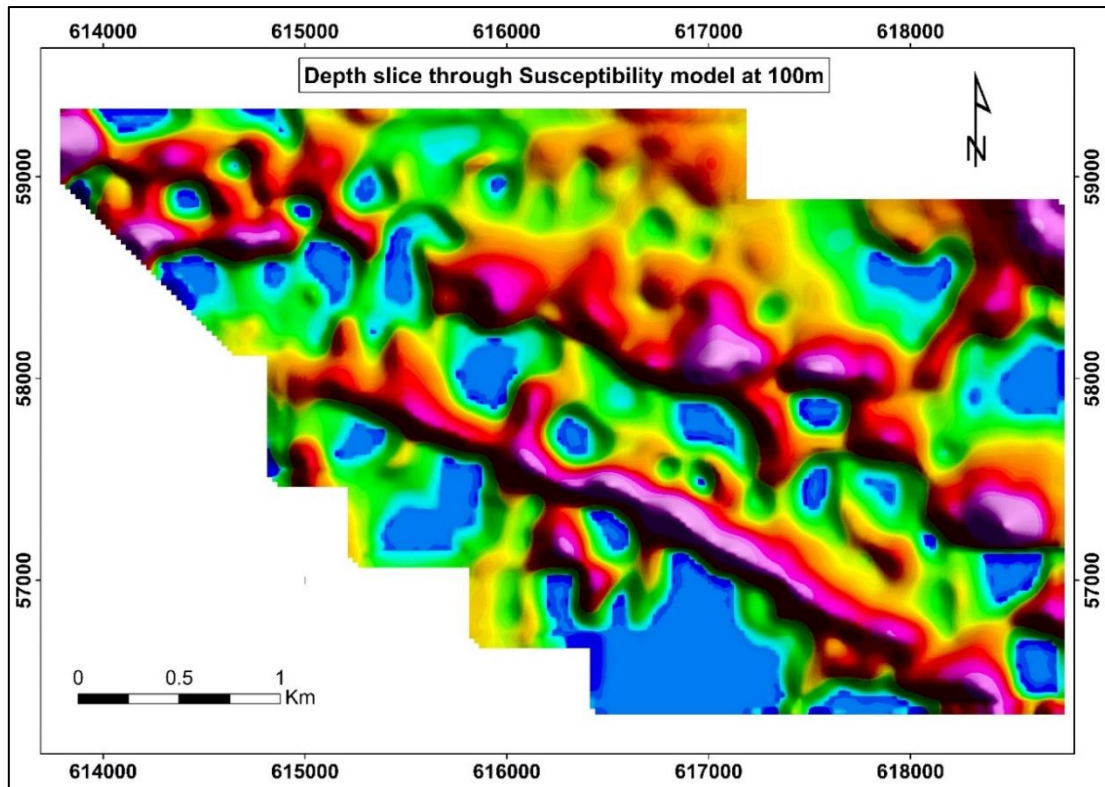
Figure 4.12: Depth slice through 3D susceptibility volume taken through 100m below terrain
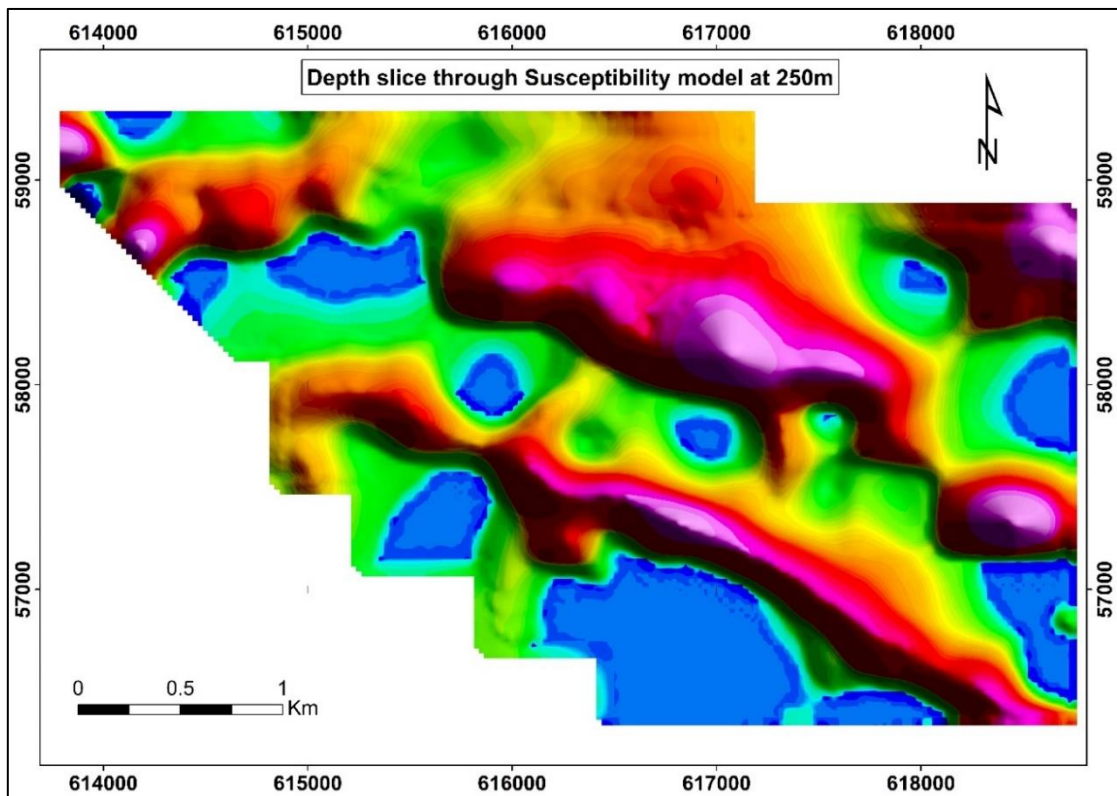

Figure 4.13: Depth slice through 3D susceptibility volume taken through 250m below terrain
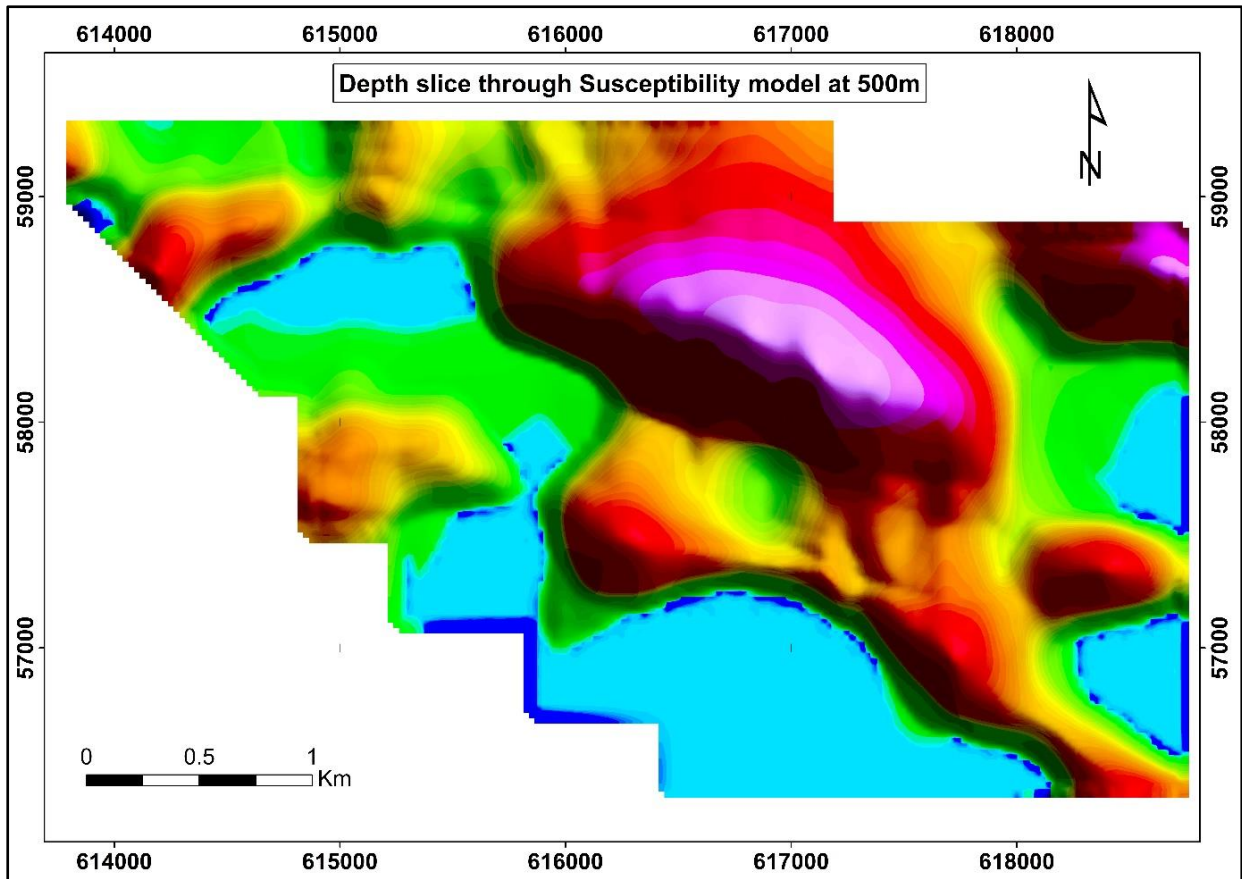
Figure 4.14: Depth slice through 3D susceptibility volume taken at 500m below terrain

4.3 DISCUSSION AND INTERPRETATION

4.3.1 Gradient IP/Resistivity anomalies

Gallas (2015) indicates that under suitable conditions, the IP method has the ability of detecting even smaller amounts of disseminated metal ores, mostly sulphides. Gold mineralization in the study area and indeed many deposits of other greenstone belts is often accompanied by metal sulphides and oxides, both of which are good conductors.

Resistivity and chargeability measurements aid in the process of mapping out chargeable and non-chargeable bodies and related rock resistivities based on the nature of the hosting geological features. Competent quartz veins for instance would record high resistivity values while, altered, sheared or fractured but mineralized zones may give low resistivity signatures (Fon et al., 2012). Therefore, to make interpretative sense of IP and resistivity maps, it is important that they are integrated with geology and geochemical data, which ideally define the initial anomaly or target zones.

In the results of this research project, the chargeability map shows significant zones of high chargeability (Figure 4.15). The high chargeability zones conform to previously identified structural trends as well as trends of the gold in soil geochemical anomalies (Figure 4.16). The anomalies to the east of the survey area appear to be controlled by almost North / South oriented fault/fracture zones. The lower eastern anomaly appears tilted towards the west as the adjoining NW/SE aligned anomaly. The NW/SE oriented anomaly covering the middle portion of the survey grid and running to the west appears to be influenced by both structure and lithology. The anomaly appears perfectly aligned with the narrow occurrence of a BIF unit ensconced in the volcanic layer (Figure 4.17). Effects of shearing induced displacement are equally evident in addition to the series of strike slip faults observed to the easter part of the surveyed area Two significant chargeable zones have been identified for further exploration as illustrated in Figure 4.18. A third anomaly appears at the north eastern corner of the surveyed area and may require future consideration.
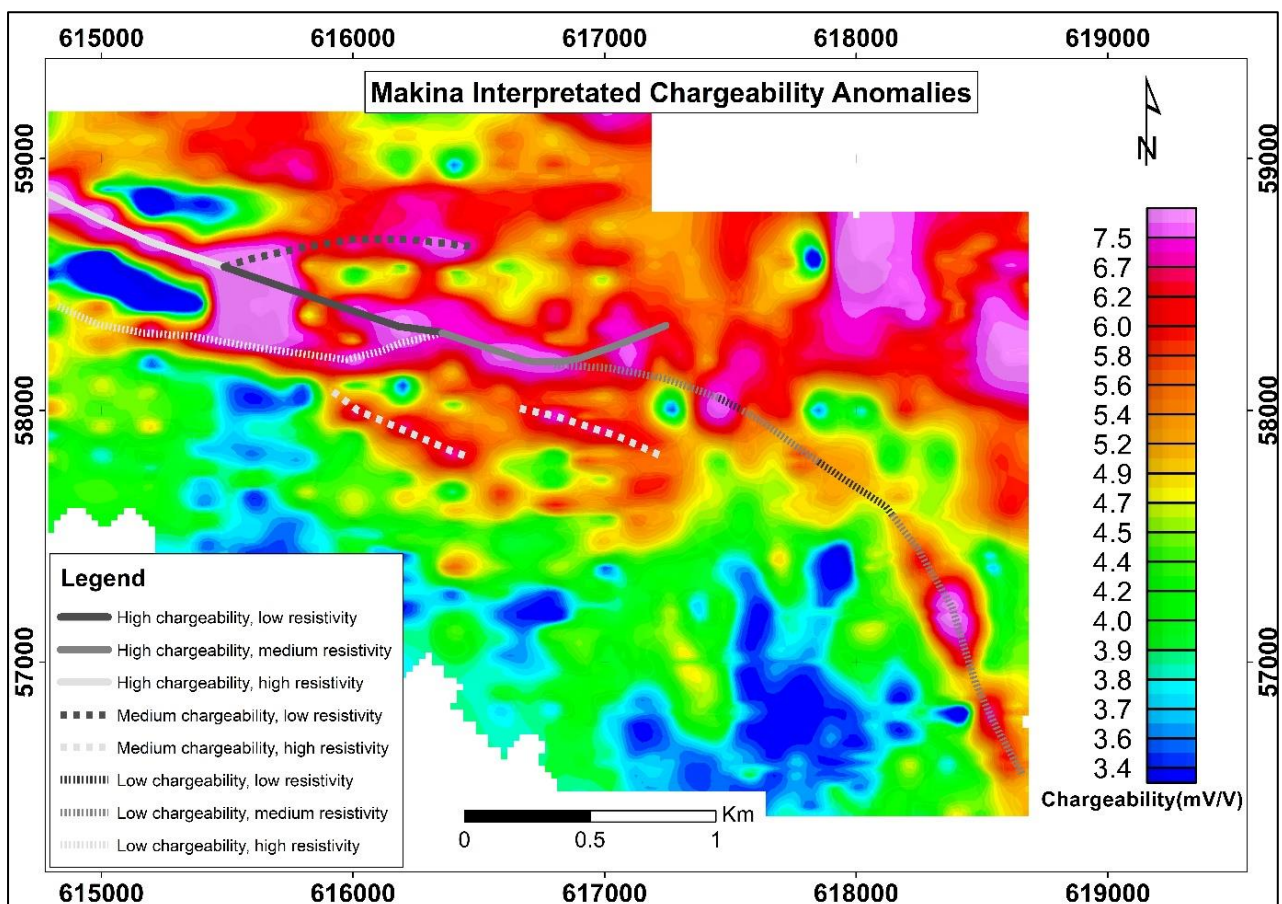

Figure 4.15: Makina Chargeability map with interpreted trend illustration of the relationship between chargeability and resistivity in the surveyed area.

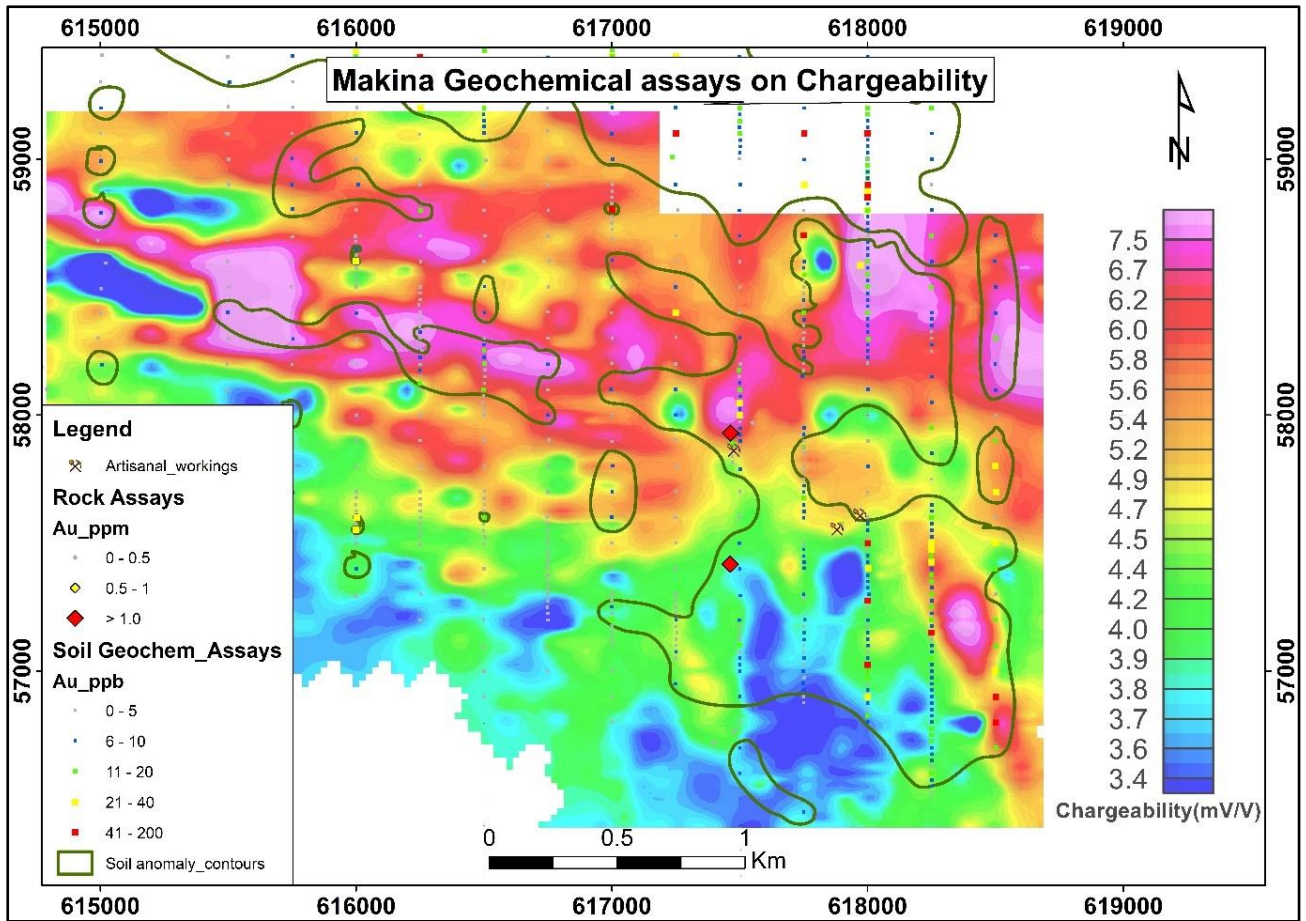Figure 4.16: Gold in soil geochemical anomalies and their interpreted trends overlaid on chargeability anomalies. The high chargeability zones can be seen to coincide with the interpreted soil anomaly trends.
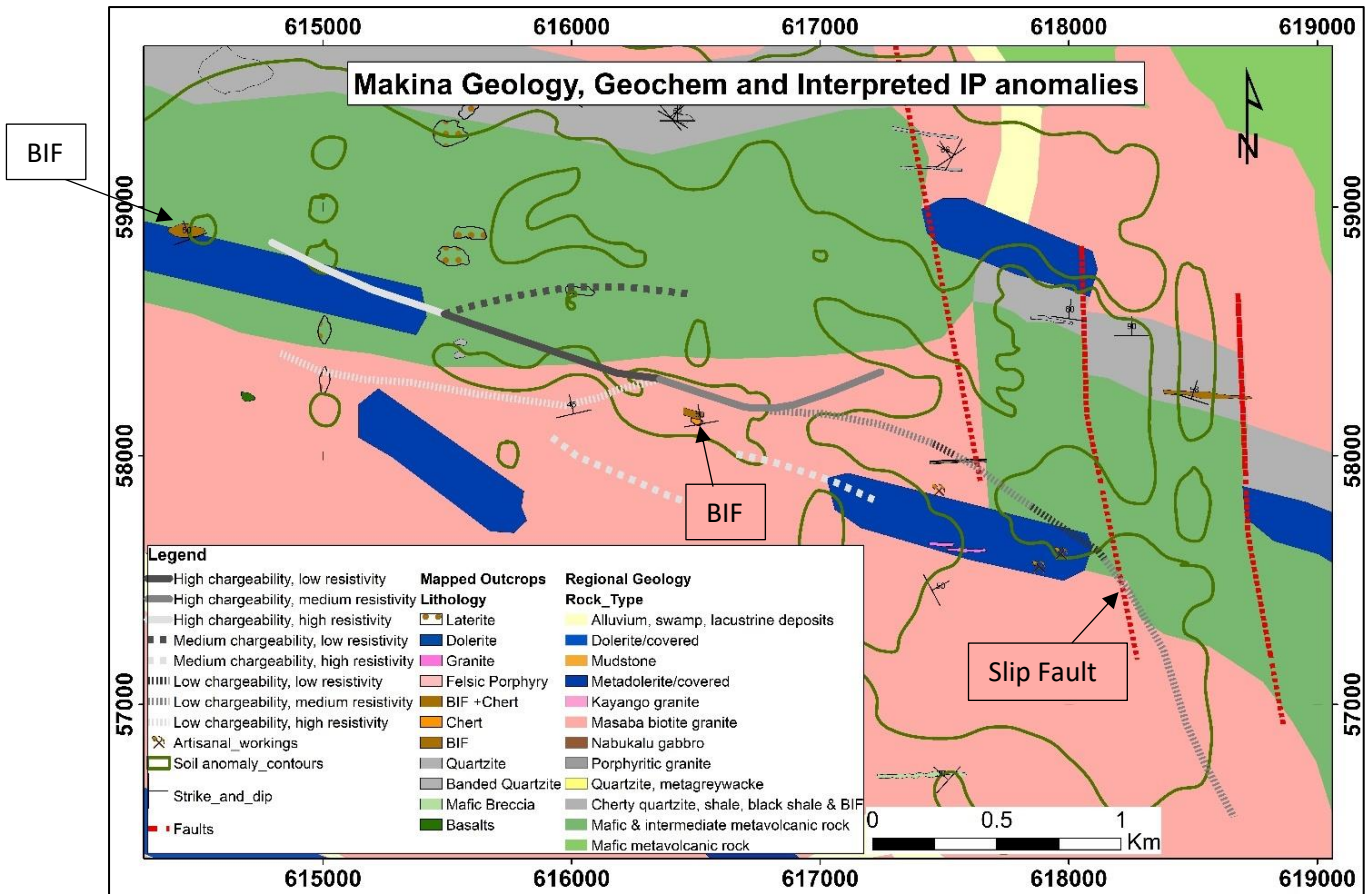
Figure 4.17:Makina Regional geology map with recently mapped Band Iron formation outcrops highlighted. The slip faults to the east coincide with geochemical anomalies and Chargeability anomalies.
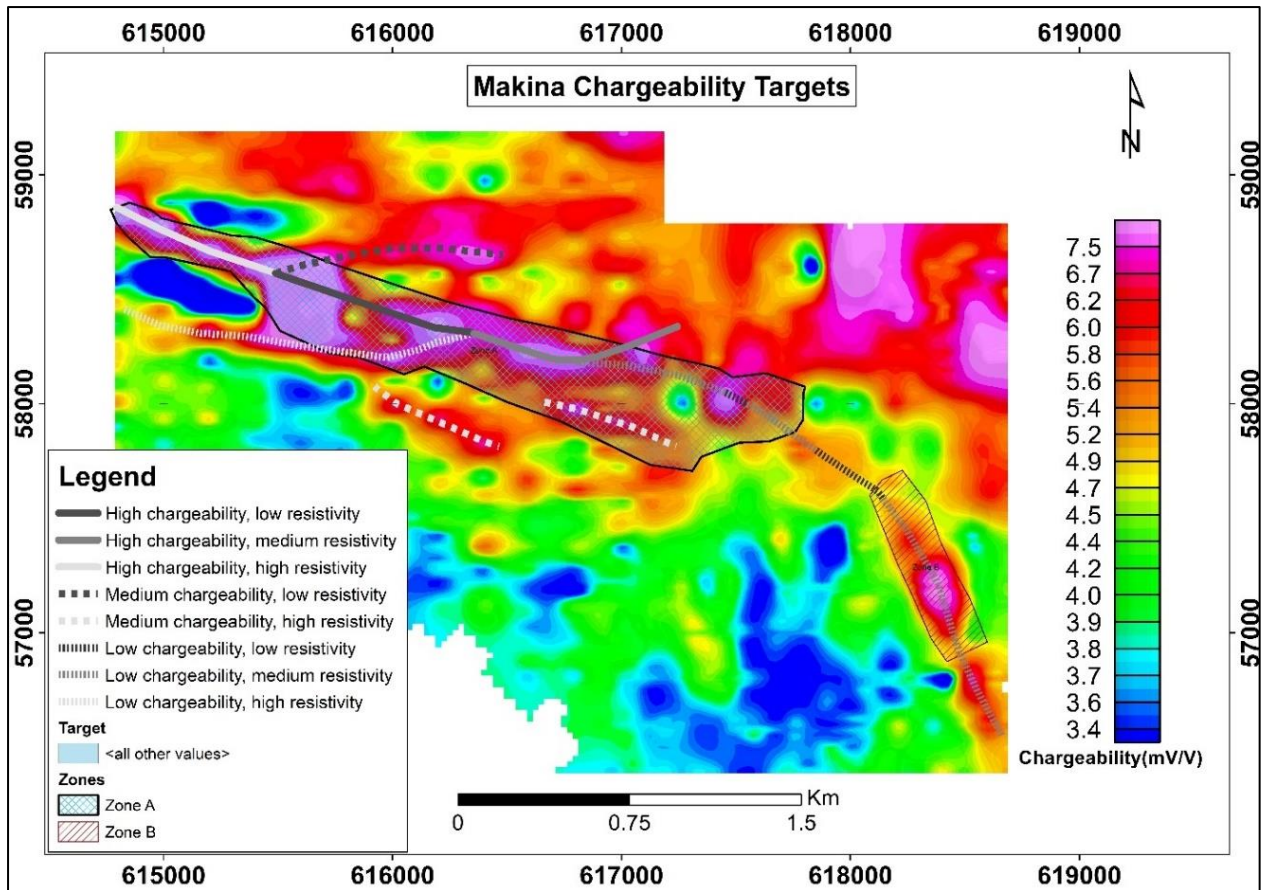
Figure 4.18: Makina Chargeability anomaly map with two high chargeability targets Highlighted.

The resistivity signatures indicate varied resistivity patterns (Figure 4.19). The low resistivity zones in the east and their orientations attest to possible fracture/ fault zones trending North/South. High resistivity zones in the area may be influenced by the presence of intrusive units (both felsic and mafic) as well as possible silicification in the volcanic rocks. Quartz veins though expected to be narrow, are also commonly represented as zones of high resistivity.
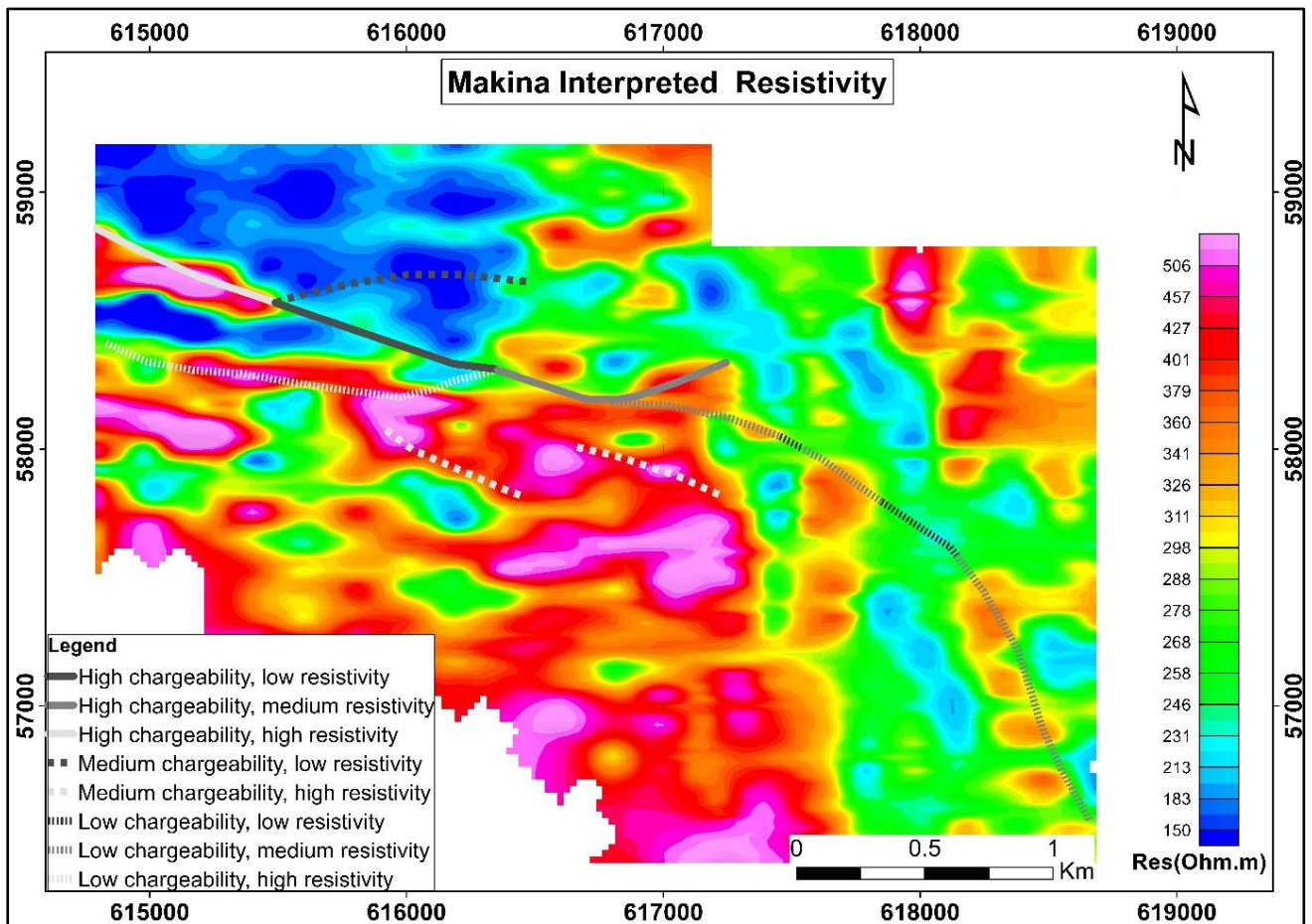
Figure 4.19: Makina Resistivity map with interpreted trend illustration of the relationship between chargeability and resistivity in the surveyed area.

Analysis of the trends and relationship between chargeability and resistivity in Makina can be summarized by the map in Figure 4.20 which shows resistivity against contoured chargeability data. The various differences in the resistivity values along the chargeable zone demonstrates the possibility of different grades and stages of structural and rheological deformations that may have occurred in the area, hence their mineralization potential. High chargeability reflects zones with good chargeable material such as sulphide mineralization. Resistivity of a particular material is linked to its electrical conductivity in that resistive bodies are said to be poor

electrical conductors while less resistive bodies are said to be good conductors. Therefore, low resistivity signifies high conductivity or occurrence of a conductive body.
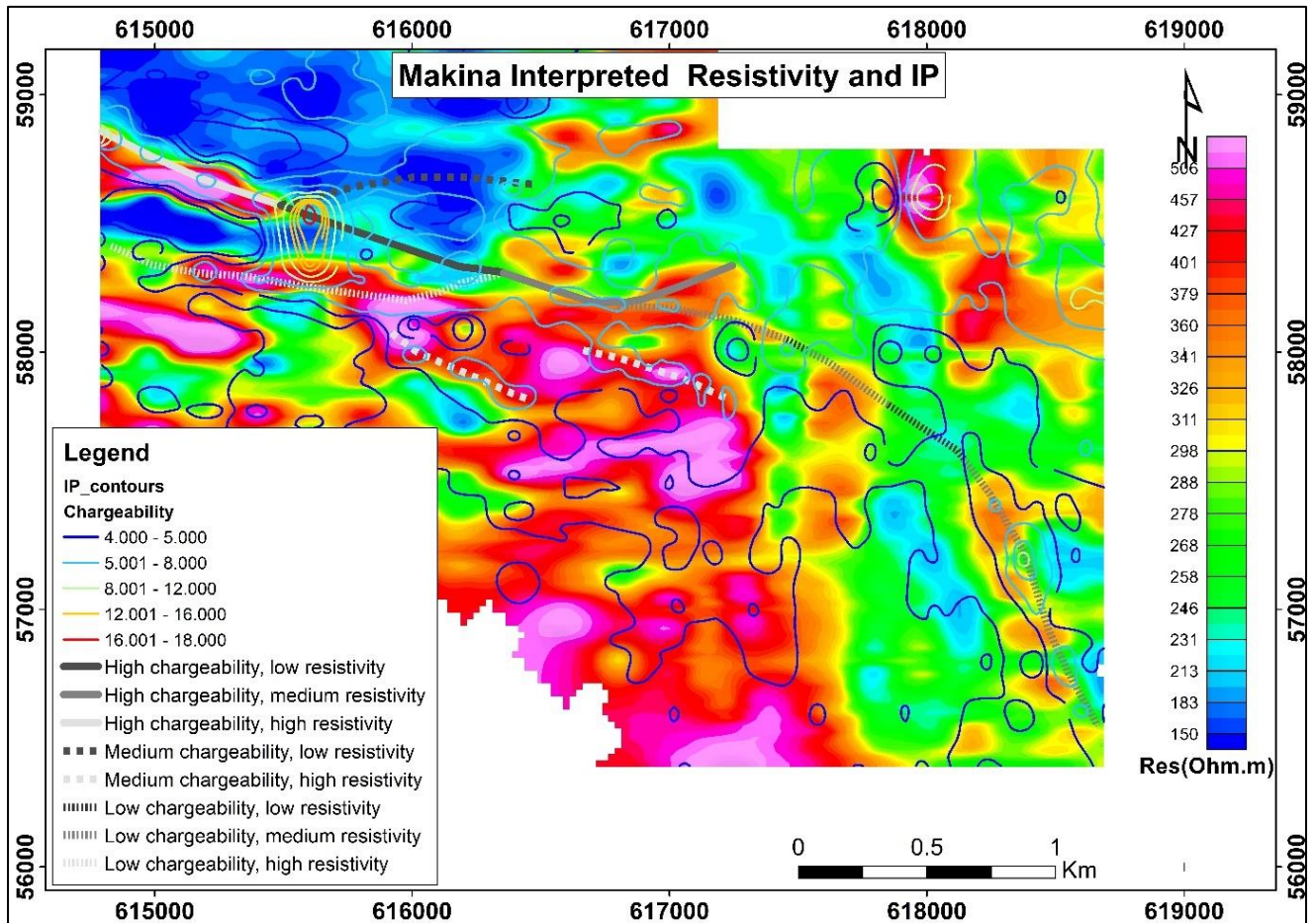
Figure 4.20: Map of Makina Chargeability contours over Resistivity data.

High chargeability anomalies are therefore, the prime target zone for occurrence of deeper mineralization and the electrical resistivity or conductivity of the chargeable zone would further improve on the nature and possible characterization of the chargeable body. These should be strongly be corroborated by geochemical results and observable surface evidence of related geological formations and mineralization.

4.3.2 Magnetic Anomalies

The magnetic anomaly maps produced from the ground magnetics data confirm to a significant level the observations from the historical aeromagnetic data. Several faults and shear patterns can be deduced from the grids. The tilt derivative map illustrates most of the structural relationships and fault orientations (Figure 4.21). The Reduced to Pole magnetic map perfectly accentuates the east -west trending features and provides a clear image of the structure suspected to control mineralization in this prospect (Figure 4.22).

The Reduced to Pole magnetic data portrays the distinct variations in the geological characterization of the prospect. The previously identified mafic dyke that runs from the Southeastern extent of the map towards the northwest is quite conspicuous in the magnetic maps. A geological map of the surveyed area has been produced from preliminary analysis of the magnetic field data and is illustrated by Figure 4.23. The interpretation suggests the occurrence of a mafic dyke cutting through mafic volcanics to the south of the area. A Banded Iron formation unit has been interpreted from the magnetic structure observed to be running from the east of the area towards the northwest and is ensconced in mafic volcanics. Towards the north, a zone of sedimentary rocks can be deduced. Two zones have been interpreted as being granitic intrusions that is, to the eastern edge of the license, bordering Tira and to the south of the mafic dyke and mafic volcanics.
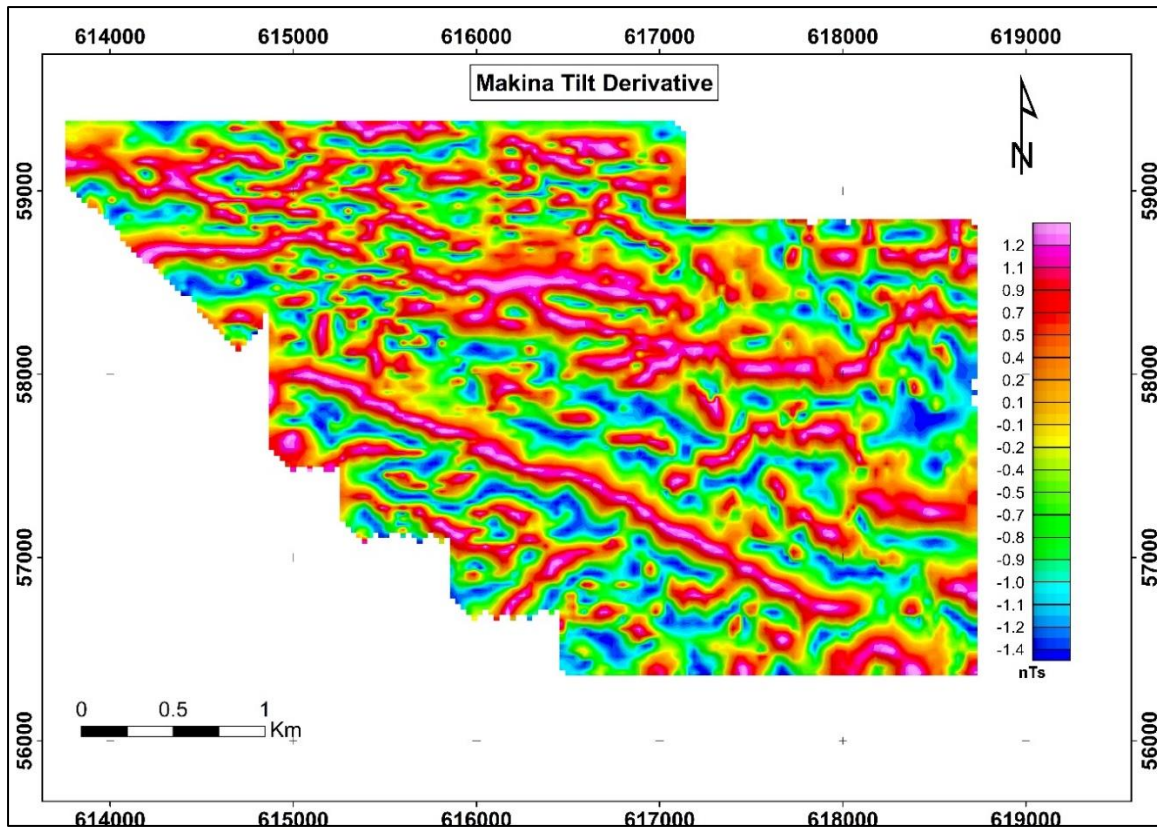
Figure 4.21: Makina Magnetics- Tilt derivative
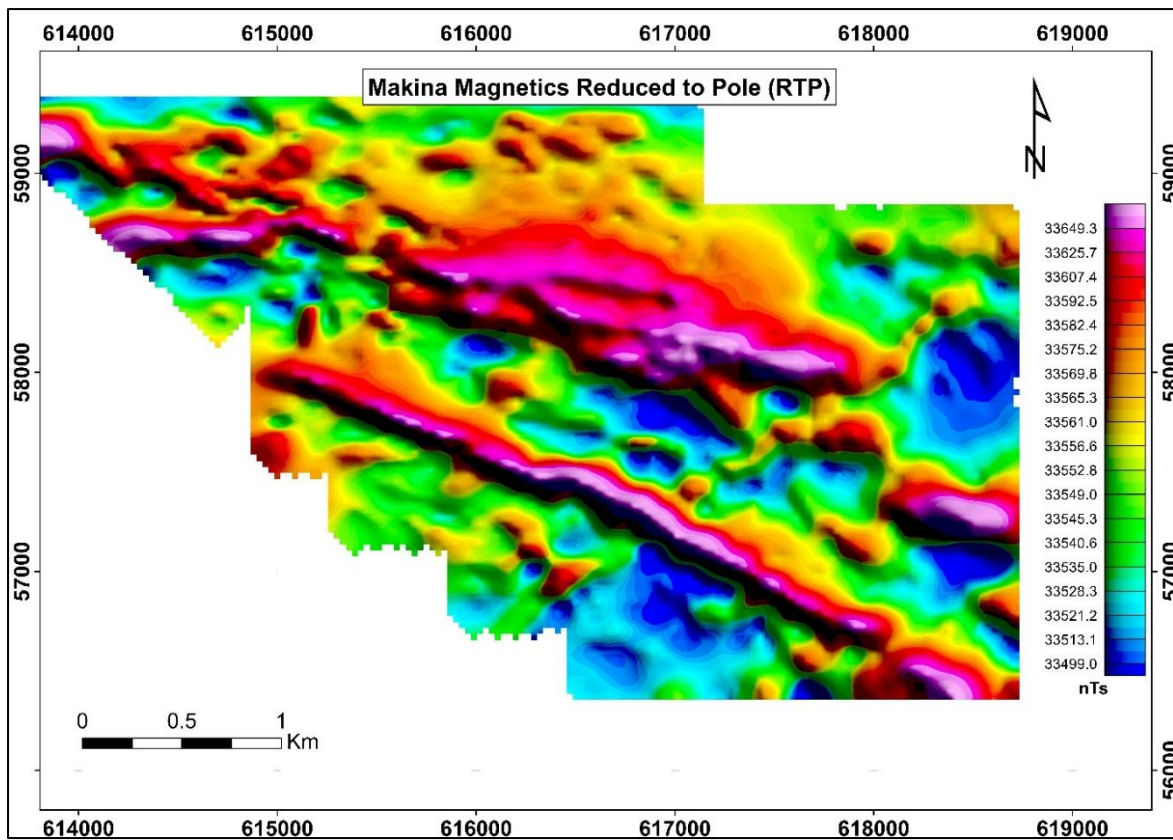
Figure 4.22: Residual Magnetics Reduced to pole (RTP)
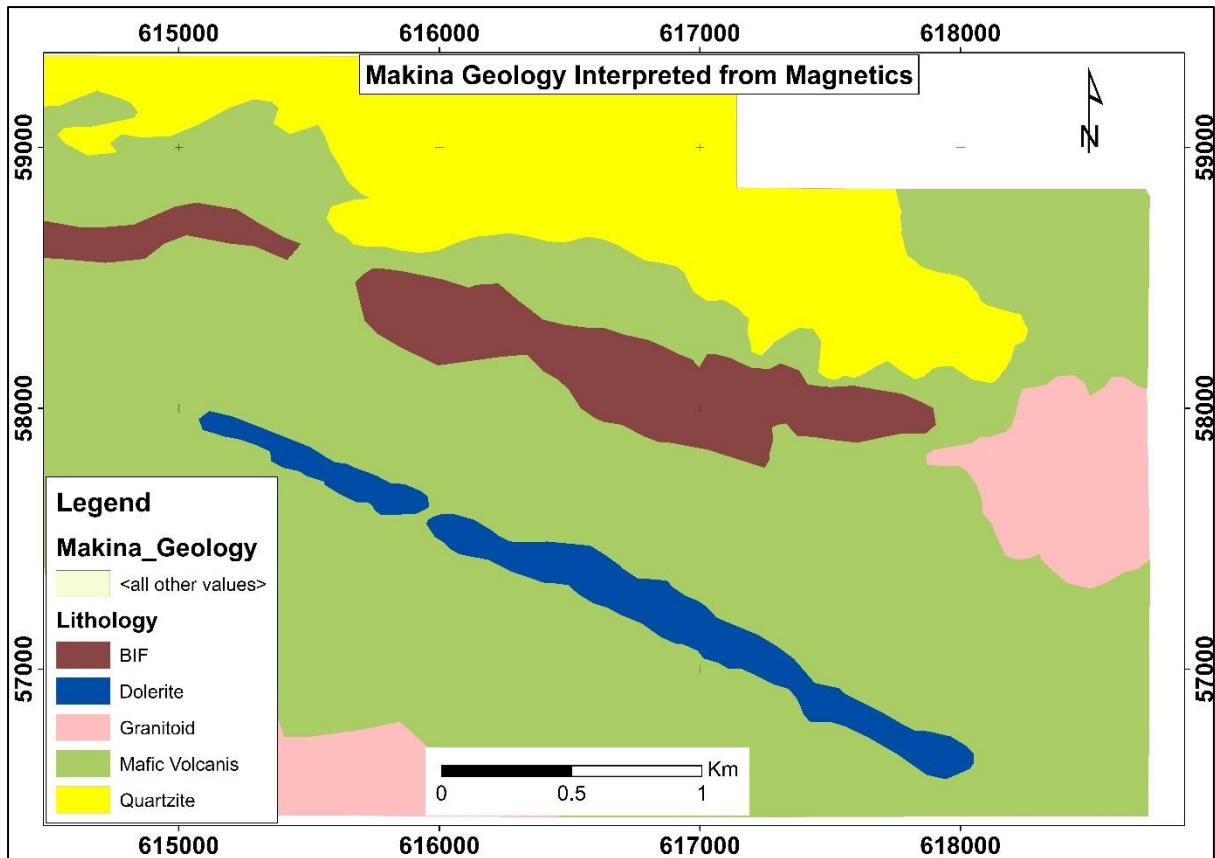
Figure 4.23: Interpreted geology map of the surveyed area as deduced and interpreted for Magnetics data.

Several faults and lineaments crosscutting all the lithologies have been interpreted and they contribute towards understanding of the structural architecture of the prospect. The interpreted lineaments reflect a general WNW strike for most of the geological structures with secondary cross cutting structures oriented towards NE and some to the NW especially at the northeastern segment. Figure 4.24 and Figure 4.25 present the interpret lineaments and Oasis Montaj.

Figure 4.24: Magnetic, reduced To Pole with interpreted structures.
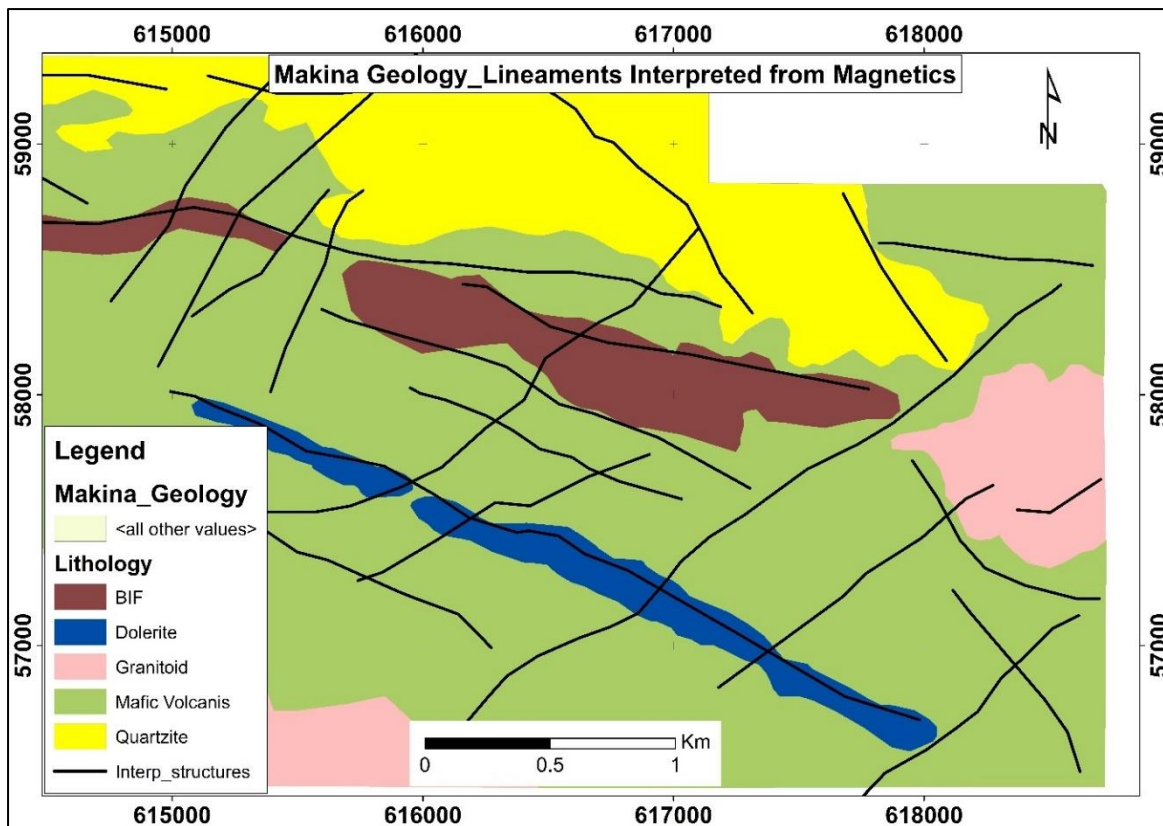
Figure 4.25: Map of the interpreted geology structural lineaments.

The targeted zones for this geophysical exploration exercise exhibit a crucial relationship between soil geochemical anomalies and the magnetic signatures Figure 4.26. This can be attributed to the specific nature of the subsurface geology as may be revealed by future subsurface studies. However, it can be said that the structural and genetic deformation events have had much influe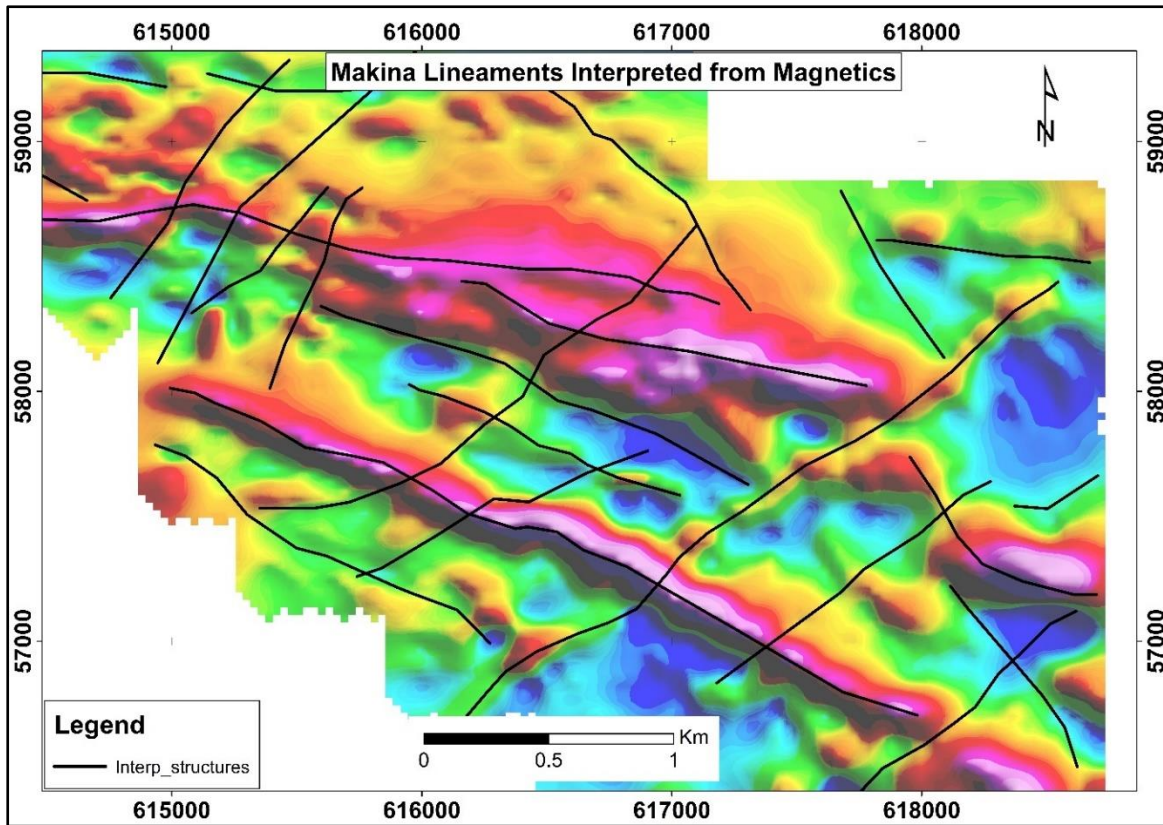nce on the nature and spread of the magnetic features in the area. Some of the events may be responsible for the occurrence or deposition of gold mineralization in the prospect.
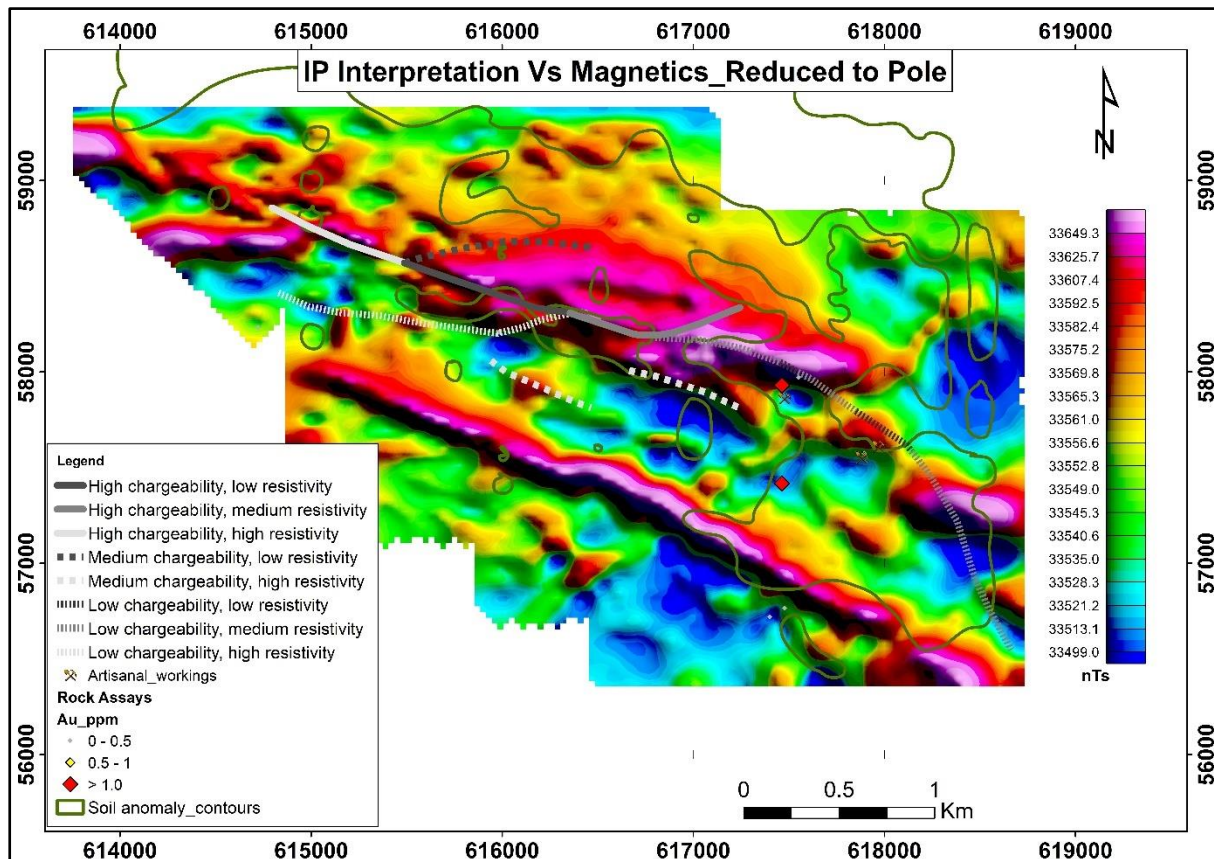
Figure 4.26: Interpreted IP anomaly distribution plotted on soil geochemical trends and Magnetics Reduced to Pole.

The Magnetic Susceptibility 3D inversion model reveals possible continuity of some of the magnetic anomalies up to 500m below surface, particularly the anomalies linked to the chargeability targets and within the anomalous soil geochemistry zones.

Superimposing the interpreted linear model of the chargeability and resistivity anomalies on the various magnetic maps has revealed a direct relation between some of the magnetic anomalies and IP anomalies. This relationship can be seen on the surface as observed in the

magnetic map in Figure 4.27, and extends at depth given the conformity illustrated in the overlay at 100m below surface (Figure 4.28).
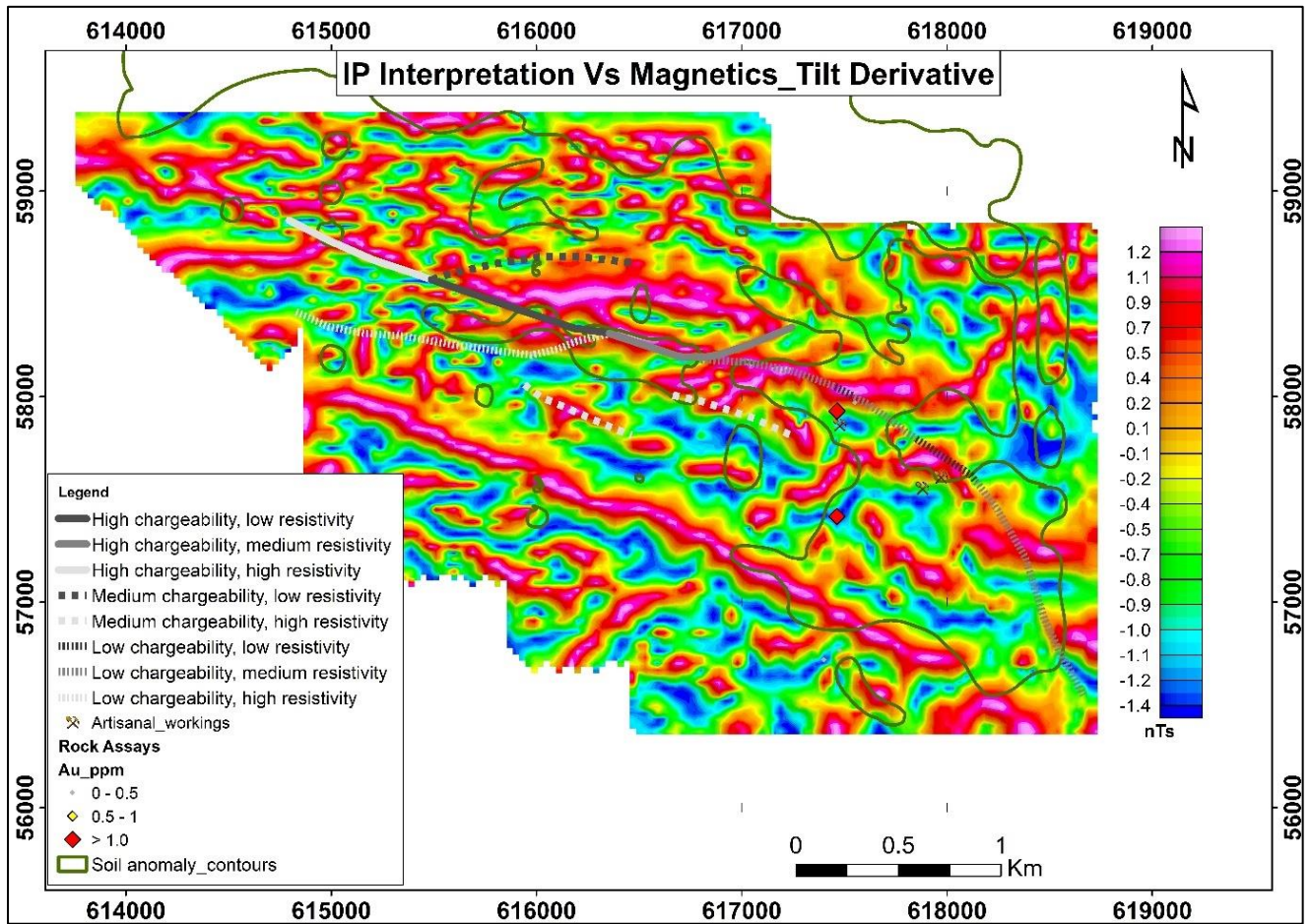
Figure 4.27: Interpretation of the IP anomalies distribution and soil anomaly trends superimposed on the magnetics Tilt Derivative map.
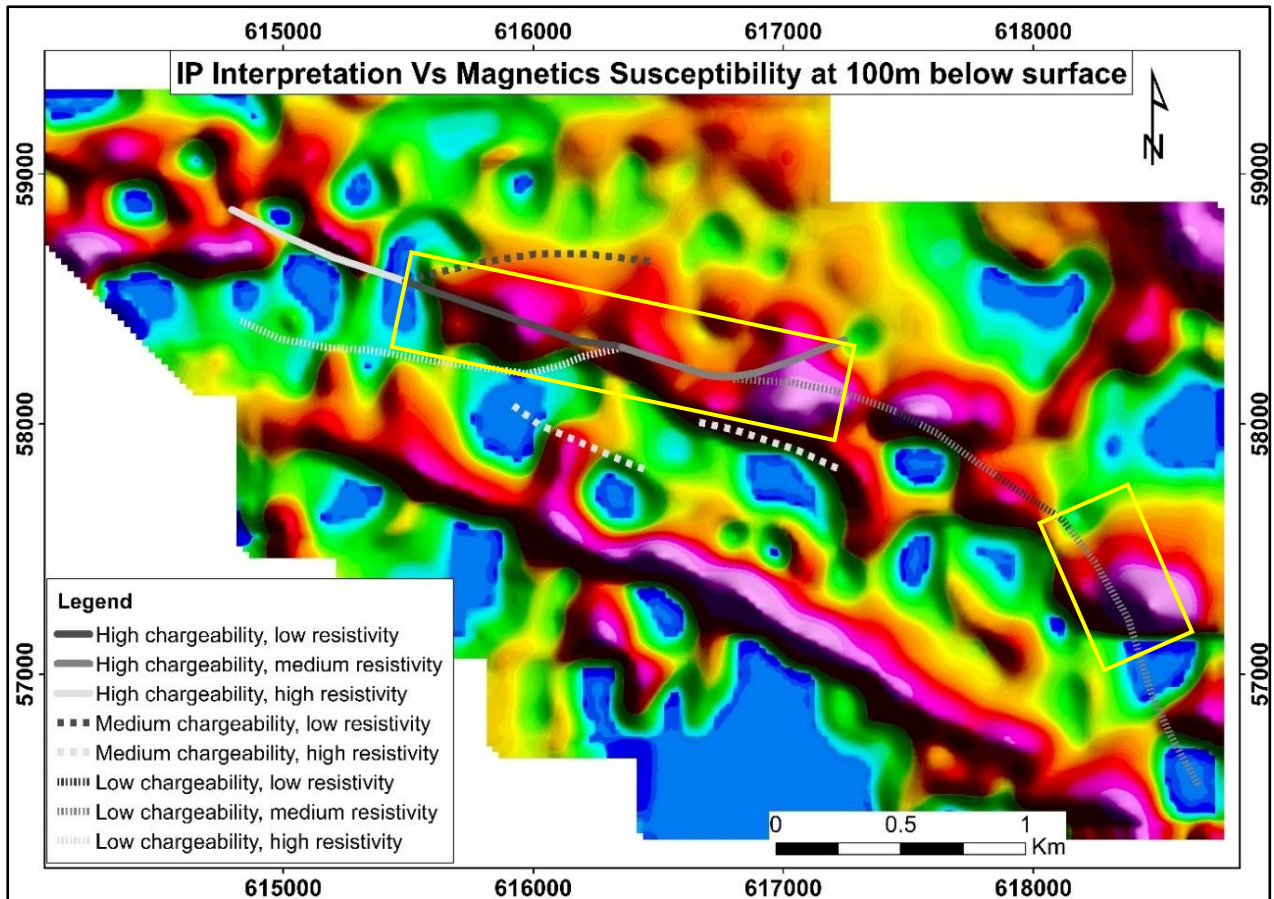
Figure 4.28: IP anomaly trend plotted over the 100m depth slice of the magnetic susceptibility model showing significant IP anomalies associated with magnetic anomalies occurring 100m below. The significant zones are highlighted by the yellow rectangles.

4.3.3 Potential gold mineralization targets

Superimposing the IP and Resistivity interpreted anomalies on the magnetics Reduced to Pole in addition to the magnetics interpretation, reveals how much the potential mineralization in the area may have been influenced by geological structures and lithology. Two zones with chargeable anomalies have been identified as potential mineralization target areas (Figure 4.29). These two zones have their chargeability anomalies coinciding with interpretable conductive bodies and well-defined magnetic anomalies. More importantly, these zones coincide well with soil geochemical anomalies and interpreted geological structures (Figure 4.30).

Figure 4.29: Makina Chargeability map with the identified IP anomaly target zones marked as Zone A and Zone B.
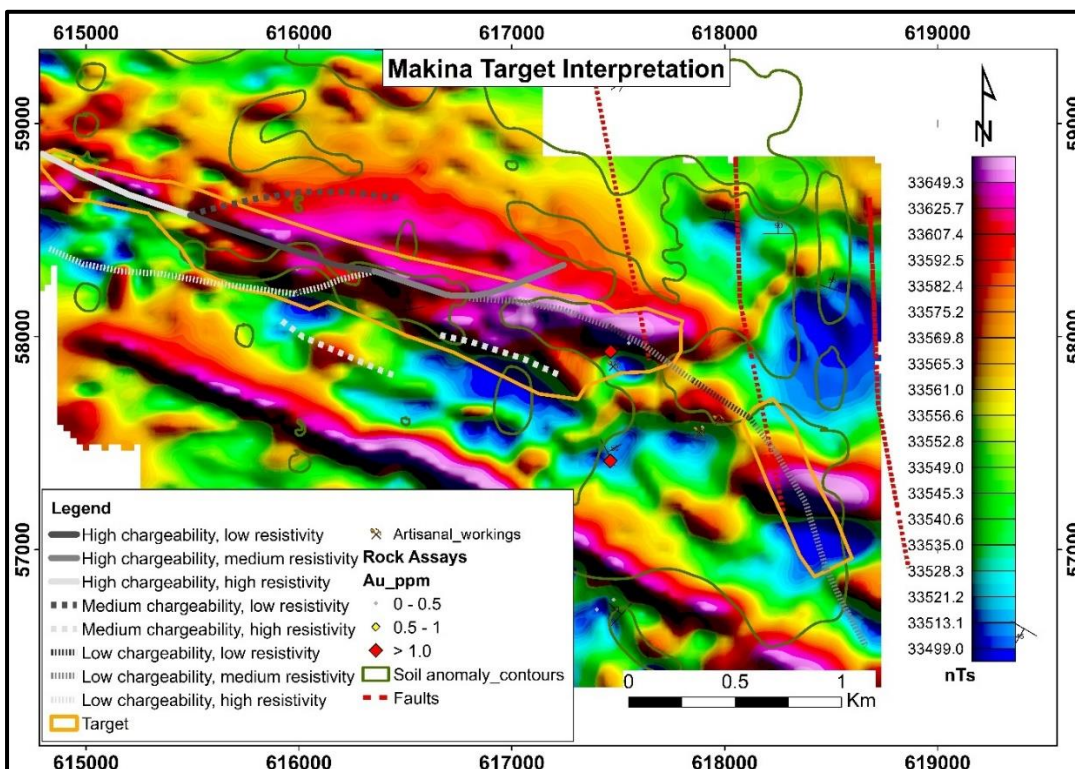
Figure 4.30: Makina Target Zones interpretation, illustrating the relationship between the identified target zones (orange polygons), ground magnetic data, soil geochemistry and geological structures/ faults.

The main target zone identified (Zone A) is the WNW - ESE oriented anomaly that can be attributed to both the occurrence of Banded Iron Formation as well as structural controls Figure 4.31). Conjugate structures as derived and indicated by the interpreted lineaments demonstra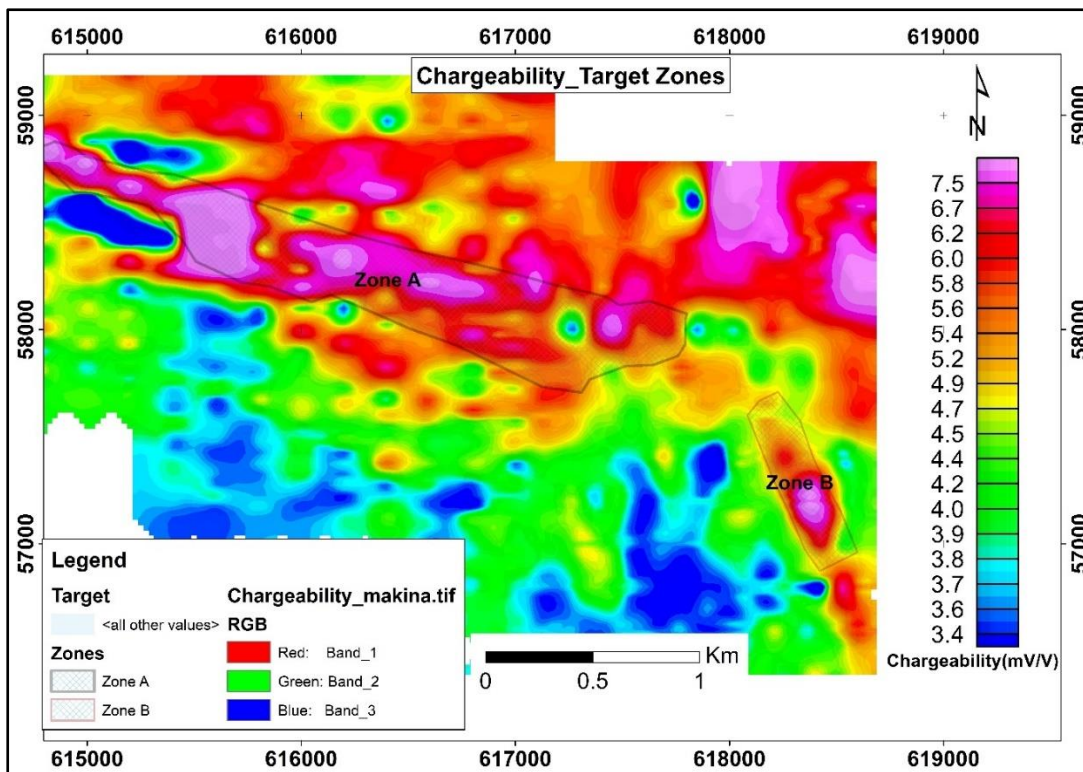te a possible interplay between the main shear and related orthogonal to oblique splay structures. This structural interplay is possibly responsible for the occurrence of mineralization. The combination of high chargeability and low to medium resistivity in this zone points to the target's high potential for hosting significant volumes of sulphides or sulphide associated mineralization. The fact that the chargeable zone coincides with the interpreted gold in soil geochemical trends as well as observed occurrences of Banded Iron Formation further raises the target's potential for hosting a significant gold deposit (Figure 4.32). The interpreted structures in this zone also indicate the possible occurrence of shear hosted vein deposits. The western-most segment of this zone although characterized by high resistivity accompanying high chargeability may still be an indication for sulphide mineralization possibly in a high silica environment. Target Zone-A stretches along strike, for about 3.2km but only as far as the area that was captured in the survey (Figure 4.31). There is possibility of its extension further towards the North west of the grid.
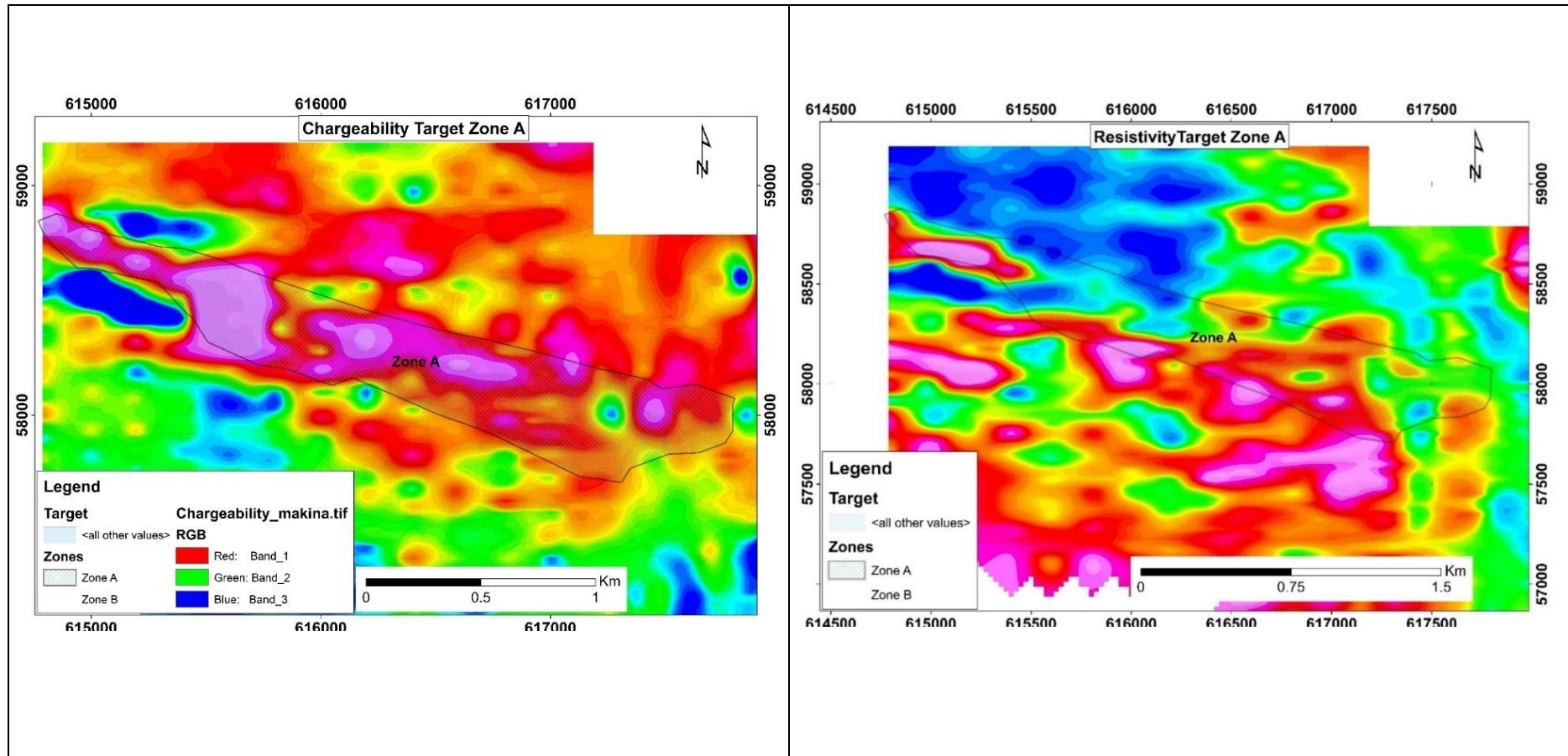
Figure 4.31: Comparison of the Changeability anomaly in Zone A with the zone's resistivity signatures on right. This comparison shows how the high chargeability target accompanied by low to moderate resistivities.
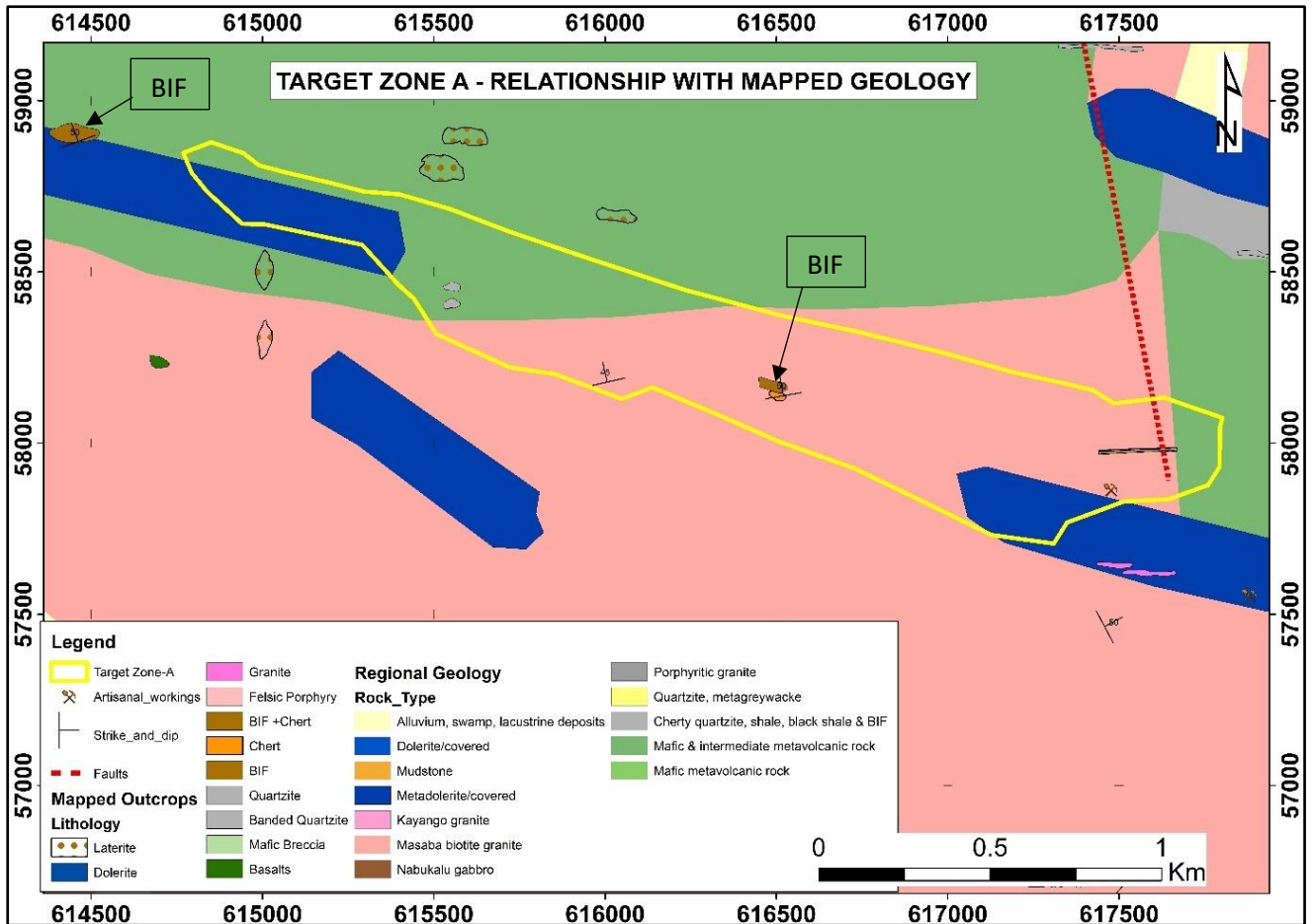
Figure 4.32: Target Zone A highlighted in yellow polygon and the associated Banded Iron Formation trend as observed from outcrop locations.

The second potential target zone (Zone B) occurs at the southeastern corner of the survey area with a Northwest strike (Figure 4.33). It stretches up to about 1.2km long. This zone is characterized by a medium to high chargeability anomaly accompanied by low to medium resistivity (Figure 4.33). The competency contrast that is seemingly depicted by the almost north-west oriented structures possibly indicate fault zones. This target zone lies conformably on the soil geochemical anomalies initially targeting the North south oriented faults and fractures associated with active artisanal gold mining (Figure 4.34). The mineralization in this zone could be an extension of that manifested at the Tira mines to the east.
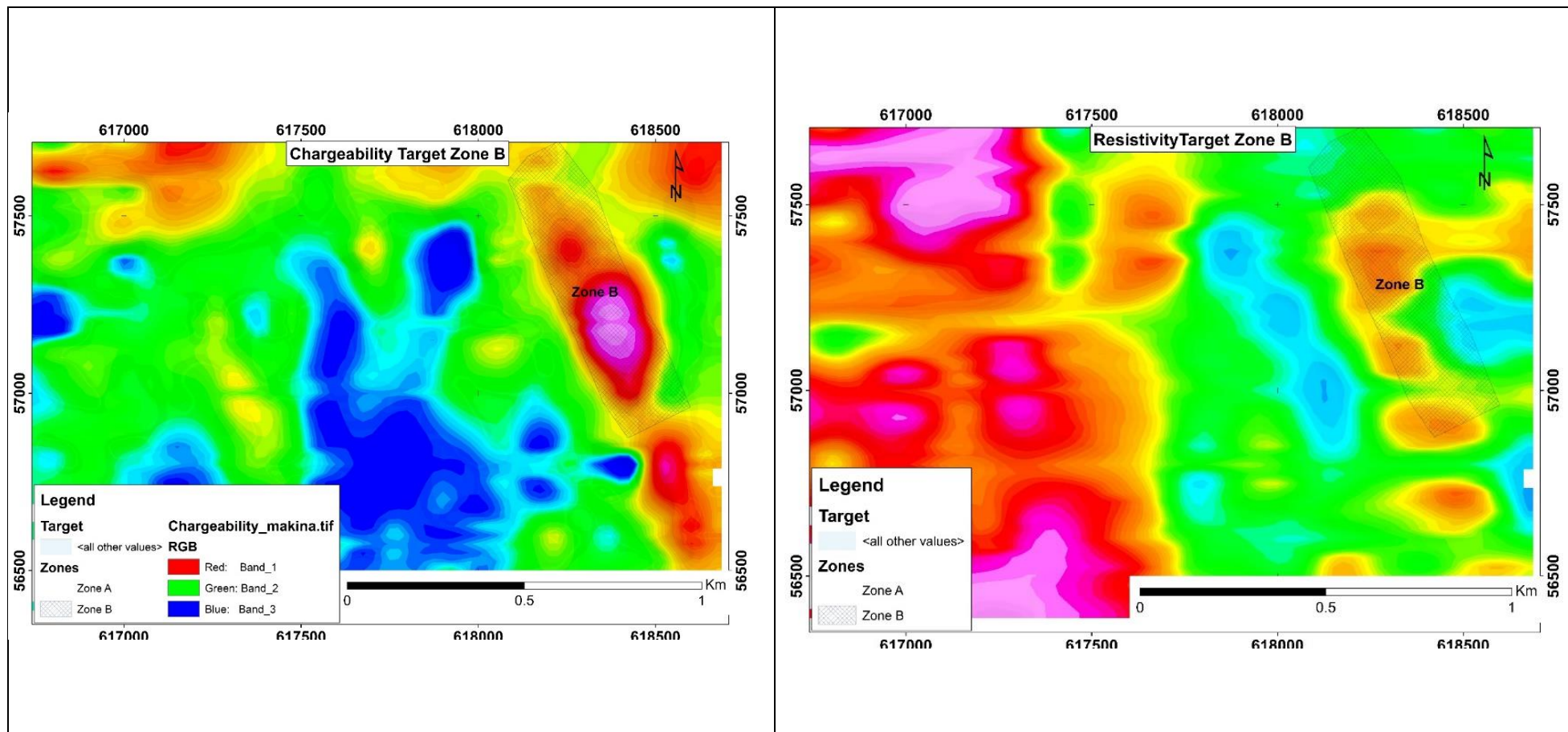
Figure 4.33: The high chargeability target zone (Zone B) on the left and the linked resistivity signatures; mostly low to medium resistivity.
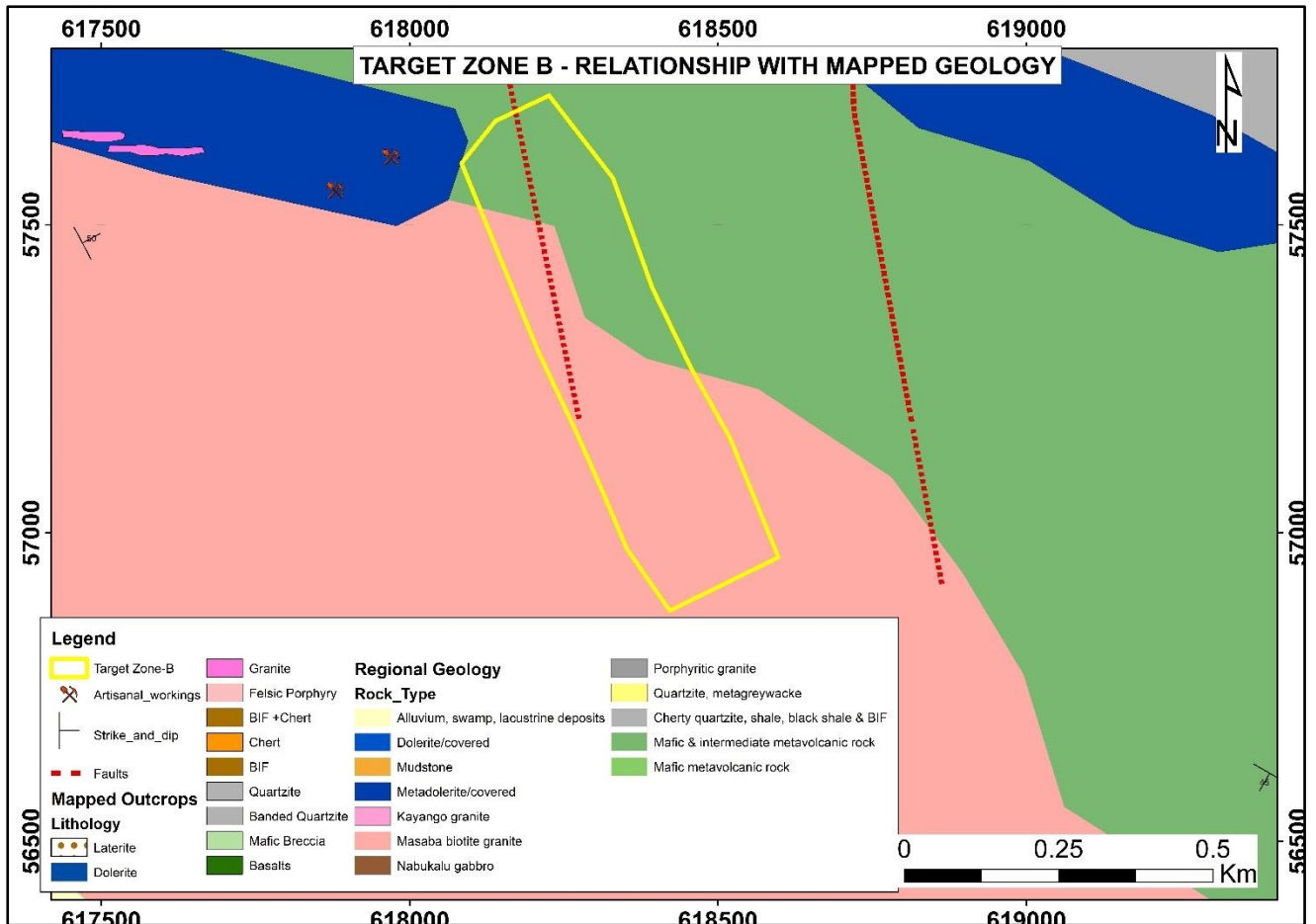
Figure 4.34: Target zone B highlighted in yellow polygon with nearby artisanal mining site and the NW oriented fault.

These two target zones have been suggested for advanced exploration in order to improve the deposit understanding and further delineating the potential gold deposits. However, there is still evidence of continuity of mineralization further to the north of the surveyed area that may be good ground for future extensive work.

Pole dipole induced polarization survey lines across the two identified target zones have been proposed as shown in Figure 4.35, Figure 4.36 and Figure 4.37. The pole dipole surveys would detail further potential of the chargeable bodies in addition to their orientation and depth extent.

The Magnetic Susceptibility inversion model also shows there's potential for the anomalous bodies extending as deep as 500m below the surface in some segments. Figure 4.38 illustrates the 3D projection of the high magnetic anomalies that have been linked to the chargeability anomalies.

The combination of IP/Resistivity and magnetics has proven useful in the delineation of subsurface features, especially features specific to occurrence of gold mineralization and could

thus be employed in the surrounding areas that contain good soil anomalies in addition to surficial evidences of gold mineralization through active artisanal mining sites. The methods applied in this study would also work well in areas where geochemical signatures may be masked by erosional events such as leaching and lateritization which are commonly encountered in the Busia gold district.
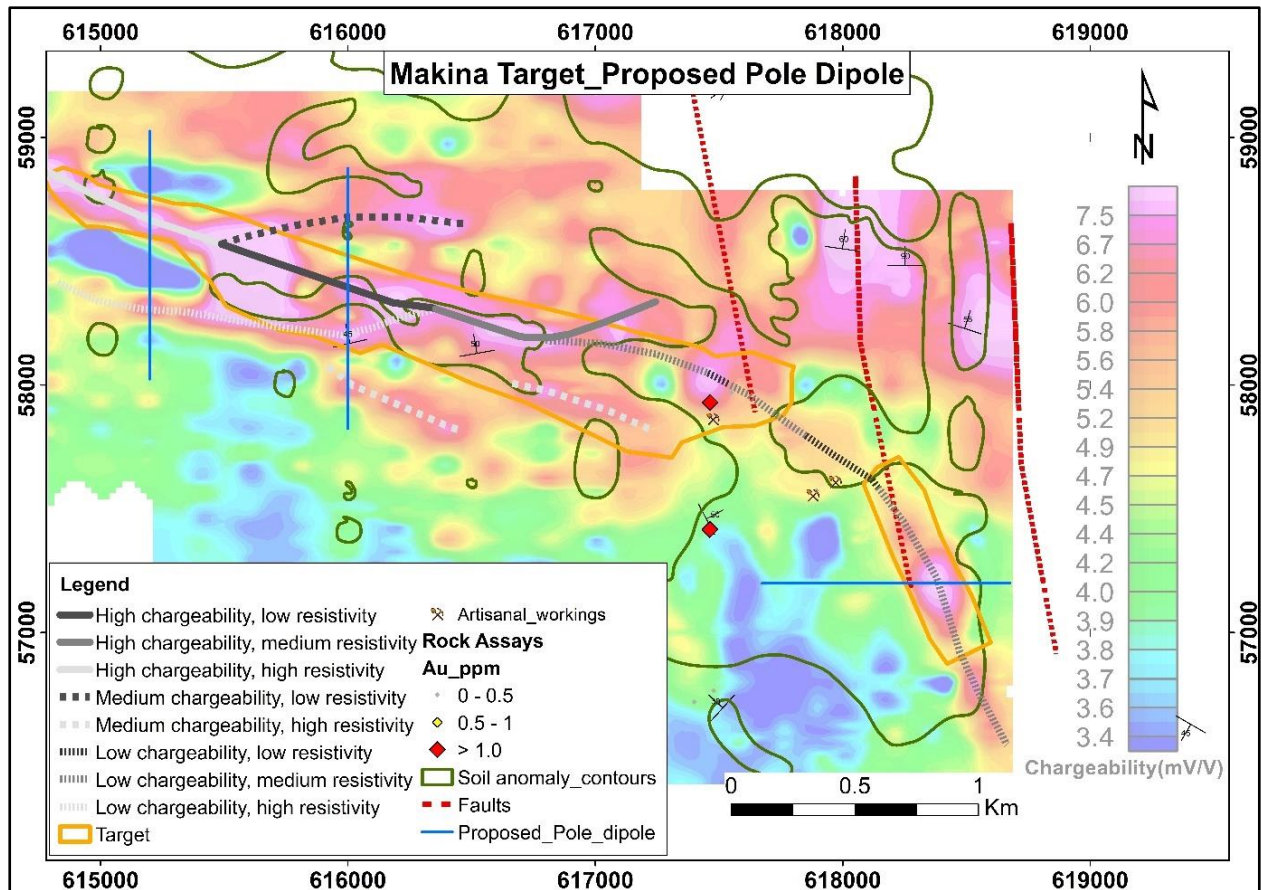
Figure 4.35: Proposed follow up Pole dipole survey lines over the identified target zones superimposed on the chargeability and geochemical maps.
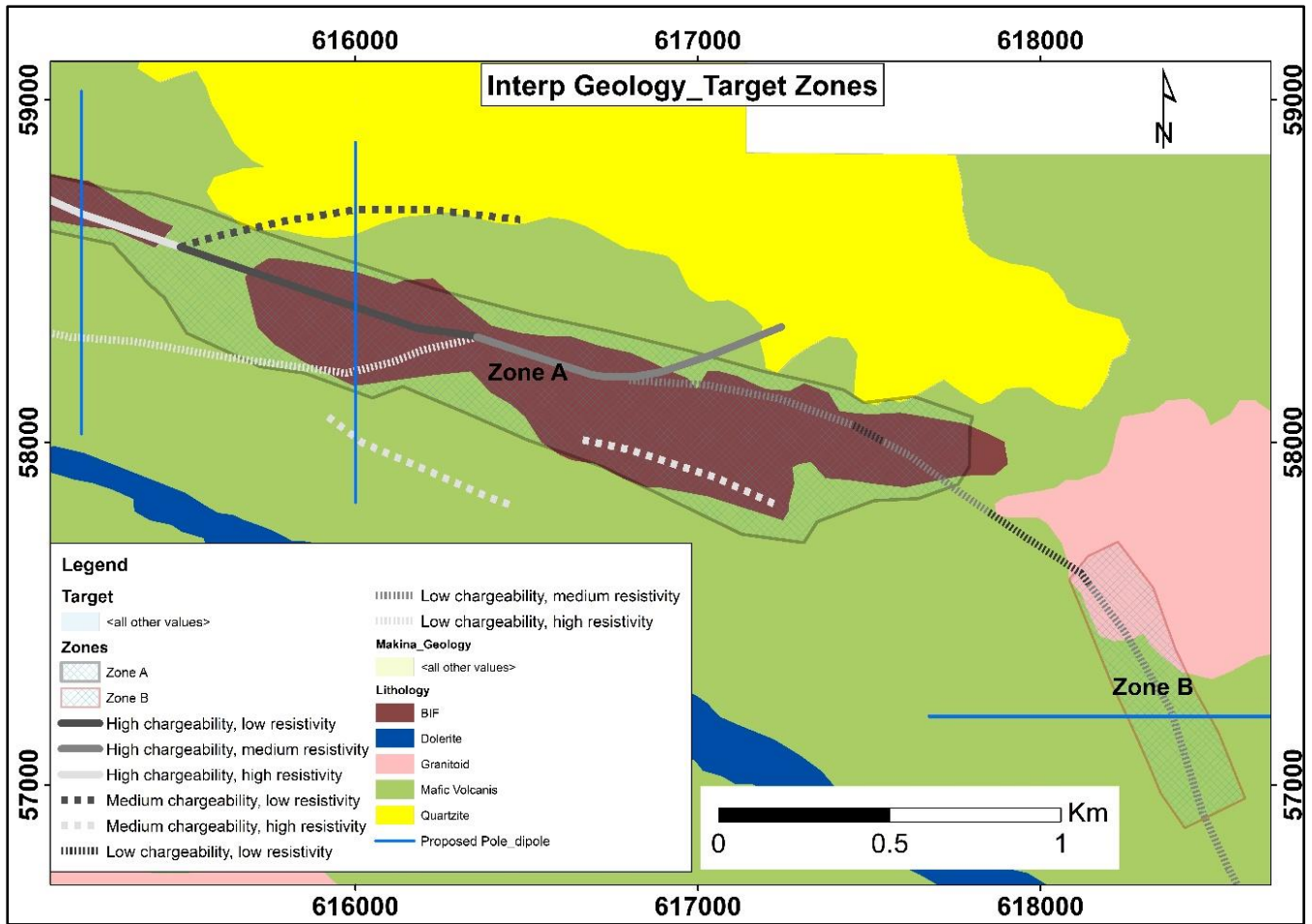
Figure 4.36: Proposed Pole dipole lines (blue lines) over the identified mineralized zones and interpreted geology.
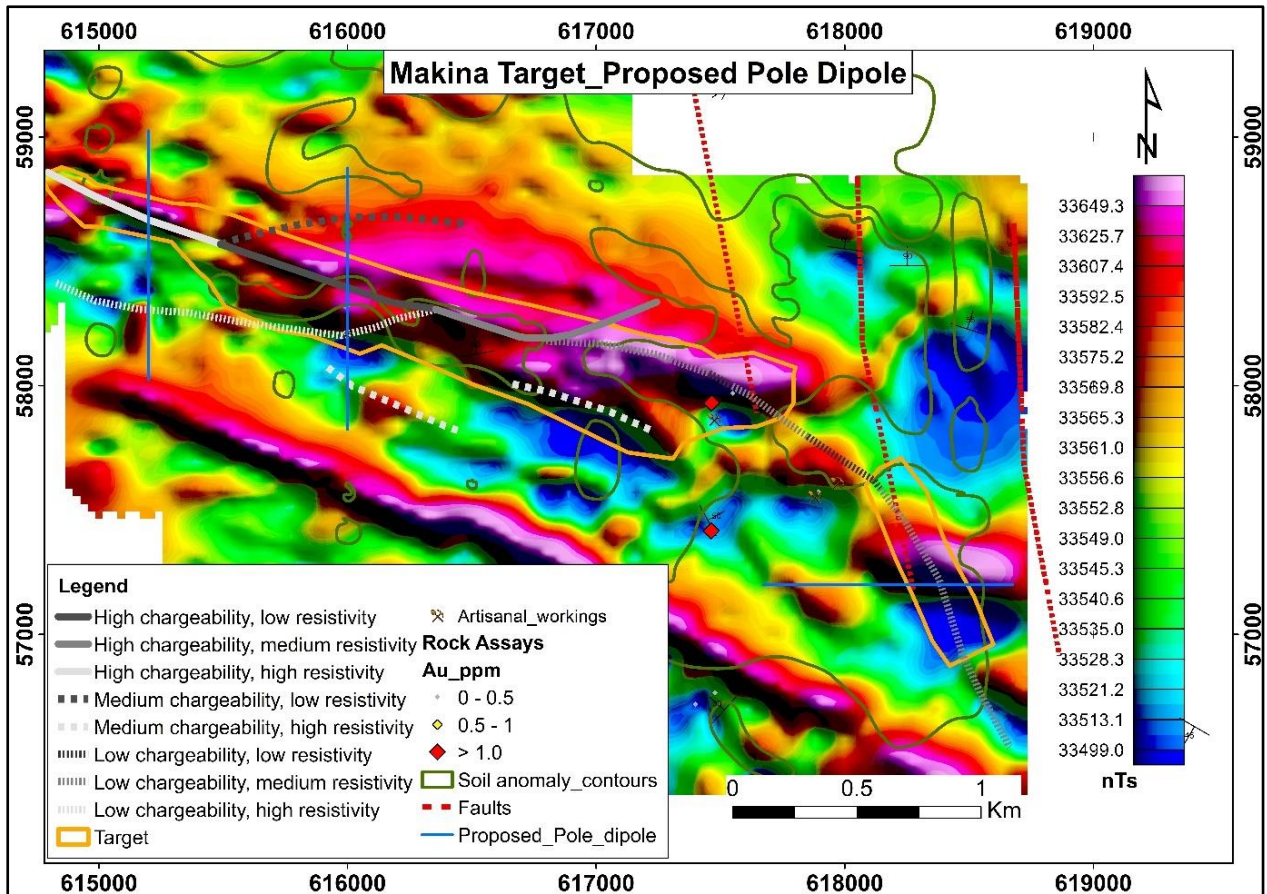
Figure 4.37: Proposed Pole dipole lines on interpreted magnetics, geochemical structural and IP data.
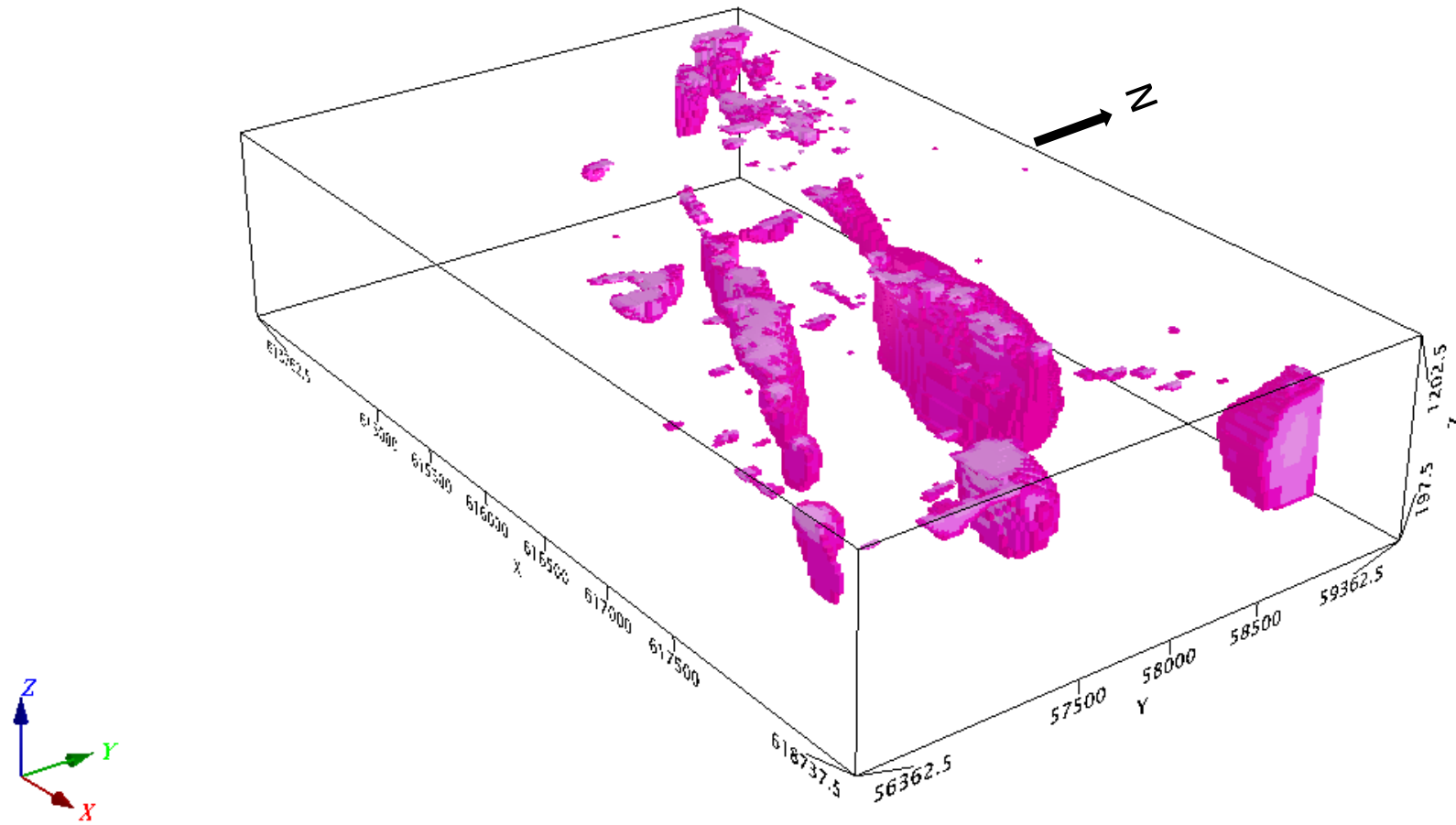
Figure 4.38: Magnetic susceptibility inversion model clipped to subsurface zones of high magnetic signatures related to identified mineralization targets.

CHAPTER 5   CONCLUSIONS AND RECOMMENDATIONS

5.1 CONCLUSIONS

Two main target zones have been delineated from the geophysical survey results. The geophysical surveys in Makina prospect have shown that the gold mineralization in this area occurs mostly in the Nyanzian volcanic facies and associated sediments while being boosted to a great degree by structural dynamics. This is evidenced by the fact that the obtained chargeability anomalies and their associated magnetic signatures occur within these lithologic facies and are equally coincident with the interpreted gold in soil geochemical anomalies. The soil geochemical analysis initially highlighted the positive relationship between gold anomalies and base metals such as lead (Pb), zinc, silver and copper, a typical suite represented in sulphide rich environments such as Volcanogenic Massive sulphide deposits. This association could be a possible occurrence in Makina especially given that most high chargeability zones (meaning sulphide occurrences) are also reflected as high magnetic anomalies potentially suggesting occurrence of Iron sulphide (pyrrhotite/ pyrite) rich bodies. The central identified target zone (Zone A) is characterized by a general WNW trending structure that appears to be sheared and fractured with an interplay of other structures oblique to the main trend. In this main zone, high chargeability is accompanied by zones high, medium and low resistivity. The less resistive segment in this zone also registers a magnetic anomaly signature that appears consistent even at depth. This relationship could point to the occurrence of mineralized quartz veins within the BIF formations. The mineralized quartz veins may be compact enough to give the high resistivity signatures while contained sulphides and the conductive BIFs account for the chargeable zones of lower resistivity. The second identified target to the south east (Zone B) is probably hosted in a fracture/ fault zone, hence the low resistivity signatures and alternating pattern of medium to low resistivity. The granitic intrusion to the northeast of this anomaly is likely to be responsible for both the proximal structural dynamics and possibly the source of mineralizing fluids. This second zone (Zone B) lies on soil geochemical anomalies that were obtained by focusing on the previously mapped N-S trending faults. The distribution of high chargeability signatures in both highly resistive and less resistive bodies demonstrates that sulphide mineralization which is associated with gold mineralization may be present as disseminated in quartz veins as well as in altered or significantly deformed host rocks. The gold mineralization in Makina is typical of the orogenic greenstone hosted model, common in most Archaean greenstone belts. Both target Zone A and B demonstrate high potential for the

occurrence of significant gold deposits. This can be supported by the fact that the two reasonably extensive zones exhibit the perfect geological architecture necessary for the occurrence of large deposits, and that evidence of gold occurrence in the same trends is provided by the flourishing artisanal activities along the identified zones. Follow up exploration is necessary to further delineate and define the deposit. The major chargeability anomalies identified are potentially future drilling targets. The narrow BIF having been encountered in few locations needs to be mapped distinctly and extensively. Before drilling the identified target zones, it would be important to conduct Pole-dipole IP and Resistivity survey over the identified Gradient IP anomalies. The Pole dipole and dipole- dipole array methods provide pseudo sections and even 3D inversion models of both the Resistivity and chargeability up to significant depths depending on the array spread. The inversion models and pseudo sections will be more useful in accurately siting drill holes and understanding the potential orientation of the mineralization at various depths below the surface. The gradient array Induced Polarization method is a faster method for mapping out the potential mineralization zones in comparison to the dipole-dipole or pole- dipole arrays methods which are rather more intensive, hence, time consuming and costly. Results from the gradient array have significantly reduced the cost and time factors that would have been incurred if the dipole-dipole or pole-dipole arrays methods were to be employed over the entire area.

5.2 RECOMMENDATIONS

It is first important to validate the results of this survey by conducting confirmatory profiles as suggested, using Pole-Dipole Induced Polarization. The confirmation and further revelation of the form of the anomaly in the subsurface would aid the design of future drill holes.

Secondly, investigations both geochemical and petrographic are necessary to distinctively identify the lithological facies existing within the prospect.

Similar exploration practices should be employed in the properties to the north as well as the western extensions, this is necessary if the full extent of the observed potential is to be ascertained.

There is potential for continuity of similar gold mineralization styles to the Kenyan side of the Busia border. The immediate grounds to the east of the border are basically underexplored, while recent works on the Uganda side have registered tremendous results recently, with a new mine being set up at the moment, coincidentally a BIF hosted deposit.

REFERENCES

Aseto, C., Ochola K., Njau., K, Malidzo J. (2018). *Mayfox Mining Company, Uganda Exploration Report.*

Boyd, G., & Wiles, C. (1984). The Newmont drill-hole EMPsystem – Examples from eastern Australia. *Geophysics, 49*, 949–56.

Clark, D. A. (1997). Magnetic petrophysics and magnetic petrology: aids to geological interpretation of magnetic surveys. *AGSO Journal of Australian Geology & Geophysics*, 83- 103.

Davies, K. A. (1956). *The geology of SE Uganda.* Memoir No. 8, Department of GeologicalSurvey and Mines, Uganda.

Dindi, E., & Maneno, J. (2016). Geological and geophysical characteristics of massive sulphide deposits: A case study of the lirhanda massive sulphide deposit of Western Kenya. *Journal of African Earth Sciences*.

Doyle, H. A. (1990). Geophysical exploration for gold. *Geophysics, 55*, 134-146.

Edwards, L. S. (1977). A modified Pseudosection for resistivity and induced-polarization. In *Geophysics* (Vol. 3, pp. 78–95.).

Fon, A. N., Che, V., & Suh, C. H. (2012). Application of Electrical Resistivity and Chargeability Data on a GIS Platformin Delineating Auriferous Structures in a Deeply Weathered Lateritic Terrain, Eastern Cameroon. *International Journal of Geosciences*, 960-971.

Gallas, J. D. (2015). Quartz prospecting with Induced Polarization (IP) and Resistivity by using Gradient and Dipole-Dipole arrays. *Brazilliand Journal of Geophysics (RBGf)*.

Groves, D., Goldfarb, R., Gebre-Mariam, Hagemann, S., & Robert, F. (1998). Orogenic gold deposits: a proposed classification in the context of their crustal distribution and relationship to other gold deposit types. *Ore Geology Reviews, 13*, pp. 7-27.

Hagemann, S. G., & Cassidy, K. F. (2000). Archean orogenic lode gold deposits. *Hagemann S. G. & Brown P. E. eds.*, 9–68.

Harris, J. (1961). Summary of the Geology of Tanganyika. *EconomicGeology; Geological Survey of Tanganyika, Memoir 1, Part IV*, ,133p. (reprinted 1981).

Henckel, J., Poulsen, K., & Sharp, T. S. (2016). Lake Victoria Goldfields. *Episodes- IUGS, 39*(2).

Ichang'i, D. (1990). *The Migori Segment of the Archean Nyanza Greenstone Belt, Kenya: Geology, Geochemistry and Economic Potential.* Ph. D Thesis, McGill University, Montreal.

Ichang'i, D. (1993). Lithostratigraphic of mineralization in Migori Segment of the Nyanza Greenstone Belt, Kenya. *5th Conference on Geol. Kenya.*, (pp. 73-84).

Ichang'i, D., & McLean, W. (1991). The Archean volcanic facies in the Migori segment, Nyanza Greenstone Belt, Kenya: Stratigraphy, Geochemistry and Mineralization. *J. African Earth Sci., 13*, 277-290.

Kearey, P., Brooks, M., & Hill, I. (2002). *An Introduction to Geophysical Exploration, Third Edition.* Blackwell Science Ltd: London.

Loke, M. (2015). *Tutorial : 2-D and 3-D electrical imaging surveys.* Unpublished.

Marjoribanks, R. (2010). *Geological Methods in Mineral Exploration and Mining.* London: Springer.

Mbonimpa, A. (2005). *The Genesis and characteristics of Gold mineralisation in the Area between River Malaba and River Solo in Busia District, South eastern Uganda.* M.Sc. Geology Thesis, Makerere University.

Mbonimpa, A. B., Barifaijo, E., & Tiberindwa, J. V. (2007). The Potential for Gold mineralisation in the Greenstne Belt of Busia District, South Eastern Uganda. *African Journal of Science and Technology, 8*(Science and Engineering Series), 116 - 134.

Moon, C. J., Whateley, K. G., & Evans, M. (2006). *Introduction to mineral exploration* (Second ed.). Blackwell Publishing.

Mroz, J. P., Urien, P., Baguma, Z., & Viallefond, L. (1991). *Gold exploration in Busia area, Uganda (Phase 1).* Bureau de recherchesgéologues et minières (BRGM).

Ngecu, W., & Gaciri, S. (1995). Lithostratigraphy provenance and facies distribution of Archean cratonic successions in western Kenya. *J. African Sci., 21*, 359-372.

Nyakecho, C., & Hagemann, S. G. (2014). An overview of gold systems in Uganda. *Australian Journal of Earth Sciences*.

Ogala, J. (1987). Mineralisation in the Migori greenstone belt, Macalder, Kenya. *J. African Geology*, 26-44.

Ogola, J., & Omenda, P. (1991). Nyanzian greenstone belts and their gold mineralisation. *IGCP no.273 Newsletter/Bulletin 1*, 61-67.

Old, R. A. (1968). *The geology of part of South-East Uganda.* PhD thesis, Leeds University, Research Institute of African Geology.

Opiyo- Aketch, N. (1991). Geochemical evidences for the tectono-magmatic emplacement of the Kenyan greenstone belt rocks from the Maseno area, western Kenya. *IGCP No. 273, Bulletin 1*, pp. 69-74. Pretoria.

Opiyo-Aketch, N. (1988). *Geology and Geochemistry of the late Archaean greenstone association in Maseno area, Kenya.* Ph. D Thesis, University of Leicester, Leicester, U.K.

Reeves, C. (2005). *Aeromagnetic Surveys: Principles, Practice and Interpretation.* Geosoft.

Robert, F. (2004). Characteristics of lode gold deposits in greenstone belts. *24ct Au workshop, Horbart, CODES Special Publication*, *5*, pp. 1-12.

Scott, W. (2014). *Geophysics for Mineral Exploration.* Matty Mitchell Room and Labrador Department of Natural Sciences.

Serwanga, C., Fiset, N., & Iga, M. (1994). *Geophysical surveys carried out on EPL 4099, Busia area, Tororo district, south eastern Uganda.* Internal Technical Report GP-2. , Geological Survey and Mines Department and United Nations Department for Development.

Sharp, T. R., Poulsen, H., & Tosdal, R. (2016). Geology of the Archean Busia-Kakamega Greenstone Belt, Western Kenya. *35th International Geological Conference.* Cape Town.

Smith, M., & Anderson, C. (2003). Gokona Gold Deposit, Northern Tanzania - Discovery and Delineation. *New Gen Gold Conference*, (pp. 10-20). Perth, Australia.

Sumner, J. (1976). Principles of Induced Polarization for Geophysical Exploration. *Elsevier Scientific*.

Tanner, P. (1973). Orogenic Cycles in East Africa. *Geological Society of America, Bulletin 84*, 2839–2850.

Telford, W., Geldart, L., & Sheriff, R. (1990). *Applied Geophysics.* (second edition ed.). Cambridge: Cambridge University Press.

Waswa, A. (2015). *Petrology and Iron ore mineralization in the Neoproterozoic Mozambique Belt rocks of Mutomo- Ikutha area, Kitui County, S.E. Kenya.* Ph. D Thesis, University of Nairobi.

Westerhof, A., Härmä, P., Isabirye, E., Katto, E., Koistinen, T., Kuosmanen, E., . . . Virransalo, P. (2014). *Geology and Geodynamic Development of Uganda with Explanation of the 1:1,000,000 -Scale Geological Map.* Special Paper 55, Geological Survey of Finland, Espoo.
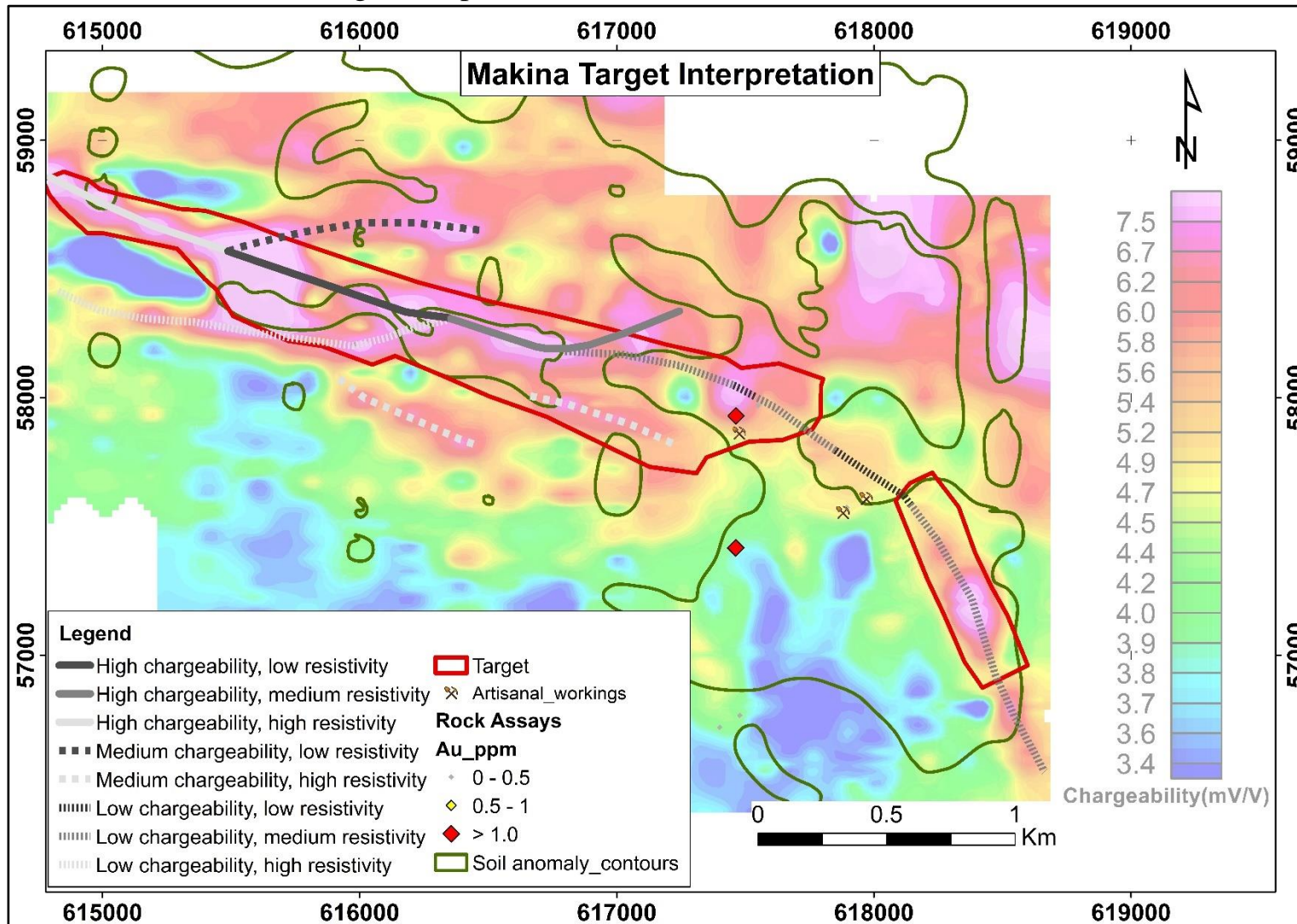
APPENDIX 1: Chargeability anomaly map of the surveyed area with the interpreted anomaly trends and identified target zones.
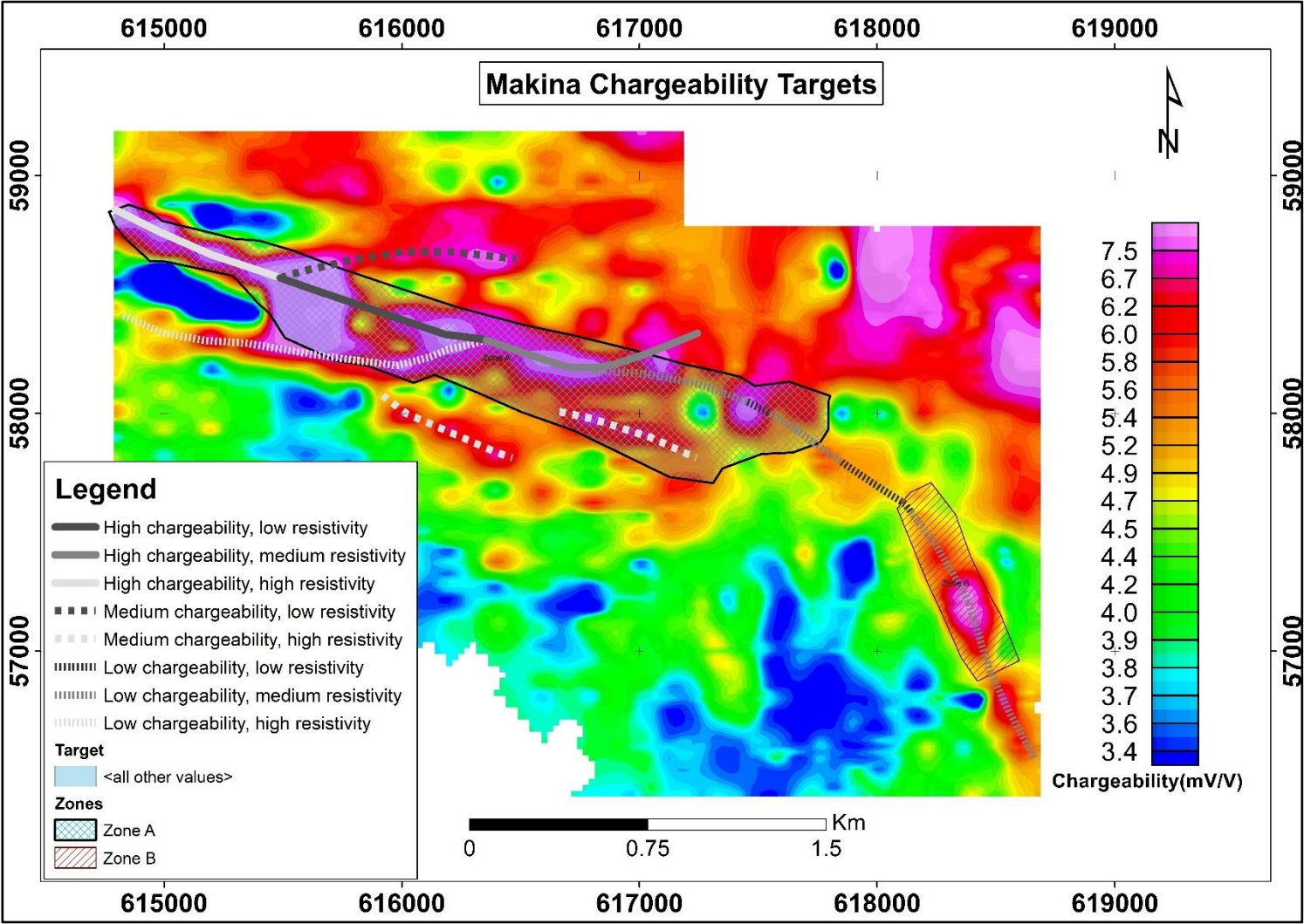
APPENDIX 2: Resistivity anomaly map of the surveyed area with identified mineralization target zones.
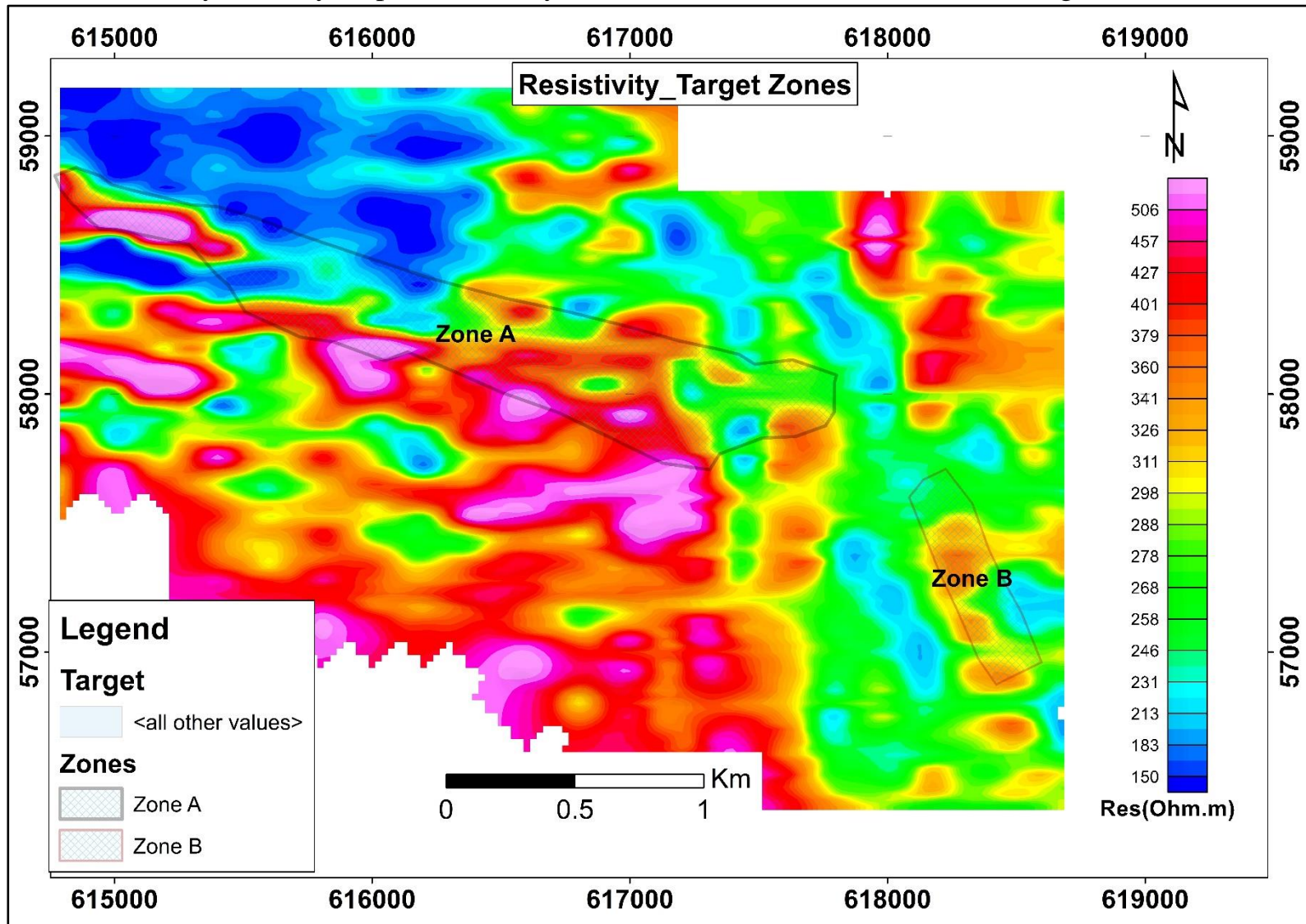
APPENDIX 3: Makina Target Interpretations

APPENDIX 4: Makina regional geology map and recently mapped outcrops

Makina Regional Geology vs Mapped Outcrops

Legend

⚒ Artisanal_workings

┼ Strike_and_dip

▪ ▪ Faults

Mapped Outcrops
Lithology
⦙∴ Laterite
■ Dolerite
■ Granite
▯ Felsic Porphyry
■ BIF +Chert
■ Chert
■ BIF
▯ Quartzite
■ Banded Quartzite
▯ Mafic Breccia

■ Basalts

Regional Geology
Rock_Type
▯ Alluvium, swamp, lacustrine deposits
■ Dolerite/covered
■ Mudstone
■ Metadolerite/covered
■ Kayango granite
▯ Masaba biotite granite
■ Nabukalu gabbro
▯ Porphyritic granite
▯ Quartzite, metagreywacke
▯ Cherty quartzite, shale, black shale & BIF
■ Mafic & intermediate metavolcanic rock
■ Mafic metavolcanic rock

0   0.5   1
▬▬▬▬▬ Km

APPENDIX 5: Makina Geology, geochemical and Induced polarization interpretations

Makina Geology, Geochem and Interpreted IP anomalies

Legend

High chargeability, low resistivity
High chargeability, medium resistivity
High chargeability, high resistivity
Medium chargeability, low resistivity
Medium chargeability, high resistivity
Low chargeability, low resistivity
Low chargeability, medium resistivity
Low chargeability, high resistivity
Artisanal_workings
Soil anomaly_contours

Strike_and_dip

Faults

Mapped Outcrops
Lithology
Laterite
Dolerite
Granite
Felsic Porphyry
BIF +Chert
Chert
BIF
Quartzite
Banded Quartzite
Mafic Breccia
Basalts

Regional Geology
Rock_Type
Alluvium, swamp, lacustrine deposits
Dolerite/covered
Mudstone
Metadolerite/covered
Kayango granite
Masaba biotite granite
Nabukalu gabbro
Porphyritic granite
Quartzite, metagreywacke
Cherty quartzite, shale, black shale & BIF
Mafic & intermediate metavolcanic rock
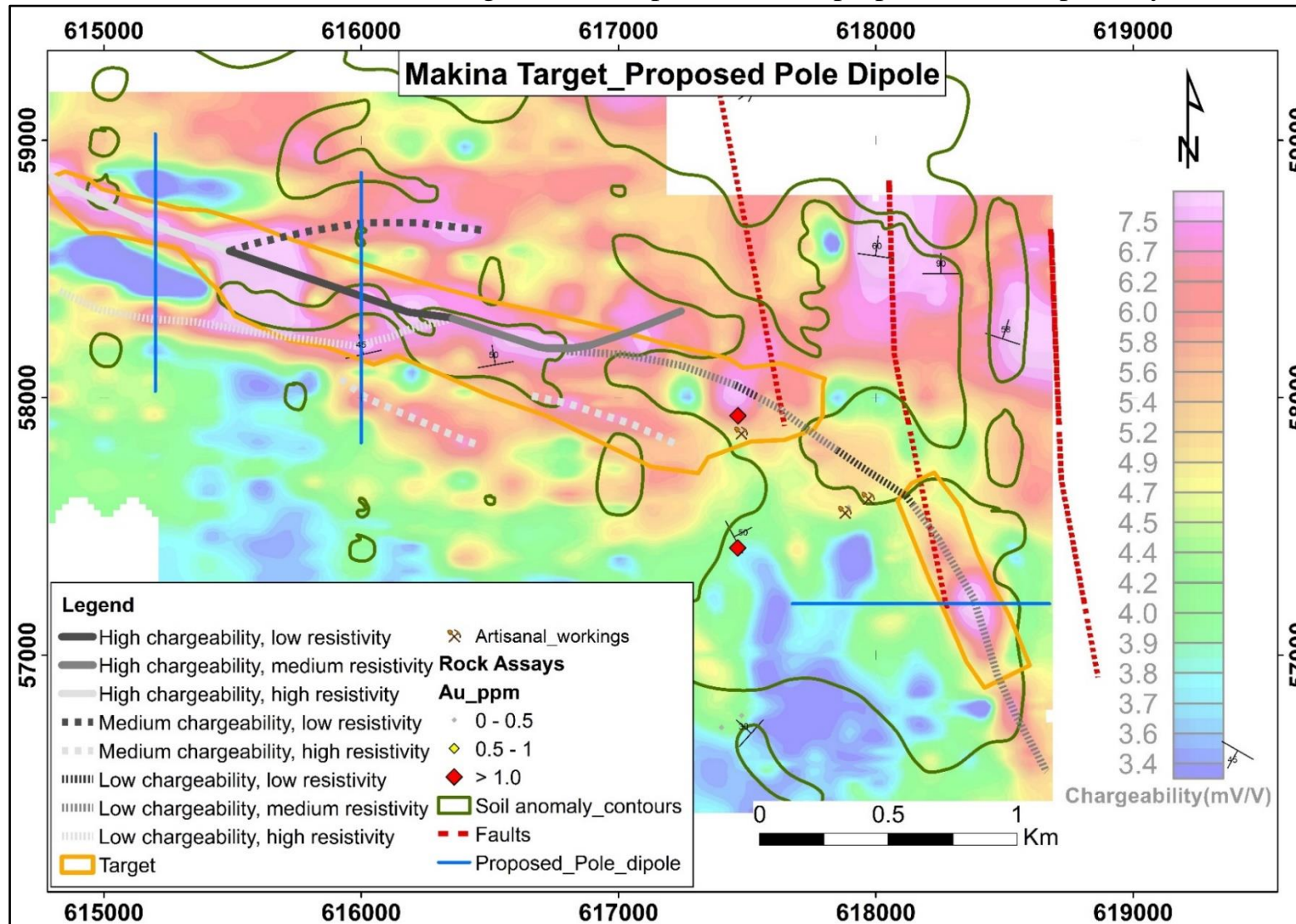Mafic metavolcanic rock

APPENDIX 6: Proposed priority Pole dipole survey lines colored in blue; L5200E, L6000E and L7200N, over the initial Gradient array lines and chargeability map, superimposed on the area google earth image.
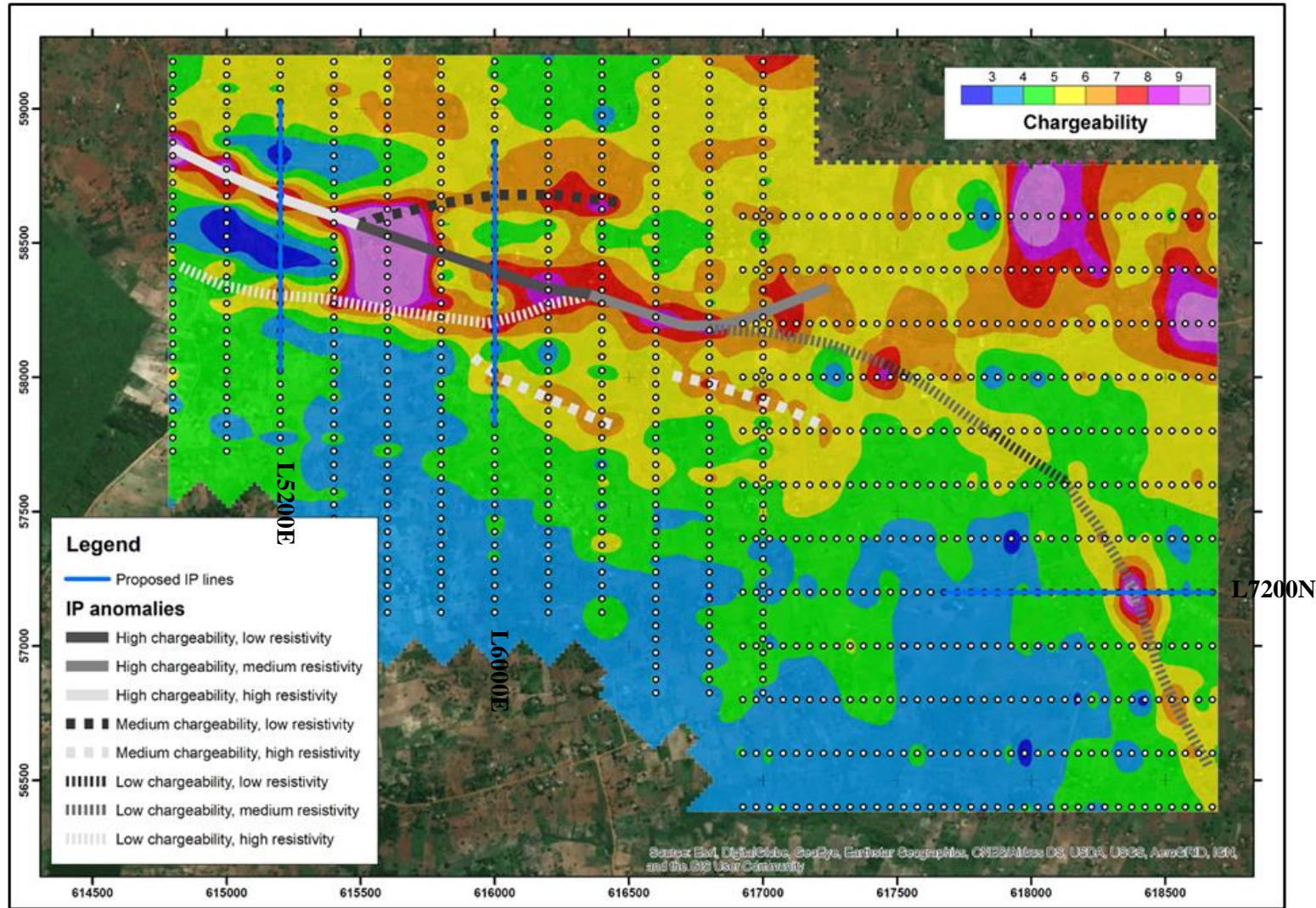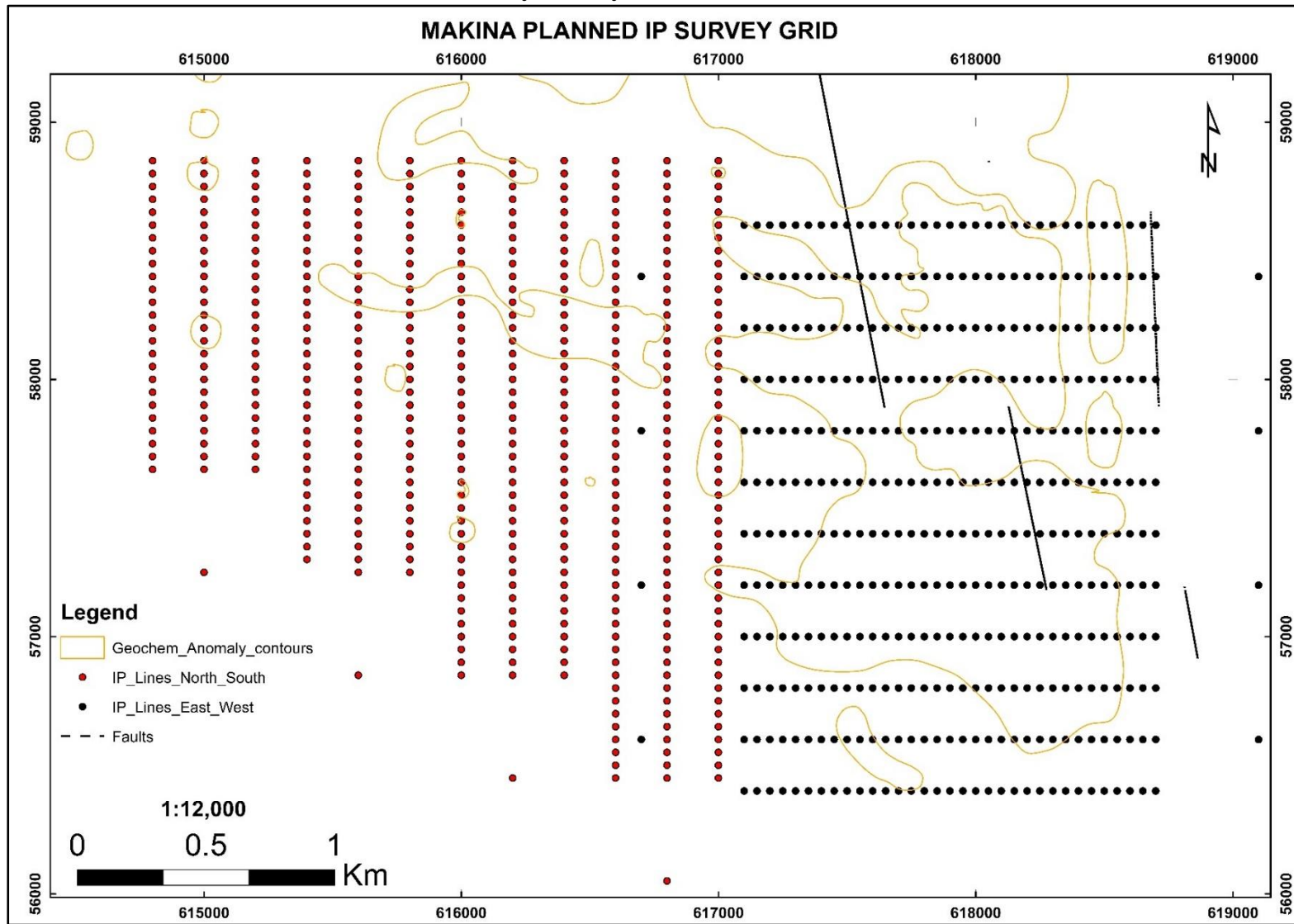
APPENDIX 7: Interpreted Chargeability and Resistivity anomalies and proposed pole-dipole lines.
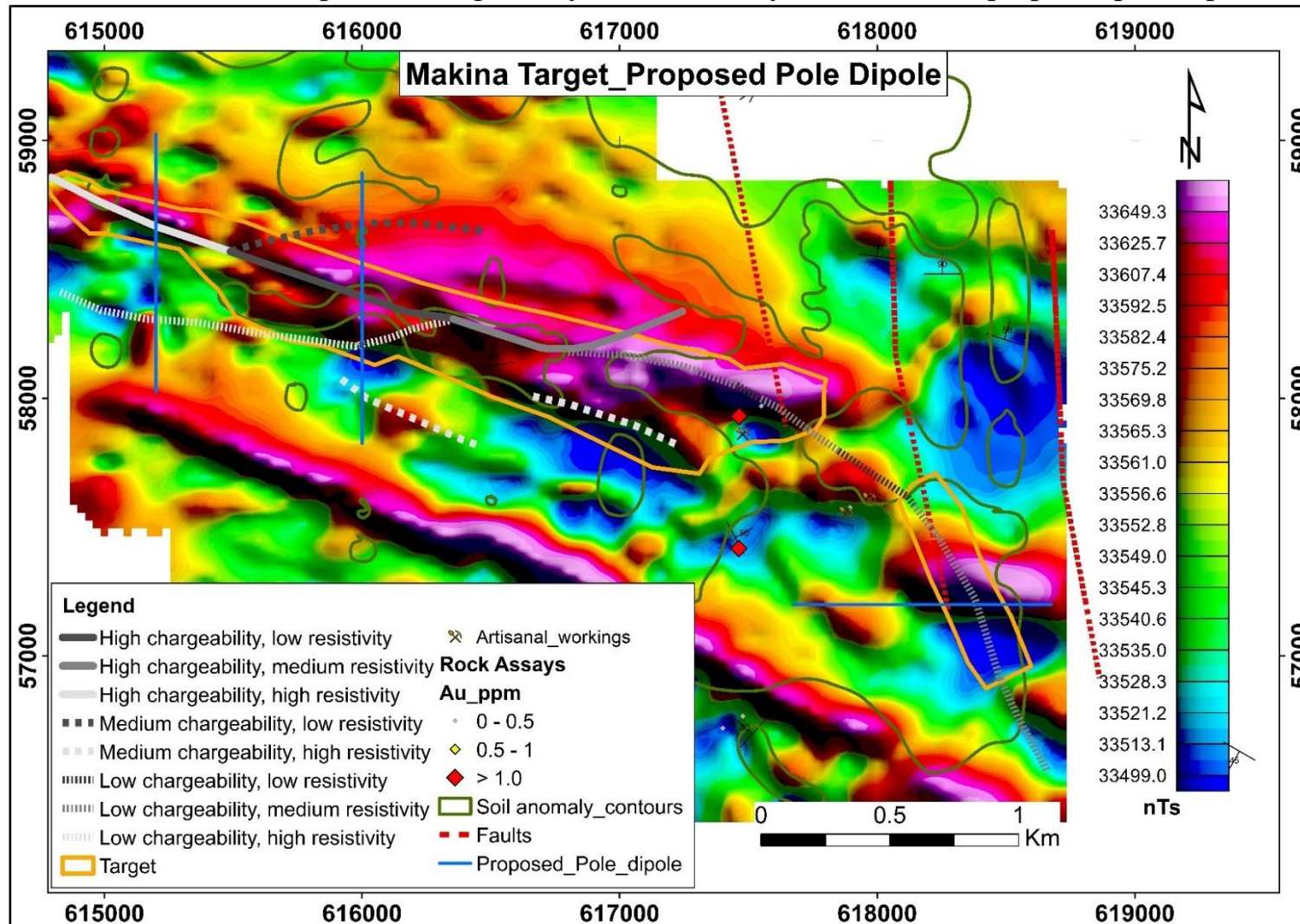
APPENDIX 8: Mineralization Target zone interpretations and proposed follow up survey lines

APPENDIX 9: Gradient IP/Resistivity survey Grid

MAKINA PLANNED IP SURVEY GRID

Legend

Geochem_Anomaly_contours

● IP_Lines_North_South

● IP_Lines_East_West

– – – Faults

1:12,000

0   0.5   1
Km

APPENDIX 10: Magnetic survey grid

MAKINA PLANNED MAGNETICS SURVEY GRID

Legend

☐ Geochem_Anomaly_contours

• Mag_Lines_North_South

• Mag_Lines_East_West

- - - Faults

1:12,000

0   0.5   1
                    Km